INAUGURAL – DISSERTATION

zur
Erlangung der Doktorwürde
der

GESAMTFAKULTÄT FÜR MATHEMATIK, INGENIEUR- UND NATURWISSENSCHAFTEN

der

RUPRECHT-KARLS-UNIVERSITÄT
HEIDELBERG

vorgelegt von

Denis Brazke

aus Rotenburg an der Fulda

Tag der mündlichen Prüfung

Asymptotic Expansion of a Non-local Isoperimetric Energy and Application to Mechanochemical Models related to Pattern Formation in Biological Membranes

Supervisor: Prof. Dr. Hans Knüpfer

Zusammenfassung

In dieser Dissertation befassen wir uns mit dem makroskopischem Grenzwert von Modellen von scharfen Grenzschichten, welche eine Näherung eines Modells von Komura, Shimokawa und Andelman (2006) zur Untersuchung von Musterbildung auf Zellmembranen basierend auf chemischen und mechanischen Wechselwirkungen in biologischen Membranen ist. Wir führen das zugehörige Minimierungsproblem auf ein nicht-lokales isoperimetrischen Problem zurück, für welches wir sub- und superkritische Regime für die relative Stärke der lokalen und nicht-lokalen Wechselwirkungen finden. Unter Benutzung der Autokorrelationsfunktion erhalten wir eine asymptotische Entwicklung der zugeörigen Energie bezüglichen des Längenparameters bis zur ersten Ordnung. Wir berechnen den Γ–Limes des Energiefunktionals im subkritischen Regime, sowie den Γ–Limes für das reskalierte Energiefunktional im kritischen Regime. Weiterhin zeigen wir höhere Regularität für die Autokorrelationsfunktion für hinreichend reguläre Gebiete zusammen mit Formeln für dessen Ableitungen ausgewertet am Ursprung.

Abstract

In this thesis, we derive a macroscopic limit for a sharp interface version of a model proposed by Komura, Shimokawa and Andelman (2006) to investigate pattern formation due to competition of chemical and mechanical forces. The problem is reformulated as a non-local isoperimetric problem, for which we identify sub- and supercritical parameter regimes in terms of the relative strength of the competing local and non-local interactions. Using the Autocorrelation Function, we find an asymptotic expansion of the energy in terms of the length scale parameter up to first order and derive the Γ–limit in the subcritical regime, and the Γ–limit of the rescaled energy in the critical regime. Concerning the analysis of the Autocorrelation Function, we show that regularity near the origin is inherited from the regularity of the corresponding set and present formulas for higher derivatives at the origin.

Contents

1. Introduction

We consider the family of nonlocal isoperimetric problems

$$E_{\gamma,\varepsilon}(\Omega) \coloneqq \mathrm{Per}(\Omega) - \frac{\gamma}{\varepsilon^{n+1}} \int_{\mathbb{R}^n} \mathcal{K}(\tfrac{z}{\varepsilon}) \int_{\mathbb{T}^n} |\chi_\Omega(x+z) - \chi_\Omega(x)| \,\mathrm{d}x \,\mathrm{d}z, \tag{1.1}$$

where $\Omega \subset \mathbb{T}^n$ is a set of finite perimeter and where $\mathbb{T}^n$, $n \geq 2$, is the n–dimensional unit flat torus. Here, $\gamma > 0$ is a fixed parameter and $\mathcal{K}$ is a radially symmetric kernel with certain integrability conditions. This class of problems appears in mathematical models of complex materials (such as pattern formation in biological membranes, see Chapter 3), diblock copolymers (see [CP10, JP17]) and cell motility (see [CMM20]). We derive various results concerning the asymptotic behaviour of $E_{\gamma,\varepsilon}$ as $\varepsilon \to 0$ such as compactness properties and Γ–convergence.

The family of functionals (1.1) is a more general sharp interface version of a model proposed in [KSA06] for the investigation of structures which arise due to competing diffusive and mechanical forces. In particular, it is relevant for the modelling of formation of so called *lipid rafts* in cell membranes. These are complex nanostructures made up of lipids, proteins, and cholesterol and are believed to be responsible for many biological phenomena such as transmembrane signaling and cellular homeostasis (see e.g. [SI97, LL15, RS05, SP13]). We comment on the relation between the diffuse and sharp interface model in Chapter 3.

This thesis is concerned with the asymptotic behaviour of $E_{\gamma,\varepsilon}$ as $\varepsilon \to 0$. More precisely we compute the Γ–limit of the family $E_{\gamma,\varepsilon}$ under suitable assumptions on $\mathcal{K}$. We identify two parameter regimes (sub– and supercritical) with respect to γ and show that the limit problem is the isoperimetric problem (with modified prefactor) in the subcritical regime. In the supercritical regime, we show that minimising sequences of $E_{\gamma,\varepsilon}$ always have unbounded perimeter. After rescaling, the energy has more subtle compactness and non-compactness properties in the critical regime. We will derive sufficient conditions for compactness and non-compactness and compute the Γ–limit in the criticial regime if the energy is rescaled by $\frac{1}{\varepsilon}$ (see Chapter 5).

Our main observation is that both the perimeter and the non–local term in (1.1) can be represented in terms of the (symmetrised) Autocorrelation Function introduced in Chapter 4:

$$c_\Omega(r) \coloneqq \fint_{\mathbb{S}^{n-1}} \int_{\mathbb{T}^n} \chi_\Omega(x+rw)\, \chi_\Omega(x) \,\mathrm{d}x \,\mathrm{d}\mathscr{H}^{n-1}(w). \tag{1.2}$$

The formulation of the energy in terms of the Autocorrelation Function (Theorem 5.6)

reveals the separation in sub- and supercritical regimes in terms of γ, and that the competing effects of the local and non-local parts of the energy (concentration versus oscillation) only appear in the zeroth order. For more details on the Autocorrelation Function, see Chapter 4.

Related Literature The Γ–convergence of (1.1) has been considered in different setups. In [Peg21], the author studied the stability of large mass minimisers of (1.1) in $\mathbb{R}^n$ (see also [MP22, GMP22]) and established the Γ–convergence in the subcritical regime under more restrictive assumptions on the kernel $\mathcal{K}$, namely that $\mathcal{K} \geq 0$. The ideas involve sharp estimates of the non–local term by the classical perimeter for the lower bound and the pointwise convergence of the non–local term proved in [DÓ2] (see also [BBM01]) for the upper bound. Apart from the different underlying geometry, we will relax the assumption of non–negativity of the kernel and recover their Γ–convergence result. We note that because of the aforementioned relaxation, a major challenge arises in the control of the non-local term. Lower bounds are more delicate since the control by the perimeter usually is achieved by estimating the integral of the difference quotient pointwise within the non-local term. If the kernel is allowed to have negative values, this estimate no longer provides a lower bound. We deal with this issue by reformulating the energy in terms of the Autocorrelation Function and shifting the desired control in terms of the perimeter to the Autocorrelation Function. This reformulation results in working with the integrated kernel (rather than the kernel itself) and allows us to relax the non-negativity.

The Γ–convergence of (1.1) in the special case where $\mathcal{K}$ is the solution to the Helmholtz equation on domains with different boundary conditions was considered in [MW23]. Their techniques are based on PDE arguments and they require the family of kernels to be solutions of the Helmholtz equation, whereas our techniques work for a larger class of kernels and are based on decay estimates. In particular, we recover the Γ–convergence result and are able to extend it to kernels which are given by $\mathcal{K} + (-\Delta)^{\frac{s}{2}}\mathcal{K} = \delta_0$ for any $1 < s \leq 2$ (see Lemma A.14).

Different classes of kernels in isoperimetric problems, where the non–local term has the same scaling as the local one (see (1.9)), were considered e.g. in [CN20, MW23, MS19, RW00]. Representing the energy in terms of the Autocorrelation Function and exploiting its fine properties has been proposed for a similar family of energies in [KS23]. There, the Autocorrelation Function was used to derive a second order expansion for the perimeter functional. However, the family of kernels is subject to different conditions and converge monotonically to a measurable function with certain integrability properties, whereas our family of kernels is assumed to form an approximation of the identity. Due to the highly singular nature of the considered kernels near the origin, our techniques require more information about the regularity of the Autocorrelation Function. Due to the aforementioned monotone convergence, higher regularity of the Autocorrelation Function is not required in [KS23]. For this purpose, we show regularity properties of the

Autocorrelation Function for higher order derivatives for a dense class of sets (see Lemma 2.18).

Lastly, non–local isoperimetric problems of the form (1.1) have also been considered in the mathematical literature in many different models, e.g. sharp interface variants of the Ohta-Kawasaki model where the non–local term is a Coulomb or Riesz type interaction (see [AFM13, ACO09, CP10, CS13, Cri18, GMS13, GMS14, JP17, MS14]). We note that, contrary to our energy, in these models the non-local term does not have the same scaling as the perimeter functional (see (1.9)).

Outline of thesis We will briefly describe how this thesis is organised. After the introduction in Chapter 1, in Chapter 2 we collect preliminary results concerning the Flat Torus $\mathbb{T}^n$ and subsets of it, in particular sets with smooth boundary and sets with finite perimeter. We also define the space of bounded variations on $\mathbb{T}^n$ and collect useful density results and compactness properties. In Chapter 3 we describe the biological setup and corresponding models in detail. We will look into diffuse and sharp interface models describing pattern formation processes in biological membranes and how these models are related. In Chapter 4 we introduce the Autocorrelation Function. Most interesting to us is the connection of the geometry of subsets of $\mathbb{T}^n$ and the regularity of the corresponding Autocorrelation Function. We will prove multiple regularity properties and derive formulas for higher derivatives at 0 as these values play a key role in the analysis concerning non-local isoperimetric problems. We will also compute Autocorrelation Functions for specific sets. In Chapter 5, we examine the asymptotic behaviour of the non-local isoperimetric energy $E_{\gamma,\varepsilon}$ as $\varepsilon \to 0$. We will find two parameter regimes with respect to γ (sub- and supercritical) with vastly different asymptotic behaviour such as compactness. In the critical regime, we derive sufficient conditions on rescalings of the energy for compactness and non-compactness. In addition, we compute the Γ–limit for the rescaled energy $\frac{1}{\varepsilon}E_{\gamma,\varepsilon}$ in the critical regime. Building on the computations in Chapter 4, we will then compute the energy for certain configurations. Auxiliary results and complicated computations are moved to the Appendix.

1.1. Statement of Results

In this section, we give the precise formulation of our setting and main results. Throughout this article, we assume $n \in \mathbb{N}$ with $n \geq 2$. Concerning the energy functional $E_{\gamma,\varepsilon}$, we are interested in the minimisation problem in case of prescribed volume fraction. We introduce the class of admissible functions

$$\mathcal{A} \coloneqq \left\{\Omega \in BV_n : |\Omega| = \theta\right\} \tag{1.3}$$

for some fixed parameter $0 < \theta < 1$, where BV_n denotes the set of all sets in $\mathbb{T}^n$ with finite perimeter (see Definition 2.14). We also fix the function $\mathcal{K} : \mathbb{R}^n \longrightarrow \mathbb{R}$ and define $\mathcal{K}_\varepsilon(z) \coloneqq \frac{1}{\varepsilon^n}\mathcal{K}(\frac{z}{\varepsilon})$. We recall the energy functional

$$E_{\gamma,\varepsilon}(\Omega) \coloneqq \mathrm{Per}(\Omega) - \frac{\gamma}{\varepsilon}\int_{\mathbb{R}^n} \mathcal{K}_\varepsilon(z) \int_{\mathbb{T}^n} |\chi_\Omega(x+z) - \chi_\Omega(x)| \,\mathrm{d}x \,\mathrm{d}z, \tag{1.4}$$

if $\Omega \in \mathcal{A}$, and $E_{\gamma,\varepsilon}(\Omega) = +\infty$ else. The kernel $\mathcal{K}$ is subject to the following conditions:

(H1) $\mathcal{K}$ is radial.

(H2) $|z|\,\mathcal{K}(z) \in L^1(\mathbb{R}^n)$.

(H3) $\displaystyle\int_{\mathbb{R}^n\setminus B_r(0)} \mathcal{K}(z)\,\mathrm{d}z \geq 0$ for all $r > 0$.

By a slight abuse of notation we also write $\mathcal{K}(z) = \mathcal{K}(|z|)$. The imposed conditions (H1)–(H3) are different from the conditions imposed on the family of kernels considered in [DÓ2] (see also [Peg21] and [MW23, Theorem 1.2]): although our family of kernels arises as L^1–dilates of $\mathcal{K}$, we relax the assumption of the non–negativity of $\mathcal{K}_\varepsilon$ by (H3). A kernels that satisfy (H3) but also has negative values is e.g.

$$\mathcal{K}(z) = \frac{\sin(|z|)}{|z|^{n+1}}\Big(\frac{\sin(|z|)}{|z|} - \cos(|z|)\Big). \tag{1.5}$$

As $E_{\gamma,\varepsilon}$ is the difference of two positive terms with the same scaling (see (1.9)), uniform control of the energy of a sequence of shapes in general does not a priori lead to control of the perimeter. However, we identify the critical parameter

$$\gamma_{\mathrm{crit}} \coloneqq \frac{n\omega_n}{2\omega_{n-1}}\bigg(\int_{\mathbb{R}^n} |z|\,\mathcal{K}(z)\,\mathrm{d}z\bigg)^{-1} \tag{1.6}$$

such that for $0 \leq \gamma < \gamma_{\mathrm{crit}}$ the perimeter is controlled by the energy, while the perimeter is not controlled for $\gamma > \gamma_{\mathrm{crit}}$.

Theorem A (Compactness and non–compactness) Suppose $\mathcal{K}$ satisfies (H1) – (H3).

a) *Compactness:* Let $0 \leq \gamma < \gamma_{\mathrm{crit}}$. Then for any sequence $\Omega_\varepsilon \in BV_n$ with $\sup_\varepsilon E_{\gamma,\varepsilon}(\Omega_\varepsilon) < \infty$ there exists $\Omega \in \mathcal{A}$ and a subsequence (not relabeled) such that $|\Omega \triangle \Omega_\varepsilon| \xrightarrow{\varepsilon\to 0} 0$.

b) *Non–compactness:* Let $\gamma \geq \gamma_{\mathrm{crit}}$. Then there exists a sequence $\Omega_\varepsilon \in \mathcal{A}$ such that $\sup_\varepsilon E_{\gamma,\varepsilon}(\Omega_\varepsilon) < \infty$, but there is no $\Omega \in \mathcal{A}$ such that $|\Omega \triangle \Omega_\varepsilon| \xrightarrow{\varepsilon\to 0} 0$ for any subsequence.

Theorem A is a special case of Theorem 5.10 and Theorem 5.12. It identifies the subcritical parameter regime $0 \leq \gamma < \gamma_{\text{crit}}$ and the supercritical parameter regime $\gamma \geq \gamma_{\text{crit}}$. We learn that the local term dominates in the subcritical regime, while in the supercritical regime the destabilising effect of the non–local interaction takes over. The failure of compactness is reflected in uniform lower bounds of the energy and the behaviour of minimising sequences:

Corollary A Suppose $\mathcal{K}$ satisfies (H1) – (H3).

a) Let $0 \leq \gamma \leq \gamma_{\text{crit}}$. Then $E_{\gamma,\varepsilon} \geq 0$ for every $\varepsilon > 0$.

b) Let $\gamma > \gamma_{\text{crit}}$. Then there exists a sequence $\Omega_\varepsilon \in \mathcal{A}$ such that

$$E_{\gamma,\varepsilon}(\Omega_\varepsilon) \xrightarrow{\varepsilon \to 0} -\infty.$$

Moreover, $\liminf_{\varepsilon \to 0} \operatorname{Per}(\Omega_\varepsilon) = \infty$ for any such sequence.

We note that in the critical case $\gamma = \gamma_{\text{crit}}$, the family of energies $E_{\gamma_{\text{crit}},\varepsilon}$ does not have the compactness property even though it is bounded from below. This is due to the fact that $0 \leq E_{\gamma_{\text{crit}},\varepsilon}(\Omega) \to 0$ for polytopes, which are able to approximate any shape of finite perimeter (see Lemma 2.16). In this case, higher order effects play a role and therefore the energy $E_{\gamma,\varepsilon}$ needs to be rescaled. We will elaborate on the rescaled functional further down.

As explained in the introduction, we are interested in the limiting behaviour of minimising sequences as $\varepsilon \to 0$. We show that the family of non–local energies Γ–converges to a local energy functional:

Theorem B (Γ–convergence) Suppose that $\mathcal{K}$ satisfies (H1) – (H3). Let $0 \leq \gamma \leq \gamma_{\text{crit}}$. Then $E_{\gamma,\varepsilon} \xrightarrow{\Gamma} E_{\gamma,0}$ with respect to the L^1–topology, where

$$E_{\gamma,0}(\Omega) := \begin{cases} (1 - \frac{\gamma}{\gamma_{\text{crit}}}) \operatorname{Per}(\Omega) & \text{if } \Omega \in \mathcal{A}, \\ +\infty & \text{else.} \end{cases}$$

In particular, for every measurable set Ω we have:

a) Liminf inequality: For every sequence of measurable sets $\Omega_\varepsilon \subset \mathbb{T}^n$ such that $|\Omega \triangle \Omega_\varepsilon| \xrightarrow{\varepsilon \searrow 0} 0$ we have $E_{\gamma,0}(\Omega) \leq \liminf_{\varepsilon \to 0} E_{\gamma,\varepsilon}(\Omega_\varepsilon)$.

b) Limsup inequality: There is a sequence of measurable sets $\Omega_\varepsilon \subset \mathbb{T}^n$ such that $|\Omega \triangle \Omega_\varepsilon| \xrightarrow{\varepsilon \searrow 0} 0$ and $\limsup_{\varepsilon \to 0} E_{\gamma,\varepsilon}(\Omega_\varepsilon) \leq E_{\gamma,0}(\Omega)$.

Theorem B is a special case of Theorem 5.18. Although the non–local term leads to a reduction of the interfacial cost by a factor of $\frac{\gamma}{\gamma_{\mathrm{crit}}}$ in the subcritical regime, the limit problem is simply the isoperimetric problem with a suitably modified prefactor.

As we have seen in Theorem A, the energy $E_{\gamma,\varepsilon}$ loses compactness if $\gamma \geq \gamma_{\mathrm{crit}}$. To restore compactness, we choose $\gamma = \gamma_\varepsilon$ depending on ε and rescale the functional suitably. By a rescaling, we mean a function $\mathbf{R} \in C^0(\mathbb{R}_+)$ such that $\mathbf{R}(\varepsilon) \xrightarrow{\varepsilon \searrow 0} +\infty$.

Theorem C (Compactness and non-compactness for rescaled energy) Suppose $\mathcal{K}$ satisfies (H1)–(H3) and let $\mathbf{R}$ be a rescaling.

a) Let $\gamma_\varepsilon > 0$ such that $\liminf_{\varepsilon\to 0}(1 - \frac{\gamma_\varepsilon}{\gamma_{\mathrm{crit}}})\mathbf{R}(\varepsilon) > 0$. Let $\Omega_\varepsilon \in BV_n$ such that $\limsup_{\varepsilon\to 0} \mathbf{R}(\varepsilon) E_{\gamma_\varepsilon,\varepsilon}(\Omega_\varepsilon) < \infty$. Then there exists $\Omega \in \mathcal{A}$ and a subsequence (not relabeled), such that $|\Omega \triangle \Omega_\varepsilon| \to 0$.

b) Let $\gamma_\varepsilon > 0$ such that $\gamma_{\mathrm{crit}} < \liminf_{\varepsilon\to 0} \gamma_\varepsilon \leq \limsup_{\varepsilon\to 0} \gamma_\varepsilon < \infty$. Then there exists $\Omega_\varepsilon \in \mathcal{A}$ such that $\mathbf{R}(\varepsilon) E_{\gamma_\varepsilon,\varepsilon}(\Omega_\varepsilon) \xrightarrow{\varepsilon \searrow 0} -\infty$.

Theorem C is a combination of Theorem 5.16 and Theorem 5.15 (see also Lemma 5.17). It provides a sufficient condition under which assumptions there exist rescalings of the energy functional $E_{\gamma,\varepsilon}$ such that compactness is restored in the critical regime $\gamma_\varepsilon \sim \gamma_{\mathrm{crit}}$. In contrast, the supercritical regime cannot be rescaled to restore compactness.

In case of the rescaling $\mathbf{R}(\varepsilon) = \frac{1}{\varepsilon}$ we have the following Γ–convergence result in two dimension, if in addition the second moment of $\mathcal{K}$ is finite.

Theorem D (Γ–convergence for rescaled energy) Let $n = 2$, $\gamma_\varepsilon > 0$ and assume that $\frac{1}{\varepsilon}(1 - \frac{\gamma_\varepsilon}{\gamma_{\mathrm{crit}}}) \xrightarrow{\varepsilon \searrow 0} \sigma > 0$. Suppose $\mathcal{K}$ satisfies (H1)–(H3) and has finite second moment. Then $\frac{1}{\varepsilon} E_{\gamma_\varepsilon,\varepsilon} \xrightarrow{\Gamma} E_0^{(1)}$ in the L^1–topology, where

$$E_0^{(1)}(\Omega) := \begin{cases} \sigma \operatorname{Per}(\Omega) & \text{if } \Omega \in \mathcal{A}, \\ +\infty & \text{else.} \end{cases}$$

In particular, for every measurable set Ω we have:

a) Liminf inequality: For every sequence of measurable sets $\Omega_\varepsilon \subset \mathbb{T}^n$ such that $|\Omega \triangle \Omega_\varepsilon| \xrightarrow{\varepsilon \searrow 0} 0$ we have $E_0^{(1)}(\Omega) \leq \liminf_{\varepsilon\to 0} \frac{1}{\varepsilon} E_{\gamma,\varepsilon}(\Omega_\varepsilon)$.

b) Limsup inequality: There is a sequence of measurable sets $\Omega_\varepsilon \subset \mathbb{T}^n$ such that $|\Omega \triangle \Omega_\varepsilon| \xrightarrow{\varepsilon \searrow 0} 0$ and $\limsup_{\varepsilon\to 0} \frac{1}{\varepsilon} E_{\gamma,\varepsilon}(\Omega_\varepsilon) \leq E_0^{(1)}(\Omega)$.

Theorem D is stated and proved in Theorem 5.21.

In the physical relevant dimension $n = 2$, the minimiser of the limit problems in Theorem B and Theorem D is known (see [CS06, Theorem 4.1]). Up to translation and rotation, it is given by $\Omega \subset \mathbb{T}^2$ being a ball (or the complement of a ball) if

$$\min\{\theta, 1-\theta\} < \frac{1}{\pi}, \tag{1.7}$$

and by a single laminate otherwise. If equality holds (1.7), both ball (or its complement) and laminate are minimisers. The isoperimetric problem in higher dimensions are (to my awareness) an open problem (see e.g. [Ros05]).

We note that the main theorems also hold without the assumption of a fixed volume fraction, i.e. for the admissible class of functions $\mathcal{A} = BV_n$. The proofs in this case can be repeated almost verbatim. Moreover, the choice of the unit flat torus in contrast to flat tori with side length $\ell > 0$ is justified by the scaling of the energy $E_{\gamma,\varepsilon}$. Most interesting to us is the limiting behaviour of $E_{\gamma,\varepsilon}$ as $\varepsilon \to 0$ and due to the scaling of the energy, we can without loss of generality consider the unit flat torus. More precisely, let $\mathbb{T}^n_\ell \coloneqq \mathbb{R}^n/(\ell\mathbb{Z})^n$ and define

$$E^{(\ell)}_{\gamma,\varepsilon}[v] \coloneqq \int_{\mathbb{T}^n_\ell} |\nabla v| - \frac{\gamma}{\varepsilon^{n+1}} \int_{\mathbb{R}^n} \mathcal{K}(\tfrac{z}{\varepsilon}) \int_{\mathbb{T}^n_\ell} \frac{|v(x+z) - v(x)|}{|\mathbb{T}^n_\ell|} \,\mathrm{d}x \,\mathrm{d}z \tag{1.8}$$

for all $v \in BV(\mathbb{T}^n_\ell, \{0,1\})$. Here, we identify the set Ω with its characteristic function $v \coloneqq \chi_\Omega$ for notational convenience. Let $u \in BV(\mathbb{T}^n, \{0,1\})$ and define the rescaled function $u_\ell \in BV(\mathbb{T}^n_\ell, \{0,1\})$ via $u_\ell(x) \coloneqq u(\frac{x}{\ell})$. Then

$$E^{(\ell)}_{\gamma,\varepsilon}[u_\ell] = \ell^{n-1} E_{\gamma,\ell^{-1}\varepsilon}[u]. \tag{1.9}$$

Thus, the limiting behaviour $\varepsilon \to 0$ as well as the subsequent analysis can be reduced to the case of the unit flat torus.

Main theorems concerning the Autocorrelation Function The arguments to prove the main theorems A – D all rely on a reformulation of the energy functional $E_{\gamma,\varepsilon}$ in terms of the Autocorrelation Function introduced in Chapter 4. More precisely, we mostly work with the following reformulation (see Theorem 5.6):

$$E_{\gamma,\varepsilon}(\Omega) = \big(1 - \tfrac{\gamma}{\gamma_{\mathrm{crit}}}\big) \operatorname{Per}(\Omega) + 2\gamma \int_0^\infty \Phi_\varepsilon(r)[c'_\Omega(r) - c'_\Omega(0)] \,\mathrm{d}r \tag{1.10}$$

where c_Ω denotes the Autocorrelation Function and Φ arises via radial integration of $\mathcal{K}$ (see (5.15)). Higher regularity of the Autocorrelation Function near the origin is of great interest as the kernel Φ_ε forms an approximation of the identity, relating the asymptotic behaviour of $E_{\gamma,\varepsilon}$ to higher derivatives of c_Ω at 0. As was shown in [Gal11, KS23] (see also

Theorem 4.7), regularity properties of the Autocorrelation Function is tightly connected to the geometry of the corresponding set. The following Theorem is proven in two dimensions for the class BV_2^∞ of sets with sufficiently regular boundary (see Definition 2.17).

Theorem E (Higher regularity of the Autocorrelation Function) Let $\Omega \in BV_2^\infty$. Then there exists $R > 0$ such that $c_\Omega \in C^\infty((0, R])$ and

$$c_\Omega''(0) = 0, \qquad\qquad c_\Omega'''(0) = \frac{1}{4\pi} \int_{\partial\Omega} \kappa^2 \, \mathrm{d}\mathscr{H}^1,$$

where $\kappa \colon \partial\Omega \longrightarrow \mathbb{R}$ denotes the curvature of Ω.

Theorem E is a combination of Theorem 4.10, Corollary 4.12 and Corollary 4.15. The fact that $c_\Omega''(0) = 0$ for the dense class of sets BV_2^∞ allows us to control possible singularities arising in the higher order convergence in the proof of Theorem D. Moreover, we will see that there exist non smooth sets for which $c_\Omega'' > 0$ (e.g. polygons, see Section 4.4.4) and $c_\Omega''(0) = +\infty$ (e.g. sets with a cusp, see Section 4.4.5).

Strategy of the proofs In the following we give an overview of the strategies of the proofs for the main theorems. Central to our proofs is the formulation of the energy in terms of the symmetrised Autocorrelation Function (see Theorem 5.6). At this stage, the radial symmetry of the kernel is crucial and the prefactor ε^{-1} of the non–local term ensures that the weight in the reformulation is an approximation of the identity. This implies that the limiting behaviour of the energy only depends on the Autocorrelation Function near the origin and the weight Φ associated to the kernel $\mathcal{K}$ (rather than the kernel itself), which allows us to treat kernels which also have negative values (see Hypothesis (H3)). As $\varepsilon \to 0$, the reformulation of the energy in terms of the Autocorrelation Function allows for a splitting into behaviour near the origin (which is controlled since the Autocorrelation Function is sufficiently regular) and far from the origin (which is small since the weight Φ_ε is an approximation of the identity).

The compactness results in Theorem A and C are shown by a sharp lower bound in terms of the perimeter functional (see Corollary 5.7) and the compact embedding of BV in L^1, while the non-compactness results are shown by construction of highly oscillating laminates (see Lemma 5.11). The lower bounds in Theorem B and D follow from sharp estimates of the Autocorrelation Function and its derivatives. The upper bound requires higher regularity of the Autocorrelation Function near the origin in order to pass to the limit.

To prove Theorem E, we observe that the Covariogram near the origin can be computed by integrals of the corresponding graph representation (see Theorem 4.10). In case of a sufficiently smooth boundary, all the functions involved in this computation are smooth, which transfers to the regularity of the Covariogram. In order to pass to the limit $r \to 0$

for higher derivatives of the Autocorrelation Function, we explicitly compute the integrals involved and relate the Covariogram back to the Autocorrelation Function using the Co-Area Formula (see Corollary 4.12 and Corollary 4.15).

1.2. Notation

We denote n-dimensional Euclidean space with $\mathbb{R}^n$, the space of vectors with integer entries with $\mathbb{Z}^n$ and the natural numbers (starting with 1) with $\mathbb{N}$. We denote the standard Inner Product and the corresponding norm by

$$x \cdot y \coloneqq \sum_{i=1}^{n} x_i y_i, \qquad |x|^2 \coloneqq x \cdot x \qquad \text{for all } x, y \in \mathbb{R}^n. \tag{1.11}$$

We denote the ball of radius $\rho > 0$ and centre $x \in \mathbb{R}^n$ by $B_\rho(x) \coloneqq \{y \in \mathbb{R}^n : |x - y| < \rho\}$, and the unit sphere by $\mathbb{S}^{n-1} \coloneqq \partial B_1(0)$. We denote the standard basis of $\mathbb{R}^n$ by $\{\mathbf{e}_1, \dots, \mathbf{e}_n\}$ and the positive real numbers by $\mathbb{R}_+$. We denote the Lebesgue measure of a Lebesgue measurable set $\Omega \subset \mathbb{R}^n$ by $|\Omega|$ and by $\mathrm{d}x$, $\mathrm{d}y$ etc. depending on the context. We denote the surface measure (or $n-1$ dimensional Hausdorff measure) by $\mathscr{H}^{n-1}$. We denote the volume of the unit ball in $\mathbb{R}^n$ by ω_n and $\sigma_n \coloneqq n\omega_n$ for its surface area.

We denote the n-dimensional flat torus by $\mathbb{T}^n \coloneqq \mathbb{R}^n/\mathbb{Z}^n$. We denote $\mathcal{Q}^n \coloneqq [0,1)^n$ for its primitive cell. Without distinction in notation, we identify $\mathcal{Q}^n$–periodic functions in $\mathbb{R}^n$ with functions defined on $\mathbb{T}^n$. We denote the unit Haar measure of a measurable set $\Omega \subset \mathbb{T}^n$ by $|\Omega|$ and by $\mathrm{d}x$, $\mathrm{d}y$ etc. depending on the context. We denote the ball of radius $\rho > 0$ and centre $x \in \mathbb{T}^n$ by $B_\rho(x) \coloneqq \{y \in \mathbb{T}^n : |x - y| < \rho\}$ where $|x - y|$ is the Riemannian distance. For more details and notational conventions, see Section 2.1.

We write $A \lesssim B$ if there exists a universal constant $C > 0$, such that $A \leq CB$. We denote $\mathcal{O}$ for the Landau symbol. Given two sets $A, B \subset X$, we define the symmetric difference $A \triangle B \coloneqq (A \setminus B) \cup (B \setminus A)$. We say that a sequence of sets Ω_ε converges in L^1 to a set Ω, if $|\Omega_\varepsilon \triangle \Omega| \xrightarrow{\varepsilon \searrow 0} 0$.

2. Preliminaries

In this chapter, we collect preliminary results necessary for the analysis concerning the Autocorrelation Function in Chapter 4 and the non-local isoperimetric energy $E_{\gamma,\varepsilon}$ in Chapter 5. In Section 2.1, we introduce and discuss the flat Torus $\mathbb{T}^n$ and its geometry. In Section 2.2, we study functions of bounded variation defined on $\mathbb{T}^n$. Of particular interest are sets of finite perimeter (see Definition 2.14) since they form the domain of the energy $E_{\gamma,\varepsilon}$.

2.1. Flat Torus

In this section, we will collect preliminary results describing the topology and geometry of the flat torus.

Definition 2.1 We define $\mathbb{T}^n := \mathbb{R}^n/\mathbb{Z}^n$.

Since $\mathbb{R}^n$ is a Lie group and $\mathbb{Z}^n$ acts smoothly, freely and proper on $\mathbb{R}^n$, the flat torus $\mathbb{T}^n$ itself is an orientable smooth closed manifold with a unique smooth structure (with respect to the canonical projection $\mathbb{R}^n \longrightarrow \mathbb{T}^n$). Moreover, $\mathbb{T}^n$ itself is a Lie group with the canonical group action

$$[x] + [y] = [x + y] \qquad \text{for all } x, y \in \mathbb{R}^n. \tag{2.1}$$

As such, there exists a unique normed Haar measure (denoted $\mathrm{d}x$, $\mathrm{d}y$ etc.). The flat torus is a flat and closed space with Lie algebra $\mathfrak{g} = \mathbb{R}^n$. In fact, all tangent spaces are identical, namely $\mathsf{T}_x\mathbb{T}^n = \mathbb{R}^n$ for all $x \in \mathbb{T}^n$, thus we identify the set of all smooth vector fields on $\mathbb{T}^n$ with the space $C^\infty(\mathbb{T}^n, \mathbb{R}^n)$. We denote the primitive cell by $\mathcal{Q}^n \cong [0,1)^n \subset \mathbb{R}^n$. Since all chart transitions are given by the identity, the smooth structure of $\mathbb{T}^n$ and $\mathbb{R}^n$ are identical. With standard abuse of notation, we use the same notation for geometric structures on $\mathbb{T}^n$ as for $\mathbb{R}^n$, meaning that $x \cdot y$ will be used as notation for the Riemannian metric and $|x|^2 = x \cdot x$. Further, given $x \in \mathbb{T}^n$, we write $x = rw =: \exp_0(rw)$ for $r > 0$ and $w \in \mathfrak{g}$ with $|w| = 1$, where $\exp_0 \colon \mathfrak{g} \longrightarrow \mathbb{T}^n$ denotes the exponential map at the identity.

We define ∇f as the unique vector field defining the gradient, i.e. the vector field satisfying

$$\nabla_X f = \nabla f \cdot X \qquad \text{for all } X \in C^\infty(\mathbb{T}^n, \mathbb{R}^n), \tag{2.2}$$

where ∇_X denotes the Lie derivative along X. We define the divergence of a smooth vector field $F \in C^\infty(\mathbb{T}^n, \mathbb{R}^n)$ via the canonical volume form $\mathrm{d}x$ (which is induced by the Riemannian metric) as the unique function $\nabla \cdot F \in C^\infty(\mathbb{T}^n)$ satisfying

$$(\nabla \cdot F)\,\mathrm{d}x \coloneqq \nabla_F(\mathrm{d}x), \tag{2.3}$$

where ∇_F is denotes the Lie derivative along F of n-forms. Using the Leibniz rule $\nabla_F(\varphi\,\mathrm{d}x) = \nabla_F(\varphi)\,\mathrm{d}x + \varphi\nabla_F(\mathrm{d}x)$ we obtain via Stoke's Theorem and $\mathrm{d}(\mathrm{d}x) = 0$ the following integration by parts formula:

$$\int_{\mathbb{T}^n} (\nabla \cdot F)\varphi\,\mathrm{d}x = -\int_{\mathbb{T}^n} F \cdot \nabla\varphi\,\mathrm{d}x. \tag{2.4}$$

2.1.1. Sets with Smooth Boundaries

In this section, we will discuss subsets of the flat torus with smooth boundary. As this class of sets will only be discussed in dimension $n = 2$, we will restrict to that case. We will define a notion of curvature of a smooth set immersed in $\mathbb{T}^2$. The procedure to define curvature is well known. However, due to the need to find the Jacobian of the Gauß map later (see Lemma 4.14) we will give the definition in detail and in such a way that it is compatible with our setup.

Definition 2.2 Let $\Omega \subset \mathbb{T}^n$ be open. Then Ω has a **smooth boundary** if $\partial\Omega \subset \mathbb{T}^n$ is a smooth immersed submanifold.

We will define the curvature $\kappa\colon \partial\Omega \longrightarrow \mathbb{R}$ of a set $\Omega \subset \mathbb{T}^2$ with smooth boundary in the following way. Let $\nu \in C^\infty(\partial\Omega, \mathbb{R}^2) \cong C^\infty(\partial\Omega, \mathsf{T}\mathbb{T}^2)$ be the Gauß map. Using the Riemannian structure on $\mathbb{T}^2$ we find a decomposition

$$\mathsf{T}\mathbb{T}^2 = \mathsf{T}\partial\Omega \oplus \mathsf{N}\partial\Omega, \tag{2.5}$$

where $\mathsf{N}\partial\Omega$ denotes the normal bundle. In particular, we have for the image of the Gauß map $\nu(x) \in \mathsf{N}_x\partial\Omega$. Moreover, the rotation operator $\bullet^\perp$ on $\mathbb{R}^2$ induces an (orientation dependent) isomorphism $\mathsf{T}\partial\Omega \cong \mathsf{N}\partial\Omega$ via

$$(x, \tau) \longmapsto (x, -\tau^\perp), \qquad (x, \mathbf{n}) \longmapsto (x, \mathbf{n}^\perp). \tag{2.6}$$

Let $I \subset \mathbb{R}$ and let $\gamma \in C^\infty(I, \mathbb{T}^2)$ be a regular curve such that $\gamma(I) \subset \partial\Omega$ with differential

$$D_s\gamma \colon \mathsf{T}_s I \longrightarrow \mathsf{T}_{\gamma(s)}\partial\Omega. \tag{2.7}$$

Let $\mathsf{T}_s I$ be spanned by the positive normed vector field $\partial_t^{(s)}$, i.e. $\mathsf{T}_s I = \langle \partial_t^{(s)} \rangle$. Since γ is regular, we find

$$\dot\gamma(s) \coloneqq (D_s\gamma)(\partial_t^{(s)}) = \alpha(\gamma(s))\, \nu^\perp(\gamma(s)) \qquad \text{for some } \alpha \in \mathbb{R} \setminus \{0\}. \tag{2.8}$$

We note that $D_\bullet\gamma \colon \mathsf{T}I \longrightarrow \mathsf{T}\partial\Omega \hookrightarrow \mathsf{T}\mathbb{T}^2$ and thus we find $\dot\gamma \colon I \longrightarrow \mathsf{T}\partial\Omega$. Again, we find the differential

$$D_s\dot\gamma \colon \mathsf{T}_s I \longrightarrow \mathsf{T}_{\dot\gamma(s)}(\mathsf{T}\partial\Omega) \cong \mathsf{N}_{\gamma(s)}\partial\Omega, \tag{2.9}$$

where $\mathsf{T}(\mathsf{T}\partial\Omega) \cong \mathsf{N}\partial\Omega$ via the canonical identification

$$(\dot\gamma(s), (\gamma(s), \tau)) \longmapsto (\gamma(s), -\tau^\perp), \qquad (\gamma(s), \mathbf{n}) \longmapsto (\dot\gamma(s), (\gamma(s), \mathbf{n}^\perp)). \tag{2.10}$$

Now, if $D_s\dot\gamma = 0$, then $\kappa(\gamma(s)) = 0$. Otherwise, since the vector spaces involved are 1 dimensional, we find a unique constant $\kappa \in \mathbb{R}$ such that

$$-\ddot\gamma^\perp(s) \coloneqq -(D_s\dot\gamma)^\perp(\partial_t^{(s)}) = \alpha(\gamma(s))\, \kappa(\gamma(s))\, \nu(\gamma(s)). \tag{2.11}$$

In that way, we can define the signed curvature $\kappa \colon \partial\Omega \longrightarrow \mathbb{R}$ via a partition of unity on segments of $\partial\Omega$ which are given by curves as described above.

Definition 2.3 Let $\Omega \subset \mathbb{T}^2$ be open with smooth boundary. We define the (signed) **curvature** $\kappa \colon \partial\Omega \longrightarrow \mathbb{R}$ as the unique value κ satisfying (2.11).

We note that this notion of curvature is extrinsic, meaning it depends on the ambient space $\mathbb{T}^2$ and its orientation.

2.2. Functions of Bounded Variation on the Torus

In this section, we will define the space of functions with bounded variation and collect properties of this space e.g. several density, representation and compactness properties.

Definition 2.4 Let $w \in \mathbb{S}^{n-1}$ and $f \in L^1(\mathbb{T}^n)$. We define the **directional variation**

along w of f via

$$V_w[f] \coloneqq \sup\Big\{ \int_{\mathbb{T}^n} f(x)\, \nabla_w \varphi(x)\, \mathrm{d}x : \varphi \in C^\infty(\mathbb{T}^n),\ \|\varphi\|_{L^\infty(\mathbb{T}^n)} \leq 1 \Big\}. \tag{2.12}$$

The definition of $BV(\mathbb{T}^n)$ differs slightly from the definition of $BV(\mathbb{R}^n)$ in that there is no support condition for test functions in the former. This is due to compactness of $\mathbb{T}^n$ as a topological space. Also, to be more precise, one should write $w \in \mathfrak{g}$ such that $|w| = 1$. As $\mathfrak{g} = \mathbb{R}^n$, we will not differ in notation.

Given a smooth function $f \in C^\infty(\mathbb{T}^n)$, the directional variation is given by

$$V_w[f] = \int_{\mathbb{T}^n} |\nabla_w f(x)|\, \mathrm{d}x \qquad \text{for all } w \in \mathbb{S}^{n-1}. \tag{2.13}$$

Indeed, we first note that given $\varphi \in C^\infty(\mathbb{T}^n)$ such that $\|\varphi\|_{L^\infty(\mathbb{T}^n)} \leq 1$, integration by parts yields

$$\int_{\mathbb{T}^n} f(x)\, \nabla_w \varphi(x)\, \mathrm{d}x \leq \Big| \int_{\mathbb{T}^n} f(x)\, \nabla_w \varphi(x)\, \mathrm{d}x \Big| \tag{2.14}$$

$$= \Big| \int_{\mathbb{T}^n} \nabla_w f(x)\, \varphi(x)\, \mathrm{d}x \Big| \tag{2.15}$$

$$\leq \int_{\mathbb{T}^n} |\nabla_w f(x)|\, \mathrm{d}x. \tag{2.16}$$

On the other hand, define the function $g(x) \coloneqq -\operatorname{sgn}(\nabla_w f(x))$, where $\operatorname{sgn}\colon \mathbb{R} \longrightarrow \mathbb{R}$ is given by $\operatorname{sgn} \coloneqq 2\chi_{\mathbb{R}_+} - 1$. Also, let $\eta_k \in C^\infty(\mathbb{T}^n)$ be a Dirac sequence (see Lemma A.1) and define $g_k \coloneqq g * \eta_k$. Then $g_k \in C^\infty(\mathbb{T}^n)$ and $g_k \to g$ in $L^1(\mathbb{T}^n)$ as $k \to \infty$. In addition, we obtain $\|g_k\|_{L^\infty(\mathbb{T}^n)} \leq 1$ using Young's convolution inequality. So the family $\{g_k\}_k$ is admissible and we compute

$$\int_{\mathbb{T}^n} f(x)\, \nabla_w g_k(x)\, \mathrm{d}x = -\int_{\mathbb{T}^n} \nabla_w f(x)\, g_k(x)\, \mathrm{d}x \xrightarrow{k\to\infty} \int_{\mathbb{T}^n} |\nabla_w f(x)|\, \mathrm{d}x, \tag{2.17}$$

from which (2.13) follows. We will also consider the total variation of a function $f \in L^1(\mathbb{T}^n)$:

Definition 2.5 Let $f \in L^1(\mathbb{T}^n)$. We define the **total variation** of f via

$$V[f] \coloneqq \sup\Big\{ \int_{\mathbb{T}^n} f(x)\, (\nabla \cdot \varphi)(x)\, \mathrm{d}x : \varphi \in C^\infty(\mathbb{T}^n, \mathbb{R}^n),\ \|\varphi\|_{L^\infty(\mathbb{T}^n, \mathbb{R}^n)} \leq 1 \Big\}. \tag{2.18}$$

If $V[f] < \infty$, then we say the function f is of **bounded variation**, and we denote $f \in BV(\mathbb{T}^n)$.

To be more precise, one should assume that φ is a smooth vector field on $\mathbb{T}^n$. As a reminder, since $\mathsf{T}_x\mathbb{T}^n = \mathbb{R}^n$ for all $x \in \mathbb{T}^n$, we identify the smooth vector fields on $\mathbb{T}^n$ with the space $C^\infty(\mathbb{T}^n, \mathbb{R}^n)$.

Similar to the directional variation, one can show that

$$V[f] = \int_{\mathbb{T}^n} |\nabla f(x)| \, \mathrm{d}x \qquad \text{for all } f \in C^\infty(\mathbb{T}^n). \tag{2.19}$$

The following theorem shows that derivatives of BV functions are Radon measures.

Theorem 2.6 Let $f \in BV(\mathbb{T}^n)$. Then there exists a Radon measure $\mu\colon \mathscr{B}(\mathbb{T}^n) \longrightarrow [0, \infty]$ and a μ–measurable function $\nu\colon \mathbb{T}^n \longrightarrow \mathbb{R}^n$, such that $|\nu| = 1$ for μ–almost–every $x \in \mathbb{T}^n$, and

$$\int_{\mathbb{T}^n} f(x) \, (\nabla \cdot \varphi)(x) \, \mathrm{d}x = -\int_{\mathbb{T}^n} \varphi(x) \cdot \nu(x) \, \mathrm{d}\mu \qquad \text{for all } \varphi \in C^\infty(\mathbb{T}^n, \mathbb{R}^n). \tag{2.20}$$

As a quick reminder: a Radon measure μ is a measure defined on the Borel–σ–Algebra $\mathscr{B}(\mathbb{T}^n)$, which is locally finite (i.e. for every $x \in \mathbb{T}^n$ there exists an open set $x \in U$ such that $\mu(U) < \infty$) and inner regular, i.e. it holds

$$\mu(U) = \sup\{\mu(K) : K \subset A, \ K \text{ is compact}\} \qquad \text{for every open set } U \subset \mathbb{T}^n. \tag{2.21}$$

Proof: Define the functional $T_f\colon C^\infty(\mathbb{T}^n) \longrightarrow \mathbb{R}$ via

$$\langle T_f, \varphi \rangle \coloneqq -\int_{\mathbb{T}^n} f(x) \, (\nabla \cdot \varphi)(x) \, \mathrm{d}x \qquad \text{for all } \varphi \in C^\infty(\mathbb{T}^n). \tag{2.22}$$

Then T_f is a linear operator and continuous with respect to $\| \cdot \|_{L^\infty(\mathbb{T}^n, \mathbb{R}^n)}$. In particular by definition of the variation $\|T_f\| = V[f]$. Using the Theorem of Stone–Weierstraß componentwise, we find that $C^\infty(\mathbb{T}^n, \mathbb{R}^n) \subset C^0(\mathbb{T}^n, \mathbb{R}^n)$ is dense, and we can extend the linear operator T_f to all of $C^0(\mathbb{T}^n)$. The statement then follows by the Riesz Representation Theorem (see [ADPM11, Appendix A.2]). ■

Corollary 2.7 Let $f \in BV(\mathbb{T}^n)$ and $w \in \mathbb{S}^{n-1}$. Then there exists a Radon measure $\mu\colon \mathscr{B}(\mathbb{T}^n) \longrightarrow [0, \infty]$ and a μ–measurable function $\nu\colon \mathbb{T}^n \longrightarrow \mathbb{R}^n$, such that $|\nu| = 1$ for μ–almost–every $x \in \mathbb{T}^n$, and

$$\int_{\mathbb{T}^n} f(x) \, \nabla_w \varphi(x) \, \mathrm{d}x = -\int_{\mathbb{T}^n} (\nu \cdot w) \varphi \, \mathrm{d}\mu \qquad \text{for all } \varphi \in C^\infty(\mathbb{T}^n). \tag{2.23}$$

Proof: Follows directly from Theorem 2.6. ■

Both Theorem 2.6 and Corollary 2.7 state that the derivatives of functions $f \in BV(\mathbb{T}^n)$ are Radon measures. We will denote these measures with $\nabla_w f := (\nu \cdot w)\mu$ and $\nabla f := \nu\mu$ so that the following integration by parts formulae hold:

$$\int_{\mathbb{T}^n} f(x)\, \nabla_w \varphi(x)\, \mathrm{d}x = -\int_{\mathbb{T}^n} \varphi \,\mathrm{d}\nabla_w f \qquad \text{for all } \varphi \in C^\infty(\mathbb{T}^n), \tag{2.24}$$

$$\int_{\mathbb{T}^n} f(x)\, (\nabla \cdot \varphi)(x)\, \mathrm{d}x = -\int_{\mathbb{T}^n} \varphi \cdot \,\mathrm{d}\nabla f \qquad \text{for all } \varphi \in C^\infty(\mathbb{T}^n, \mathbb{R}^n). \tag{2.25}$$

Also, with slight abuse of notation, we write

$$V[f] = \int_{\mathbb{T}^n} |\nabla f|, \qquad V_w[f] = \int_{\mathbb{T}^n} |\nabla_w f|. \tag{2.26}$$

We will now continue to establish several useful properties of the space BV when it comes to L^1–convergence.

Lemma 2.8 Let $f_k \in BV(\mathbb{T}^n)$ and $f \in L^1(\mathbb{T}^n)$ such that $f_k \to f$ in $L^1(\mathbb{T}^n)$. Then

$$V[f] \le \liminf_{k\to\infty} V[f_k], \qquad V_w[f] \le \liminf_{k\to\infty} V_w[f_k] \qquad \text{for all } w \in \mathbb{S}^{n-1}. \tag{2.27}$$

Proof: Let $w \in \mathbb{S}^{n-1}$ and $\varphi \in C^\infty(\mathbb{T}^n)$ with $\|\varphi\|_{L^\infty(\mathbb{T}^n)} \le 1$. Since

$$\liminf_{k\to\infty} \int_{\mathbb{T}^n} f_k(x)\, \nabla_w \varphi(x)\, \mathrm{d}x \le \liminf_{k\to\infty} V_w[f_k], \tag{2.28}$$

we obtain from $f_k \to f$ in $L^1(\mathbb{T}^n)$

$$\int_{\mathbb{T}^n} f(x)\, \nabla_w \varphi(x)\, \mathrm{d}x = \lim_{k\to\infty} \int_{\mathbb{T}^n} f_k(x)\, \nabla_w \varphi(x)\, \mathrm{d}x \le \liminf_{k\to\infty} V_w[f_k]. \tag{2.29}$$

An analogue argument works for the total variation. ■

Lemma 2.9 Let $f \in BV(\mathbb{T}^n)$. Then there exists a sequence $f_k \in C^\infty(\mathbb{T}^n)$, such that $f_k \to f$ in $L^1(\mathbb{T}^n)$ and

$$V[f_k] \xrightarrow{k\to\infty} V[f], \qquad V_w[f_k] \xrightarrow{k\to\infty} V_w[f], \qquad \text{for all } w \in \mathbb{S}^{n-1}. \tag{2.30}$$

Proof: Let $\eta_k \in C^\infty(\mathbb{T}^n)$ be the Dirac sequence as in Appendix A.1 and define $f_k := f * \eta_k$. Then $f_k \in C^\infty(\mathbb{T}^n)$ for all $k \in \mathbb{N}$ and $f_k \to f$ in $L^1(\mathbb{T}^n)$, so it remains to prove that

the variations converge. Let $w \in \mathbb{S}^{n-1}$ and $\varphi \in C^\infty(\mathbb{T}^n)$ such that $\|\varphi\|_{L^\infty(\mathbb{T}^n)} \leq 1$. We compute

$$\int_{\mathbb{T}^n} f_k(x)\, \nabla_w \varphi(x)\, \mathrm{d}x = \int_{\mathbb{T}^n} f(x)\, \nabla_w (\eta_k * \varphi)(x)\, \mathrm{d}x \leq V_w[f]. \tag{2.31}$$

Together with Lemma 2.8 we obtain

$$V_w[f] \leq \liminf_{k\to\infty} V_w[f_k] \leq \limsup_{k\to\infty} V_w[f_k] \leq V_w[f], \tag{2.32}$$

so convergence holds. An analogue argument works for the total variation. ■

The proof of Lemma 2.9 shows that convolution with a smooth Dirac sequence is compatible with the weak topology of $BV(\mathbb{T}^n)$. However, the space $C^\infty(\mathbb{T}^n)$ is not dense in the space $BV(\mathbb{T}^n)$ with respect to the norm

$$\|f\|_{BV(\mathbb{T}^n)} \coloneqq \|f\|_{L^1(\mathbb{T}^n)} + V[f] \qquad \text{for all } f \in BV(\mathbb{T}^n). \tag{2.33}$$

Indeed, using (2.19) we have $\|\varphi\|_{BV(\mathbb{T}^n)} = \|\varphi\|_{W^{1,1}(\mathbb{T}^n)}$ for all $\varphi \in C^\infty(\mathbb{T}^n)$ and by definition we know that $C^\infty(\mathbb{T}^n)$ is dense in $W^{1,1}(\mathbb{T}^n)$ with respect to $\|\cdot\|_{W^{1,1}(\mathbb{T}^n)}$ (see also e.g. [Heb99, Theorem 2.4]). However $\chi_{B_r(0)} \in BV(\mathbb{T}^n) \setminus W^{1,1}(\mathbb{T}^n)$ and thus cannot be approximated strongly by smooth functions.

Using the compact embedding for Sobolev spaces $W^{1,1}(\mathbb{T}^n) \longrightarrow L^1(\mathbb{T}^n)$ we obtain the following compactness result:

Theorem 2.10 Let $f_k \in BV(\mathbb{T}^n)$ such that $\sup_k \|f_k\|_{L^1(\mathbb{T}^n)} + V[f_k] < \infty$. Then there exists $f \in BV(\mathbb{T}^n)$ and a subsequence (not relabeled) such that $f_k \to f$ in $L^1(\mathbb{T}^n)$.

Proof: Using Lemma 2.9 we find $g_k \in C^\infty(\mathbb{T}^n)$ such that

$$\|f_k - g_k\|_{L^1(\mathbb{T}^n)} + |V[f_k] - V[g_k]| < \frac{1}{k} \qquad \text{for all } k \in \mathbb{N}. \tag{2.34}$$

Together with (2.19) we thus obtain $\sup_k \|g_k\|_{W^{1,1}(\mathbb{T}^n)} < \infty$. Using the Theorem of Rellich-Kondrachov (see Theorem A.3) we find $f \in L^1(\mathbb{T}^n)$ such that after a selection of a subsequence (not relabeled) we have $g_k \to f$ in $L^1(\mathbb{T}^n)$. Using (2.34) we obtain $f_k \to f$ in $L^1(\mathbb{T}^n)$. Furthermore, using Lemma 2.8 we find

$$V[f] \leq \liminf_{k\to\infty} V[f_k] < \infty \tag{2.35}$$

by assumption, showing that $f \in BV(\mathbb{T}^n)$. ■

The following proposition was taken from [Gal11] and adapted to the geometry of the torus:

Proposition 2.11 Let $0 < r < \frac{1}{2}$, $w \in \mathbb{S}^{n-1}$ and $f \in L^1(\mathbb{T}^n)$. Then

$$\frac{1}{r}\int_{\mathbb{T}^n} |f(x+rw) - f(x)|\,\mathrm{d}x \leq V_w[f], \qquad \lim_{r\to 0}\frac{1}{r}\int_{\mathbb{T}^n} |f(x+rw) - f(x)|\,\mathrm{d}x = V_w[f]. \tag{2.36}$$

As a reminder, we use the notation $rw \coloneqq \exp_0(rw)$, where $\exp_0 \colon \mathfrak{g} \longrightarrow \mathbb{T}^n$ is the exponential map at the identity. A more precise notation would be $x + rw = \exp_x(rw)$, where we used that $\mathbb{T}^n$ is a an Abelian group. We chose to keep the notation as in e.g. [KS23].

Proof: We will first consider $f \in C^\infty(\mathbb{T}^n)$. We use Hadamard's lemma to compute

$$|f(x+rw) - f(x)| \leq r\int_0^1 |\nabla_w f(x+trw)|\,\mathrm{d}t. \tag{2.37}$$

Integrating with respect to x yields after an application of Tonelli's theorem

$$\frac{1}{r}\int_{\mathbb{T}^n} |f(x+rw) - f(x)|\,\mathrm{d}x \leq \int_0^1\int_{\mathbb{T}^n} |\nabla f(x+trw)\cdot w|\,\mathrm{d}x\,\mathrm{d}t \overset{(2.13)}{=} V_w[f]. \tag{2.38}$$

By density, this inequality is valid for all $f \in L^1(\mathbb{T}^n)$, which establishes the first statement.

Let us now turn our attention to the second statement: let $\eta_k \in C^\infty(\mathbb{T}^n)$ be a Dirac sequence (see Lemma A.1) and define $f_k \coloneqq f * \eta_k$. We use Fatou's lemma and Young's convolution inequality to deduce

$$V_w[f_k] = \int_{\mathbb{T}^n} |\nabla_w f_k(x)|\,\mathrm{d}x \leq \liminf_{r\to 0}\int_{\mathbb{T}^n} \frac{|f_k(x+rw) - f_k(x)|}{r}\,\mathrm{d}x \tag{2.39}$$

$$\leq \liminf_{r\to\infty}\int_{\mathbb{T}^n} \frac{|f(x+rw) - f(x)|}{r}\,\mathrm{d}x. \tag{2.40}$$

Using the lower semicontinuity of V_w with respect to the L^1–convergence (see Lemma 2.8) we obtain

$$V_w[f] \leq \liminf_{k\to\infty} V_w[f_k] \leq \liminf_{r\to\infty}\int_{\mathbb{T}^n} \frac{|f(x+rw) - f(x)|}{r}\,\mathrm{d}x, \tag{2.41}$$

which shows the claim. ■

Corollary 2.12 Let $f \in BV(\mathbb{T}^n)$. Then

$$V[f] = \frac{1}{2\omega_{n-1}}\int_{\mathbb{S}^{n-1}} V_w[f]\,\mathrm{d}\mathscr{H}^{n-1}(w). \tag{2.42}$$

Proof: Let us first consider $f \in C^\infty(\mathbb{T}^n)$. Then we compute

$$\int_{\mathbb{S}^{n-1}} V_w[f] \,\mathrm{d}\mathscr{H}^{n-1}(w) = \int_{\mathbb{T}^n} |\nabla f(x)| \int_{\mathbb{S}^{n-1}} \Big| \frac{\nabla f(x)}{|\nabla f(x)|} \cdot w \Big| \,\mathrm{d}\mathscr{H}^{n-1}(w) \,\mathrm{d}x \tag{2.43}$$

$$\overset{\text{A.10}}{=} 2\omega_{n-1} \int_{\mathbb{T}^n} |\nabla f(x)| \,\mathrm{d}x \overset{(2.19)}{=} 2\omega_{n-1} V[f]. \tag{2.44}$$

The statement then follows by density of smooth functions (see Lemma 2.9). ■

Functions of bounded variation in general have very low regularity as the notion of derivative is very weak. However, it is still strong enough to allow for the following version of the Coarea formula:

Theorem 2.13 Let $f \in BV(\mathbb{T}^n)$ and define $E_t \coloneqq \{x \in \mathbb{T}^n : f(x) > t\}$ for all $t \in \mathbb{R}$. Then

$$V[f] = \int_{\mathbb{R}} \mathrm{Per}(E_t) \,\mathrm{d}t, \tag{2.45}$$

where $\mathrm{Per}(E_t) \coloneqq V[\chi_{E_t}]$.

Proof: We separate the proof in multiple steps. We will first show that the integrand is measurable and proceed by showing the statement for smooth functions. The general result will be dealt with via density. We denote $D \coloneqq \{\varphi \in C^\infty(\mathbb{T}^n, \mathbb{R}^n) : \|\varphi\|_{L^\infty(\mathbb{T}^n,\mathbb{R}^n)} \leq 1\}$.

Step 1: The Integrand is measurable. The set E_t is measurable since f is measurable. Thus, the function $(x,t) \longmapsto \chi_{E_t}(x)$ is measurable in $\mathbb{T}^n \times \mathbb{R}$. Let $\varphi \in D$. Then $(x,t) \longmapsto \chi_{E_t}(x)(\nabla \cdot \varphi)(x)$ is measurable in $\mathbb{T}^n \times \mathbb{R}$ and hence

$$t \longmapsto \int_{\mathbb{T}^n} \chi_{E_t}(x)(\nabla \cdot \varphi)(x) \,\mathrm{d}x \tag{2.46}$$

is an $\mathbb{R}$ measurable function by Fubinis Theorem. As $C^\infty(\mathbb{T}^n, \mathbb{R}^n)$ is separable (see [RF10, Section 12.3]), we find an at most countable and dense set $D' \subset D$ with respect to uniform convergence. We obtain that

$$t \longmapsto \mathrm{Per}(E_t) = \sup_{\varphi \in D'} \int_{\mathbb{T}^n} \chi_{E_t}(x)(\nabla \cdot \varphi)(x) \,\mathrm{d}x \tag{2.47}$$

is the supremum of at most countably many $\mathbb{R}$ measurable functions. Hence $t \longmapsto \mathrm{Per}(E_t)$ is an $\mathbb{R}$ measurable function.

Step 2: Upper bound in (2.45). We note that

$$\int_{\mathbb{R}} \mathrm{Per}(E_t) \,\mathrm{d}t = \int_{\mathbb{R}} \sup_{\varphi \in D} \left\{ \int_{E_t} (\nabla \cdot \varphi)(x) \,\mathrm{d}x \right\} \mathrm{d}t \geq \sup_{\varphi \in D} \left\{ \int_{\mathbb{R}} \int_{E_t} (\nabla \cdot \varphi)(x) \,\mathrm{d}x \,\mathrm{d}t \right\} \tag{2.48}$$

On the other hand, by definition we have

$$V[f] = \sup_{\varphi \in D} \int_{\mathbb{T}^n} f(x)(\nabla \cdot \varphi)(x)\,\mathrm{d}x. \tag{2.49}$$

Thus, comparing the preceding lines we aim to show that

$$\int_{\mathbb{T}^n} f(x)(\nabla \cdot \varphi)(x)\,\mathrm{d}x = \int_{\mathbb{R}} \int_{E_t} (\nabla \cdot \varphi)(x)\,\mathrm{d}x\,\mathrm{d}t \qquad \text{for all } \varphi \in D. \tag{2.50}$$

Notice that due to Stokes Theorem

$$\int_{\mathbb{T}^n} (\nabla \cdot \varphi)(x)\,\mathrm{d}x = 0 \qquad \text{for all } \varphi \in D. \tag{2.51}$$

We observe that

$$\chi_{E_t}(x) = \begin{cases} 1 \text{ for all } t < f(x), \\ 0 \text{ for all } t \geq f(x), \end{cases} \qquad \chi_{E_t}(x) - 1 = \begin{cases} 0 \quad \text{for all } t < f(x), \\ -1 \text{ for all } t \geq f(x). \end{cases} \tag{2.52}$$

and thus obtain for $x \in \mathbb{T}^n$

$$f(x) = \begin{cases} \displaystyle\int_0^{f(x)} \mathrm{d}t = \int_0^{\infty} \chi_{E_t}(x)\,\mathrm{d}t & \text{if } f(x) > 0, \\ \displaystyle -\int_{f(x)}^0 \mathrm{d}t = \int_{-\infty}^0 \chi_{E_t}(x) - 1\,\mathrm{d}t & \text{if } f(x) \leq 0. \end{cases} \tag{2.53}$$

We now compute for an arbitrary $\varphi \in D$ with Fubini's Theorem

$$\begin{aligned} \int_{\mathbb{R}} \int_{\mathbb{T}^n} \chi_{E_t}(x)(\nabla \cdot \varphi)(x)\,\mathrm{d}x\,\mathrm{d}t &= \int_0^{\infty} \int_{\mathbb{T}^n} \chi_{E_t}(x)(\nabla \cdot \varphi)(x)\,\mathrm{d}x\,\mathrm{d}t && (2.54) \\ &\quad + \int_{-\infty}^0 \int_{\mathbb{T}^n} \chi_{E_t}(x)(\nabla \cdot \varphi)(x) - (\nabla \cdot \varphi)(x)\,\mathrm{d}x\,\mathrm{d}t && (2.55) \\ &= \int_{\mathbb{T}^n} (\nabla \cdot \varphi)(x) \int_0^{\infty} \chi_{E_t}(x)\,\mathrm{d}t\,\mathrm{d}x && (2.56) \\ &\quad + \int_{\mathbb{T}^n} (\nabla \cdot \varphi)(x) \int_{-\infty}^0 \chi_{E_t}(x) - 1\,\mathrm{d}t\,\mathrm{d}x && (2.57) \\ &= \int_{\mathbb{T}^n} (\nabla \cdot \varphi)(x)\, f(x)\,\mathrm{d}x, && (2.58) \end{aligned}$$

which was the claim.

Step 3: The statement for smooth functions. Due to step 2 it remains to show the reversed

inequality. Let $f \in BV(\mathbb{T}^n) \cap C^\infty(\mathbb{T}^n)$. We define $m\colon \mathbb{R} \longrightarrow \mathbb{R}$ via

$$m(t) \coloneqq \int_{\mathbb{T}^n} (1 - \chi_{E_t}) |\nabla f(x)| \,\mathrm{d}x \qquad \text{for all } t \in \mathbb{R}. \tag{2.59}$$

By definition m is a non-decreasing function and thus is differentiable almost everywhere. Furthermore $0 \leq m \leq V[f]$. By monotone convergence we obtain

$$V[f] = \lim_{t\to\infty} m(t) = \lim_{t\to\infty} m(t) - m(-t) = \int_{\mathbb{R}} m'(t) \,\mathrm{d}t. \tag{2.60}$$

Our goal is to show that $\mathrm{Per}(E_t) \leq m'(t)$ for almost every $t \in \mathbb{R}$. To do so, let $t \in \mathbb{R}$ such that m is differentiable in t. Let $h > 0$ and define the cut-off function $\eta\colon \mathbb{R} \longrightarrow \mathbb{R}$ via

$$\eta(s) = \begin{cases} 0 & \text{for all } s < t, \\ \frac{s-t}{h} & \text{for all } t < s < t + h, \\ 1 & \text{for all } s > t + h. \end{cases} \qquad \text{for all } s \in \mathbb{R}. \tag{2.61}$$

Then η is Lipschitz continuous and $\eta' = \frac{1}{h}\chi_{(t,t+h)}$. We obtain for any $\varphi \in D$ via the chain rule

$$\begin{aligned} -\int_{\mathbb{T}^n} \eta(f(x)) \,(\nabla \cdot \varphi)(x) \,\mathrm{d}x &= \int_{\mathbb{T}^n} \eta'(f(x)) \,\nabla f(x) \cdot \varphi(x) \,\mathrm{d}x && (2.62) \\ &= \frac{1}{h} \int_{E_t \setminus E_{t+h}} \nabla f(x) \cdot \varphi(x) \,\mathrm{d}x && (2.63) \\ &\leq \frac{1}{h} \int_{E_t \setminus E_{t+h}} |\nabla f(x)| \,\mathrm{d}x && (2.64) \\ &\leq \frac{m(t+h) - m(t)}{h}. && (2.65) \end{aligned}$$

Taking the limit $h \to 0$ we obtain

$$-\int_{E_t} (\nabla \cdot \varphi)(x) \,\mathrm{d}x \leq m'(t) \tag{2.66}$$

and thus $\mathrm{Per}(E_t) \leq m'(t)$.

Step 4: Conclusion. We choose $f_k \in BV(\mathbb{T}^n) \cap C^\infty(\mathbb{T}^n)$ such that $f_k \to f$ in $L^1(\mathbb{T}^n)$ and $V[f_k] \to V[f]$ as $k \to \infty$ (see Lemma 2.9). We define $E_t^k \coloneqq \{x \in \mathbb{T}^n : f_k(x) > t\}$. Using Step 3 we obtain with Fatou's Lemma

$$V[f] = \lim_{k\to\infty} V[f_k] \geq \liminf_{k\to\infty} \int_{\mathbb{R}} \mathrm{Per}(E_t^k) \,\mathrm{d}t \geq \int_{\mathbb{R}} \liminf_{k\to\infty} \mathrm{Per}(E_t^k) \,\mathrm{d}t. \tag{2.67}$$

Thus, we aim to show $\liminf_{k\to\infty} \mathrm{Per}(E_t^k) \geq \mathrm{Per}(E_t)$ for almost all $t \in \mathbb{R}$. We observe

that with Tonelli's Theorem

$$\int_{\mathbb{R}} \int_{\mathbb{T}^n} |\chi_{E_t^k}(x) - \chi_{E_t}(x)| \, \mathrm{d}x \, \mathrm{d}t = \int_{\mathbb{T}^n} \int_{\mathbb{R}} |\chi_{E_t^k}(x) - \chi_{E_t}(x)| \, \mathrm{d}t \, \mathrm{d}x \tag{2.68}$$

$$= \int_{\mathbb{T}^n} |f_k(x) - f(x)| \, \mathrm{d}x \xrightarrow{k\to\infty} 0. \tag{2.69}$$

Thus $\chi_{E_t^k} \to \chi_{E_t}$ in $L^1(\mathbb{T}^n)$ for almost every $t \in \mathbb{R}$. The claim now follows from the lower-semicontinuity of the Perimeter Functional (see Lemma 2.8). ■

2.2.1. Sets of Finite Perimeter

In the analysis concerning the Autocorrelation Function in Chapter 4 we need to work with sets $\Omega \subset \mathbb{T}^n$ rather than functions $f \in BV(\mathbb{T}^n)$. In particular, in order to avoid strong oscillations at the boundary, we introduce a class which we will work with later when it comes to higher regularity of the Autocorrelation Function.

Definition 2.14 Let $\Omega \subset \mathbb{T}^n$. We call Ω a **set of finite perimeter**, if $\chi_\Omega \in BV(\mathbb{T}^n)$. We define the set

$$BV_n \coloneqq \{\Omega \subset \mathbb{T}^n : \chi_\Omega \in BV(\mathbb{T}^n)\}. \tag{2.70}$$

If $\Omega \in BV_n$, we define $\mathrm{Per}(\Omega) \coloneqq V[\chi_\Omega]$.

Using Gauß' Theorem, one can show that every set $\Omega \subset \mathbb{R}^n$ with smooth boundary is an element of BV_n and in addition

$$\mathrm{Per}(\Omega) = \mathscr{H}^{n-1}(\partial\Omega), \tag{2.71}$$

where $\mathscr{H}^{n-1}$ is the $n-1$ dimensional Hausdorff measure (constructed similarly to the Euclidean version). However, there exist open sets $U \in BV_n$ such that $\mathscr{H}^{n-1}(U) = +\infty$. The following lemma shows that sets with smooth boundary can approximate sets in BV_n.

Lemma 2.15 Let $\Omega \in BV_n$. Then there exist $\Omega_k \in BV_n$ such that:

a) Ω_k is open for all $k \in \mathbb{N}$.

b) $|\Omega_k| = |\Omega|$ for all $k \in \mathbb{N}$.

c) $\partial\Omega_k$ is smooth for all $k \in \mathbb{N}$.

d) $|\Omega_k \triangle \Omega| \xrightarrow{k\to\infty} 0$.

e) $\mathrm{Per}(\Omega_k) \xrightarrow{k\to\infty} \mathrm{Per}(\Omega)$.

Proof: We adapt the proof [Leo13, Lemma 1.15] to the geometry of the Torus.

Step 1: Generating appropriate smooth sets. Let $\varphi_k \in C^\infty(\mathbb{T}^n)$ be a Dirac sequence (see Lemma A.1) and define $w_k \coloneqq \chi_\Omega * \varphi_k$. Then $w_k \in C^\infty(\mathbb{T}^n)$, $0 \leq w_k \leq 1$, $w_k \to w$ in $L^1(\mathbb{T}^n)$ and $\|\nabla w_k\|_{L^1(\mathbb{T}^n,\mathbb{R}^n)} \to \mathrm{Per}(\Omega)$.

Let $0 < t < 1$ and fix $k \in \mathbb{N}$. We define the sets $\Omega_{k,t} \coloneqq \{x \in \mathbb{T}^n : w_k(x) > t\}$. Then $\Omega_{k,t}$ is open by the regularity of w_k, and using Sard's Theorem (see Theorem A.8) we obtain that $\partial\Omega_{k,t}$ is smooth for almost all $0 < t < 1$. We note that $\{\partial\Omega_{k,t}\}_t$ is pairwise disjoint and by definition

$$\begin{aligned}\|w_k - \chi_\Omega\|_{L^1(\mathbb{T}^n)} &\geq \int_{\Omega_{k,t}\setminus\Omega} |w_k(x) - \chi_\Omega(x)|\,\mathrm{d}x + \int_{\Omega\setminus\Omega_{k,t}} |w_k(x) - \chi_\Omega(x)|\,\mathrm{d}x && (2.72)\\ &= \int_{\Omega_{k,t}\setminus\Omega} w_k(x)\,\mathrm{d}x + \int_{\Omega\setminus\Omega_{k,t}} |w_k(x) - 1|\,\mathrm{d}x && (2.73)\\ &\geq t|\Omega_{k,t}\setminus\Omega| + (1-t)|\Omega\setminus\Omega_{k,t}|. && (2.74)\end{aligned}$$

Thus $|\Omega \triangle \Omega_{k,t}| \to 0$ as $k \to \infty$ for every $0 < t < 1$.

To obtain convergence of the perimeter, we first use the Coarea Formula (see Theorem 2.13) and then Fatou's Lemma to obtain

$$\mathrm{Per}(\Omega) = \lim_{k\to\infty} V[w_k] = \lim_{k\to\infty} \int_{\mathbb{R}} \mathrm{Per}(\Omega_{k,t})\,\mathrm{d}t \geq \int_0^1 \liminf_{k\to\infty} \mathrm{Per}(\Omega_{k,t})\,\mathrm{d}t. \tag{2.75}$$

However, due to the lower semicontinuity of the Perimeter Functional (see Lemma 2.8) we obtain

$$0 \leq \int_0^1 \liminf_{k\to\infty} \mathrm{Per}(\Omega_{k,t}) - \mathrm{Per}(\Omega)\,\mathrm{d}t \leq 0, \tag{2.76}$$

and thus $\liminf_{k\to\infty} \mathrm{Per}(\Omega_{k,t}) = \mathrm{Per}(\Omega)$ for almost all $t \in (0,1)$. Choosing suitable $k \in \mathbb{N}$ and $0 < t < 1$, we obtained a sequence $\Omega_k \in BV_n$ such that assertions a), c) and d) and e) hold. It remains to modify this sequence to ensure assertion b).

Step 2: Correcting mass deficit. Using Lemma A.7 we find $x, x' \in \partial\Omega$ such that

$$\lim_{r\to 0} \frac{|\Omega \cap B_r(x)|}{|B_r(x)|} = \lim_{r\to 0} \frac{|\Omega \cap B_r(x')|}{|B_r(x')|} = \frac{1}{2}. \tag{2.77}$$

For $i \in \mathbb{N}$ we now define

$$D_i \coloneqq (\Omega \cup B_{\frac{1}{i}}(x)) \setminus B_{\frac{1}{i}}(x') \subset \mathbb{T}^n. \tag{2.78}$$

Then $|D_i \triangle \Omega| \xrightarrow{i\to\infty} 0$ and

$$\mathrm{Per}(D_i) \leq \mathrm{Per}(\Omega) + \mathrm{Per}(B_{\frac{1}{i}}(x)) + \mathrm{Per}(B_{\frac{1}{i}}(x')) \xrightarrow{k\to\infty} \mathrm{Per}(\Omega). \tag{2.79}$$

From the lower semicontinuity of the Perimeter Functional (see Lemma 2.8) we therefore obtain $\mathrm{Per}(D_i) \xrightarrow{i\to\infty} \mathrm{Per}(\Omega)$. As in Step 1 we now construct $D_{i,j} \in BV_n$ such that $D_{i,j} \in BV_n$ is open for all $i, j \in \mathbb{N}$, $\partial D_{i,j}$ is smooth for all $i, j \in \mathbb{N}$ and

$$|D_i \triangle D_{i,j}| \xrightarrow{j\to\infty} 0, \qquad \mathrm{Per}(D_{i,j}) \xrightarrow{j\to\infty} \mathrm{Per}(D_i) \qquad \text{for all } i \in \mathbb{N}. \tag{2.80}$$

If $|D_{i,j}| = |\Omega|$, then we are done. If not, then we have two cases to consider:

- Assume $|D_{i,j}| > |\Omega|$. By our choice of x we know that there exists $i^* \in \mathbb{N}$ such that

$$|E \cap B_{\frac{1}{i}}(x)| > \frac{1}{4}|B_{\frac{1}{i}}(x)| \qquad \text{for all } i \geq i^*. \tag{2.81}$$

  We also observe that by construction from Step 1 (as mollification changes the support slightly, see Lemma A.2) that there exists $j^*(i) \in \mathbb{N}$ such that

$$B_{(\frac{4}{5})^{\frac{1}{n}}\frac{1}{i}}(x) \subset D_{i,j} \qquad \text{for all } j \geq j^*. \tag{2.82}$$

  We define

$$E_{i,j} \coloneqq D_{i,j} \setminus B_{r_{i,j}}(x), \tag{2.83}$$

  where $r_{i,j} > 0$ is chosen such that $|B_{r_{i,j}}(x)| = |D_{i,j}| - |\Omega| > 0$. We observe that $|E_{i,j}| = |\Omega|$ and we aim to show that $r_{i,j} \leq (\frac{4}{5})^{\frac{1}{n}}\frac{1}{i}$ for i, j sufficiently large, since in that case $E_{i,j}$ has a smooth boundary. Indeed, for $i > i^*$ we estimate.

$$\begin{aligned} |D_i| &= |\Omega| + |B_{\frac{1}{i}}(x) \setminus \Omega| - |\Omega \cap B_{\frac{1}{i}}(x')| && (2.84)\\ &= |\Omega| + |B_{\frac{1}{i}}(x)| - |\Omega \cap B_{\frac{1}{i}}(x)| - |\Omega \cap B_{\frac{1}{i}}(x')| && (2.85)\\ &\overset{(2.81)}{<} |\Omega| + |B_{\frac{1}{i}}(x)| - \frac{1}{4}|B_{\frac{1}{i}}(x)| = |\Omega| + \frac{3}{4}|B_{\frac{1}{i}}(x)|. && (2.86) \end{aligned}$$

  Now, for $0 < \delta < \frac{4}{5} - \frac{3}{4}$, using (2.80), there exists $\bar{j}^*(i) \in \mathbb{N}$ such that

$$\big||D_{i,j}| - |D_i|\big| < \delta|B_{\frac{1}{i}}(x)| \qquad \text{for all } j > \bar{j}^*. \tag{2.87}$$

  And therefore

$$\big||D_{i,j}| - |\Omega|\big| \leq \big||D_{i,j}| - |D_i|\big| + \big||D_i| - |\Omega|\big| < (\delta + \tfrac{3}{4})|B_{\frac{1}{i}}(x)| < \frac{4}{5}|B_{\frac{1}{i}}(x)|, \tag{2.88}$$

  which in turn implies the desired bound $r_{i,j} \leq (\frac{4}{5})^{\frac{1}{n}}\frac{1}{i}$ for $i > i^*$ and $j > \max\{j^*, \bar{j}^*\}$.

- Assume $|D_{i,j}| < |\Omega|$. By our choice of x' we know that there exists $i_* \in \mathbb{N}$ such that

$$|E \cap B_{\frac{1}{i}}(x')| < \frac{3}{4}|B_{\frac{1}{i}}(x')| \qquad \text{for all } i > i_* - 1. \tag{2.89}$$

Analogous to the previous case, we find $j_*, \bar{j}_* \in \mathbb{N}$ such that

$$F_{i,j} \coloneqq D_{i,j} \cup B_{r_{i,j}}(x') \tag{2.90}$$

is correcting the mass deficit similarly to $E_{i,j}$ in the previous item for $i > i_*$ and $j > \max\{j_*, \bar{j}_*\}$.

Step 3: Conclusion. We are now in the position to select a sequence $\Omega_k \in BV_n$ with the desired properties. Let $k \in \mathbb{N}$. We define

$$i_k \coloneqq 1 + \max\{i_*, i^*, k\}, \qquad j_k \coloneqq 1 + \max\{j_*(i_k), j^*(i_k), \bar{j}_*(i_k), \bar{j}^*(i_k), k\}, \tag{2.91}$$

and

$$\Omega_k \coloneqq \begin{cases} D_{i_k,j_k} & \text{if } |D_{i_k,j_k}| = |\Omega|, \\ E_{i_k,j_k} & \text{if } |D_{i_k,j_k}| > |\Omega|, \\ F_{i_k,j_k} & \text{if } |D_{i_k,j_k}| < |\Omega|. \end{cases} \tag{2.92}$$

Then $\{\Omega_k\}_k$ satisfies all the assertions a) – e). ■

The second step of the proof of Lemma 2.15 provides an algorithm how to adjust approximating sets such that the masses are the same. Analogously, we find that polytopes are dense in BV_n similar to sets with smooth boundaries.

Lemma 2.16 Let $\Omega \in BV_n$. Then there exist $\Omega_k \in BV_n$ such that:

a) Ω_k is open for all $k \in \mathbb{N}$.

b) $|\Omega_k| = |\Omega|$ for all $k \in \mathbb{N}$.

c) Ω_k is a polytope for all $k \in \mathbb{N}$.

d) $|\Omega_k \triangle \Omega| \xrightarrow{k\to\infty} 0$.

e) $\mathrm{Per}(\Omega_k) \xrightarrow{k\to\infty} \mathrm{Per}(\Omega)$.

As a reminder, a set $P \subset \mathbb{T}^n$ is a polytope, if the canonical projection to the primitive cell is a polytope in $\mathbb{R}^n$. An equivalent characterisation is as superlevel sets of continuous piecewise affine functions, as every polytope in $\mathbb{R}^n$ is given by the superlevel set of an affine function.

Proof: We use the notation from the proof of Lemma 2.15 except for the definition of $\Omega_{k,t}$. Instead, using Lemma A.4, we find a piecewise affine linear function $v_k \in C^0(\mathbb{T}^n)$ such that

$$\|v_k - w_k\|_{W^{1,1}(\mathbb{T}^n)} < \frac{1}{k} \qquad \text{for all } k \in \mathbb{N}. \tag{2.93}$$

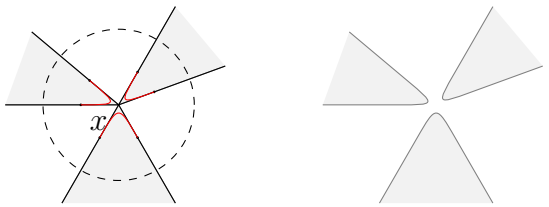

Figure 2.1.: Smoothing process used in the proof of Lemma 2.18

.

We define $\Omega_{k,t} \coloneqq \{x \in \mathbb{T}^n : v_k(x) > t\}$. Then $\Omega_{k,t}$ is a polytopal domain and the remaining assertions follow analogously to the proof of Lemma 2.15. ■

Even though sets with smooth boundary are a dense class of sets in BV_n, the boundaries are still allowed to have high oscillations. This effect might be problematic later in the analysis concerning the Autocorrelation Function (see Section 4.3). Thus, we will introduce a class of sets which do not have high oscillations in the boundary.

Definition 2.17 We define

$$BV_n^\infty \coloneqq \left\{\Omega \in BV_n : \begin{smallmatrix}\Omega \text{ is open, } \partial\Omega \text{ is smooth, and } \nu^{-1}(\{w\}) \text{ has finitely} \\ \text{many connected components for all } w \in \mathbb{S}^{n-1}\end{smallmatrix}\right\}. \tag{2.94}$$

In this thesis, we will primarily work with the space BV_2^∞ as it is only involved in the computations concerning the Autocorrelation Function in two space dimensions (see Section 4.3). The conditions defining the space BV_2^∞ ensure that the boundary does not have high oscillations. It also allows us to reduce computations of the Autocorrelation Function of the corresponding set through local graph representations (see Lemma 4.10). A useful property of the space BV_2^∞ is its density in BV_2.

Lemma 2.18 Let $\Omega \in BV_2$. Then for every $\varepsilon > 0$ there exists $\Omega_\varepsilon \in BV_2^\infty$, such that

$$|\Omega_\varepsilon| = |\Omega|, \qquad |\Omega_\varepsilon \triangle \Omega| + |V[\chi_\Omega] - [\chi_{\Omega_\varepsilon}]| < \varepsilon. \tag{2.95}$$

Proof: Using Lemma 2.16, it suffices to show that every polytope $\Omega \subset \mathbb{T}^2$ can be approximated as in (2.95). We construct a set in $\Omega_\varepsilon \in BV_2^\infty$ with the desired properties. We note that Ω has a smooth boundary except in its finitely many vertices. Without loss of generality we can also assume that Ω is connected, else repeat the below argument son each connected component of Ω.

Step 1: Smoothing of vertex. Let $m > 0$ and define $f\colon \mathbb{R} \longrightarrow \mathbb{R}$ via $f(x) \coloneqq m|x|$ for all $x \in \mathbb{R}$. We choose $\varphi \in C_c^\infty(\mathbb{R})$ such that $\operatorname{supp}(\varphi) = [-\frac{1}{2}, \frac{1}{2}]$, $\varphi \geq 0$, $\|\varphi\|_{L^1(\mathbb{R})} = 1$ and

$\varphi(y) = \varphi(-y)$ for all $y \in \mathbb{R}$. In addition, we define $\varphi_\varepsilon(y) \coloneqq \frac{1}{\varepsilon}\varphi(\frac{y}{\varepsilon})$ for all $y \in \mathbb{R}$ and the convolution

$$f_\varepsilon(x) \coloneqq m \int_{\mathbb{R}} |x-y|\, \varphi_\varepsilon(y)\, \mathrm{d}y \qquad \text{for all } x \in \mathbb{R}. \tag{2.96}$$

Then $f_\varepsilon \in C^\infty(\mathbb{R})$, $f_\varepsilon(x) = f(x)$ for all $|x| \geq \frac{\varepsilon}{2}$ and f_ε is strictly convex. Moreover, we compute

$$\|f' - f_\varepsilon'\|_{L^1(\mathbb{R})} = 2\int_0^{\frac{\varepsilon}{2}} \left| 1 - \int_{-\frac{\varepsilon}{2}}^{x} \varphi_\varepsilon(y)\,\mathrm{d}y + \int_x^{\frac{\varepsilon}{2}} \varphi_\varepsilon(y)\,\mathrm{d}y \right| \mathrm{d}x \tag{2.97}$$

$$\leq \varepsilon + 2\int_0^{\frac{\varepsilon}{2}} \int_0^y \varphi_\varepsilon(y)\,\mathrm{d}x\,\mathrm{d}y \lesssim \varepsilon, \tag{2.98}$$

where we used Fubini's Theorem in the last line. Thus $\|f - f_\varepsilon\|_{W^{1,1}(\mathbb{R})} \xrightarrow{\varepsilon \searrow 0} 0$.

Step 2: Construction of Ω_ε. We will use the function f_ε from Step 1 to smooth vertices. Let $\mathcal{V}$ be the finite set of vertices of Ω. Let $x \in \mathcal{V}$ be a vertex and let $\delta > 0$ be sufficiently small. Since the set Ω is assumed to be connected, the set $\Omega \cap B_\delta(x)$ can be represented by the epigraph of the function $f(x) = m|x|$. Then we define $\tilde{\Omega}_\varepsilon \coloneqq \Omega$ outside $\cup_{x\in\mathcal{V}} \Omega \cap B_\delta(x)$ and $\tilde{\Omega}_\varepsilon \cap B_\delta(x)$ as the epigraph of f_ε from Step 1 (pulled back accordingly) for $\varepsilon > 0$ sufficiently small. Due to the convergence $f_\varepsilon \to f$ in $W^{1,1}$ we have

$$\big||\Omega| - |\tilde{\Omega}_\varepsilon|\big| + |\operatorname{Per}(\Omega) - \operatorname{Per}(\tilde{\Omega}_\varepsilon)| \lesssim \varepsilon. \tag{2.99}$$

Since $\tilde{\Omega}_\varepsilon^c$ has non-empty interior, we can find a ball $B_\varepsilon \subset \tilde{\Omega}_\varepsilon^c$ such that for ε sufficiently small $|B_\varepsilon| = \big||\Omega| - |\tilde{\Omega}_\varepsilon|\big|$. The set $\Omega_\varepsilon \coloneqq \tilde{\Omega}_\varepsilon \cup B_\varepsilon$ now satisfies the desired assertions. ■

3. Biological Model

In this chapter, we will take a closer look at mechanochemical models describing pattern formation in biological membranes. We will compare certain diffuse and sharp interface variants, the physical and mathematical model assumptions and in which way these models are related or approximated. In order to do so, we make the following defintion.

Definition 3.1 Let $F\colon L^1(\mathbb{T}^n) \longrightarrow \mathbb{R} \cup \{+\infty\}$. We define the **domain** of F via

$$\mathrm{dom}(F) \coloneqq \{u \in L^1(\mathbb{T}^n) : F[u] < \infty\}. \tag{3.1}$$

We call F a **Diffuse Interface Model** if $\mathrm{dom}(F) \subset W^{1,2}(\mathbb{T}^n)$. We call F a **Sharp Interface Model** if $\mathrm{dom}(F) \subset BV(\mathbb{T}^n, \{0,1\})$. If F is a sharp interface model, we write $F(\Omega) \coloneqq F[\chi_\Omega]$ for all $\Omega \in BV_n$.

As is already indicated in the notations section, sharp interface models are typically functionals acting on sets rather than functions.

This chapter is organised as follows. In Section 3.1 we will discuss the biological setup and the relevant concepts of the situations we aim to model. In Section 3.2 we describe what we mean by a mechanochemical model by exploring chemical and mechanical energies and combining them suitably. In Section 3.3 we will compare diffuse and sharp interface models qualitatively and quantitatively.

3.1. Biological Setup

We are interested in finding fine scale patterns in biological systems, specifically the formation of so called *lipid rafts* in membranes of vesicles or cells. These are complex nanostructures made up of certain lipids, proteins and cholesterol and are believed to be responsible for many biological phenomena such as transmembrane signaling and cellular homeostasis (see e.g. [SI97, LL15, RS05, SP13]).

Lipids (or more precisely phospholipids) are organic molecules that are insoluble in water, but soluble in polar fluids. Most types are amphipathic, meaning that one spatial end of the molecule is hydrophilic, the other hydrophobic. More precisely, they consist of a polar

head group and two hydrophobic tails usually made up of fatty acids. Due to their shape and amphipatic nature, lipids spontaneously group together and form closed structures like micelles and lipid bilayers in aqueous environments (see [AJL+02]).

On the one hand, having formed a closed structure, lipid bilayers act as a barrier from the inside to the outside as it is impermeable to most hydrophilic molecules. On the other hand, single lipid molecules can move freely around within the bilayer. Being only nanometres thick, this property makes them behave like 2D fluids and gives certain lipids (like e.g. sphingolipids) the possibility to group together due to attractive forces (like e.g. the van der Waals forces) holding them together to form domains, called raft domains. They can be thought of as transient phase separation in the fluid bilayer, where sphingolipids are more concentrated. Another mechanism to form raft domains comes from a mutual effect of the proteins imbedded in the membrane and the bending of the membrane, i.e. both the simultaneous influence of mechanical and chemical interactions (see [PYG06, HZ01]).

Experiments show that these domains form fine scale patterns. In [RKG05], a vesicle adhered to a solid substrate with a lipid bilayer membrane composed of sphingomyelin, cholesterol and dioleoylphosphatidylcholine (DOPC) is considered. They observe a fine scale pattern formation in regions in which the vesicle was not adhered. From an initially homogeneous mixture they describe a phase separation into DOPC which in time transforms from periodically organised laminates that become unstable to hexagonal array of circular domains which appear to be stable. In addition, the shape of the vesicle changes as well and simultaneously the width of the pattern. The authors of [RKG05] also describe a second experiment where a large circular domain made up of sphingomyelin evolves into an organised stripe pattern over time which appearing to be stable. Similar observations were made e.g. in [PYG06, KG10, SMNT17].

In summary, fine scale patterns are observed in a lipid bilayer that change simultaneously with the shape of the vesicle itself. The experiments show periodically organised stripe pattern or hexagonally organised circular patterns. Our aim is to model the situation at hand with the following physical assumptions:

- The lipid bilayer is modeled as a 2D immersed surface in $\mathbb{R}^3$.
- The membrane consists of a binary mixture.
- The lipid bilayer behaves like a 2D fluid, the binary mixture is able to diffuse.

3.2. Mechanochemical Models

Mechanochemical models describe phenomena in which chemical and mechanical forces are driving the system. We will present several models and briefly describe the physical

interpretation. We will proceed by combining these models and describe certain approximations thereof to derive the energy model $E_{\gamma,\varepsilon}$ analysed in Chapter 5. We will restrict to energy models as these are the most relevant in this thesis.

Phase separation energies *Cahn–Hilliard* type models describe chemical phase separation processes and concentration effects of binary mixtures and are generally of the form

$$\mathrm{CH}[f] \coloneqq \int_U \mathcal{W}(\phi) + \frac{b^2}{2}|\nabla\phi(x)|^2 \,\mathrm{d}x, \tag{3.2}$$

where $U \subset \mathbb{R}^n$ is a reference domain, $\mathcal{W}\colon \mathbb{R} \longrightarrow \mathbb{R}$ is a so called *double well potential*, and $b > 0$ is parameter related to line tension. The double well potential describes chemical interaction while the gradient contribution is a regularisation term, making oscillations energetically less favourable. To have a well-defined energy, the argument has at least to be of class $W^{1,2}$, thus energy models of this type are diffuse interface models.

Mathematically, the function $\mathcal{W}$ usually satisfies the following conditions:

- $\mathcal{W} \in C^0(\mathbb{R})$.
- There exist $a_1, a_2 \in \mathbb{R}$, $a \neq b$, such that $\mathcal{W}(a_1) = \mathcal{W}(a_2) = 0$ and $\mathcal{W}(x) > 0$ otherwise.
- $\mathcal{W}$ is non degenerate at $\pm\infty$.

Non degeneracy usually comes in the following forms:

- **Growth Condition:** $1 + |x|^q \lesssim \mathcal{W}(x)$ for some $q > 0$.
- $\liminf\limits_{x\to\pm\infty} \mathcal{W}(x) > 0$.

By redefining the arguments $f \longmapsto \frac{f-a_1}{a_2-a_1}$, we can without loss of generality assume that $a_1 = -1$ and $a_2 = +1$. We will refer to ± 1 as the pure phases.

The Direct Method of the Calculus of Variations ensures the existence of a minimiser u of class $W^{1,2}$ since the energy is convex in the highest order of derivatives. Also, the properties on $\mathcal{W}$ drive the minimiser of CH to be close to the pure phases ± 1. However, since the minimiser is of class $W^{1,2}$, jump discontinuities cannot occur. Thus there is a transition layer between the phases $u \approx -1$ and $u \approx +1$.

Bending energies In the context of biology, bending energies were introduced in [Can70] to explain the non-convex shape of red blood cells (see also [Hel73]). Examples of such energies are *Helfrich type energies*. These are energies of 2D immersed smooth surfaces in $\mathbb{R}^3$ and are of the form

$$\mathrm{Hel}(\Sigma) \coloneqq \kappa \int_\Sigma (H - H_0)^2 \,\mathrm{d}\mathscr{H}^2 + \kappa' \int_\Sigma K \,\mathrm{d}\mathscr{H}^2, \tag{3.3}$$

where H denotes the mean curvature of Σ and K the Gauß curvature of Σ and $\kappa, \kappa' > 0$ are bending moduli. The parameter H_0 is called spontaneous curvature. Using the Gauß–Bonnet Theorem, the second term in the energy can be written as

$$\int_\Sigma K \,\mathrm{d}\mathscr{H}^2 = 2\pi\chi(\Sigma), \tag{3.4}$$

where $\chi(\Sigma)$ denotes the Euler Characteristic of Σ, i.e. a topological quantity. Since we are only interested in immersed sets which do not have a topological defect (i.e. $\chi(\Sigma) = 0$), we will omit the second term in the energy and only work with the mean curvature contribution.

Mathematically, Helfrich type energies are hard to deal with, especially if $H_0 \neq 0$. In particular, it is hard to find strictly positive lower bounds. While in the case $H_0 = 0$ there is a lower bound (which is given by 4π), in general there is not a strictly positive lower bound available if $H_0 \neq 0$. Moreover, if $H_0 \neq 0$, then the energy lacks and invariances and semi-continuity properties. In particular, the functional is not lower semi-continuous with respect to weak convergence (see [GeB93]) and not conformally invariant (see [MS20]).

Coupling mechanical and chemical interactions: Combining the above mentioned models is not an easy task as they operate on two different domains: the Cahn-Hilliard type energies act on sufficiently regular functions, while the Helfrich type energies act on sufficiently smooth sets. One way to overcome this difficulty is to reformulate the Helfrich type energies to act on sufficiently smooth functions by means of localisation. By using a representation as a graph via a function $h\colon U \longrightarrow \mathbb{R}$, we find that at $z = h(x, y)$ we have

$$2H(z) = \frac{(1 + h_x^2)h_{yy} + (1 + h_y^2)h_{xx} - 2h_x h_y h_{xy}}{(1 + |\nabla h|^2)^{\frac{3}{2}}} \tag{3.5}$$

$$= \frac{\Delta h}{\sqrt{1 + |\nabla h|^2}} - \frac{h_{xx}h_x^2 + h_{yy}h_y^2 + 2h_x h_y h_{xy}}{(1 + |\nabla h|^2)^{\frac{3}{2}}}. \tag{3.6}$$

Assuming small gradients and reducing to the linear contribution, we obtain an approximation of the form

$$H(z) \approx \frac{1}{2}\Delta h(x, y). \tag{3.7}$$

Using this approximation, the Helfrich energy can be formally approximated as follows:

$$\tilde{\mathrm{Hel}}(h) = \kappa \int_U (\Delta h - H_0)^2 \,\mathrm{d}x. \tag{3.8}$$

We are now in the position to combine chemical and mechanical energies by virtue of adding their contributions $\mathrm{CH} + \tilde{\mathrm{Hel}}$. As of now, the variable for the chemical energy and the variable for the mechanical energy are not coupled. This will be dealt with by setting

$H_0 = \Lambda\phi$, where $\Lambda \in \mathbb{R}$ is a coupling constant. This results in

$$\mathrm{MC}[\phi, h] = \int_U \mathcal{W}(\phi) + \frac{b^2}{2}|\nabla\phi|^2 + \frac{\kappa}{4}(\Delta h)^2 - \Lambda^2\phi^2 + \Lambda\phi\Delta h \,\mathrm{d}x. \tag{3.9}$$

We will call models of this type *mechano–chemical models*. Furthermore, we will call the variable ϕ the *order variable*, and the variable h the *displacement variable*.

In the literature, there are multiple different energies similar to MC in various aspects. In [Tan96], the corresponding gradient flow is solved numerically with a curved reference domain U and concludes that the coupling as performed above strongly influences the formation of protrusions in the membrane. More recent asymptotic analysis was conducted in [EH21] (see also [EHS22]) on curved surfaces. Further application of mechano chemical models can be found in the study of Diblock copolymers (see e.g. [RW00]).

The experiments conducted in [RKG05] are considered in [KSA06] and analyse a mechano-chemical model of the form (see also [LA87])

$$\mathcal{E}[\phi, h] = \int \frac{a_4}{4}\phi^4 + \frac{a_2}{2}\phi^2 - \mu\phi + \frac{b}{2}|\nabla\phi|^2 + \frac{\sigma}{2}|\nabla h|^2 + \frac{\kappa}{2}|\Delta h|^2 + \Lambda\phi\Delta h \,\mathrm{d}x, \tag{3.10}$$

where $a_4 > 0$ for stability purposes, $a_2 > 0$ is proportional to temperature, $\mu > 0$ denotes the chemical potential and $\sigma > 0$ the surface tension of the membrane. In [KSA06] the authors performed a linear stability analysis and concluded that in the parameter regime $\Lambda^2 > b\sigma$, the homogenuous system becomes unstable and might lead to fine-scale patterns. More specifically, they conclude that the model predicts a change from striped to hexagonal patterns by increasing the line tension b, or decreasing the coupling constant Λ^2 (see also [HG96]).

3.3. Comparison of Sharp and Diffuse Interface Models

Under additional physical assumptions on the system, namely that the elastic stress relaxes much faster than the typical time scale of diffusion, the dependence of h in the mechano-chemical energies can be removed. In [FHLZ16], the authors worked with a reformulation of the energy model in (3.10). Using the Euler–Lagrange equation $\frac{\delta\mathcal{E}}{\delta h} = 0$, they reformulated the energy $\mathcal{E}$ in terms of the order parameter only. The resulting energy is non-local (as it involves a solution operator to an elliptic equation) and is given by

$$\mathcal{F}_{q,\varepsilon}[u] = \frac{1}{\varepsilon}\int_{\mathbb{T}^2} W(u) + (1-q)\varepsilon^2|\nabla u|^2 - u^2 + u(\mathbf{1} - \varepsilon^2\Delta)^{-1}u \,\mathrm{d}x, \tag{3.11}$$

where the non-linear terms are absorbed in the double well potential W and the effective parameters are given in terms of the physical parameters via

$$q = 1 - \frac{\sigma b}{\Lambda^2}, \qquad \varepsilon^2 = \frac{\kappa}{\sigma L^2}. \tag{3.12}$$

To develop some intuition for the non-local energy $\mathcal{F}_{q,\varepsilon}$, we perform a formal expansion of the non-local term which reveals

$$u(\mathbf{1} - \varepsilon^2\Delta)^{-1}u = u^2 + \varepsilon^2 u\Delta u + \varepsilon^4 u\Delta^2 u + \mathcal{O}(\varepsilon^6). \tag{3.13}$$

Using integration by parts, we find an approximate energy for the non-local energy $\mathcal{F}_{q,\varepsilon}$ by a local energy functional

$$\tilde{\mathcal{F}}_{q,\varepsilon}[u] = \frac{1}{\varepsilon}\int_{\mathbb{T}^2} W(u) - q\varepsilon^2|\nabla u|^2 + \varepsilon^4|\Delta u|^2 \,\mathrm{d}x \tag{3.14}$$

for which it was shown that there exists $\tilde{q}_* > 0$ sucht that $\tilde{F}_{q,\varepsilon} \xrightarrow{\Gamma} \tilde{c}_q \operatorname{Per}$ in the L^2 topology for all $q < \tilde{q}_*$ (see [CDMFL11, CSZ11]). So the non-local energy $\mathcal{F}_{q,\varepsilon}$ behaves qualitatively like the local energy functional $\tilde{\mathcal{F}}_{q,\varepsilon}$.

In order to find a sharp interface variant of $\mathcal{F}_{q,\varepsilon}$ we can use an approximation of the local contribution in terms of the Perimeter functional. More precisely, in the Modica–Mortola theory there is a connection between diffuse and sharp interface energies in the framework of Γ–convergence, namely (see [CS06, Mod87])

$$\int_{\mathbb{T}^n} \frac{1}{\varepsilon}W(u) + (1-q)\varepsilon|\nabla u|^2 \,\mathrm{d}x \xrightarrow{\Gamma} c_{W,q}\int_{\mathbb{T}^n} |\nabla u| \tag{3.15}$$

in the L^1 topology as $\varepsilon \to 0$, where

$$c_{W,q} = 2\sqrt{1-q}\int_{-1}^{1}\sqrt{W(s)}\; ds. \tag{3.16}$$

Naively, this would suggest to correspondingly replace the local diffuse interface term in $\mathcal{F}_{q,\varepsilon}$ by its sharp interface counterpart as in (3.15). In particular, we note that for $\mathcal{K}$ being the Fundamental Solution to the Helmholtz equation, namely

$$\mathcal{K} - \Delta\mathcal{K} = \delta_0 \qquad \text{in } \mathbb{R}^n, \tag{3.17}$$

$\mathcal{F}_{q,\varepsilon}$ in (3.11) is a corresponding diffuse interface model of the non-local isoperimetric energy

$$E_{\gamma,\varepsilon}(\Omega) \coloneqq \operatorname{Per}(\Omega) - \frac{\gamma}{\varepsilon^{n+1}}\int_{\mathbb{R}^n}\mathcal{K}(\tfrac{z}{\varepsilon})\int_{\mathbb{T}^n}|\chi_\Omega(x+z) - \chi_\Omega(x)|\,\mathrm{d}x\,\mathrm{d}z \tag{3.18}$$

analysed in Chapter 5. Here, we identified the function $u \in BV(\mathbb{T}^2, \{\pm 1\})$ with the set

$\Omega \in BV_2$ via $\Omega \longmapsto u = 2\chi_\Omega - 1$. The energy $\mathcal{F}_{q,\varepsilon}$ has been considered in [FHLZ16] where it was shown that there exists $\bar{q} > 0$, such that $\mathcal{F}_{q,\varepsilon}$ Γ–converges to a constant multiple of the perimeter functional (a sharp interface model) for all $0 < q < \bar{q}$. We note that the results of [FHLZ16] do not contain a characterisation or estimation of $\bar{q}$, nor the constant appearing in their Γ–limit. This is due to a non-linear interpolation inequality shown in [CDMFL11], which has no explicit description of the constants involved (see also [CSZ11]).

Our main result (see Theorem B) is similar to that of [FHLZ16] in that we find two regimes for a parameter related to the relative strength of the non–local interaction (for our energy γ, in [FHLZ16] it is q), and the limit problem in the subcritical regime is the isoperimetric problem. The interpretation is the same as in [FHLZ16], namely in the subcritical parameter regime, fine scale pattern formation does not occur in contrast to experimental results (e.g. stripe patterns or hexagonal array of balls, see [RKG05, KG10]). The analysis of the energy $E_{\gamma,\varepsilon}$ suggest that fine scale patterns occur in the supercritical regime (see Section 5.4.2), but for fixed $\varepsilon > 0$, since in the supercritical regime high oscillations are preferred. This leads to a failure of compactness and to an asymptotically unbounded energy.

Furthermore, our result shows that quantitatively, the sub- and supercritical regimes of the diffuse and sharp interface models differ. In particular, the critical value q_{crit} of the corresponding sharp interface model (using the relations (3.15) and (3.16)) is given by

$$q_{\text{crit}} = 1 - \left(2\gamma_{\text{crit}} \int_{-1}^{1} \sqrt{W(s)}\, ds\right)^{-2}. \tag{3.19}$$

For $\mathcal{K}$ as in (3.17), we can explicitly compute the corresponding critical value of the sharp interface model and it is given by $\gamma_{\text{crit}} = 1$ (see Lemma A.13). However, one cannot equate the parameter q_{crit} with the corresponding critical value $\bar{q}$ (the threshold for Γ–convergence) in [FHLZ16]. Indeed, for a suitable double well potential with $\|W\|_{L^\infty(-1,1)} < \frac{1}{16}$ we would obtain $q_{\text{crit}} < 0$. This shows, that $\bar{q} = q_{\text{crit}}$ cannot hold, since the result of [FHLZ16] shows that $\bar{q} > 0$. This is probably due to the fact that the sharp interface model neglects effects which might occur due to non–linearity (i.e. the double well potential W) such as asymmetry, compressibility of the chemical substance, or behaviour at infinity or the vanishing order at the roots. In particular, the interpolation inequality used in [FHLZ16] in order to show $\bar{q} > 0$ only works for double well potentials W which have quadratic roots and superquadratic growth (see also [CSZ11, Section 3]). The sharp interface model does not contain information about the double well potential W other than the quantity $\int_{-1}^{1} \sqrt{W(s)}\, ds$, which is unrelated to the aforementioned properties.

4. Autocorrelation Function

In this chapter, we introduce and study the Covariogram and the Autocorrelation Function of measurable subsets of the flat Torus $\mathbb{T}^n$. Our interest is its application to non-local isoperimetric problems motivated by [KS23] (see also [BKMC23]) and in particular to the models with periodic boundary conditions described in Chapter 3. For a measurable subset $\Omega \subset \mathbb{T}^n$ we define its Covariogram $C_\Omega \colon \mathbb{T}^n \longrightarrow \mathbb{R}$ via

$$C_\Omega(x) \coloneqq |\Omega \cap (\Omega + x)| \qquad \text{for all } x \in \mathbb{T}^n. \tag{4.1}$$

In [Gal11] (see also [Mat86]), the author studied the same quantity in the Euclidean setting. Namely, given a measurable set $\Omega \subset \mathbb{R}^n$ with finite measure, the Covariogram $\mathscr{C}_\Omega \colon \mathbb{R}^n \longrightarrow \mathbb{R}$ is given by

$$\mathscr{C}_\Omega(z) \coloneqq |\Omega \cap (\Omega + z)| \qquad \text{for all } z \in \mathbb{R}^n, \tag{4.2}$$

where $|\cdot|$ denotes the Lebesgue measure on $\mathbb{R}^n$. It is shown for example that $\mathscr{C}_\Omega$ is a Lipschitz function if and only if Ω is a set of finite perimeter (with estimates of the Lipschitz constant in terms of the perimeter of Ω) and the inequality

$$|\mathscr{C}_\Omega(z) - \mathscr{C}_\Omega(z')| \leq \mathscr{C}_\Omega(0) - \mathscr{C}_\Omega(z - z') \qquad \text{for all } z, z' \in \mathbb{R}^n. \tag{4.3}$$

This inequality essentially shows that the Lipschitz continuity and the regularity of the Covariogram only depend on the behaviour of $\mathscr{C}_\Omega$ in $z = 0$. Applications of the Covariogram can be found e.g. in convex geometry (see [MRS93, Nag93, AB15, Bia02, EL11, Wil17]), the theory of random sets (see [MC70, Gal11, EL11]) and non-local isoperimetric problems (see [KS23, BKMC23]).

This chapter is organised as follows: In Section 4.1 we will define the Covariogram and the Autocorrelation Function and collect basic properties. In Section 4.2 and Section 4.3 we will take a closer look into regularity properties of the Covariogram and the Autocorrelation Function and show that the behaviour of C_Ω and c_Ω at the origin is tightly related to the geometry of Ω. In particular, in Section 4.2 we will show that C_Ω and c_Ω are Lipschitz functions if and only if $\Omega \in BV_n$ (see Theorem 4.7). Moreover, we derive a formula for the second derivative. In Section 4.3 we proceed with higher regularity properties in dimension $n = 2$. More precisely, we will show that C_Ω and c_Ω are smooth

functions around the origin if $\Omega \subset \mathbb{T}^2$ is sufficiently smooth (see Theorem 4.10) and find

$$c''_\Omega(0) = 0, \qquad c'''_\Omega(0) = \int_{\partial\Omega} \kappa^2 \, \mathrm{d}\mathscr{H}^1, \tag{4.4}$$

where $\kappa \colon \partial\Omega \longrightarrow \mathbb{R}$ denotes the curvature. Finally, we will discuss some explicit examples in Section 4.4, building upon techniques developed in the prior sections. This includes balls, laminates and polytopes. With these explicit results, we are able to show that $\Omega \longmapsto c''_\Omega(0)$ in contrast to the lower derivatives is neither upper-, nor lower semicontinuous with respect to L^1–convergence (see Lemma 4.19).

4.1. Covariogram and Autocorrelation Function of Measurable Sets

We will shortly recall the setup. The precise definitions can be found in Chapter 2. Let $n \in \mathbb{N}$ with $n \geq 2$ and define $\mathbb{T}^n \coloneqq \mathbb{R}^n/\mathbb{Z}^n$ the n–dimensional flat torus endowed with the unit Haar measure (denoted by $|\cdot|$ or $\mathrm{d}x, \mathrm{d}y$ etc.). We denote the surface measure with $\mathscr{H}^{n-1}$. We also define translates of sets by

$$A + z \coloneqq \{x + z : x \in A\} \qquad \text{for all } A \subset \mathbb{T}^n,\ z \in \mathbb{T}^n. \tag{4.5}$$

We also define ω_n to be the measure of the unit ball in $\mathbb{R}^n$ and $\sigma_n = n\omega_n$ the measure of the unit sphere. We start by defining the Covariogram of a set and its (radially symmetrised) Autocorrelation Function:

Definition 4.1 Let $\Omega \subset \mathbb{T}^n$ be measurable. We define the **Covariogram** $C_\Omega \colon \mathbb{T}^n \longrightarrow \mathbb{R}$ via

$$C_\Omega(x) \coloneqq |\Omega \cap (\Omega + x)| \qquad \text{for all } x \in \mathbb{T}^n. \tag{4.6}$$

We define the (radially symmetrised) **Autocorrelation Function** $c_\Omega \colon \mathbb{R} \longrightarrow \mathbb{R}$ via

$$c_\Omega(r) \coloneqq \frac{1}{\sigma_n} \int_{\mathbb{S}^{n-1}} C_\Omega(rw) \, \mathrm{d}\mathscr{H}^{n-1}(w) \qquad \text{for all } r \in \mathbb{R}. \tag{4.7}$$

We note, that the Covariogram of a set $\Omega \subset \mathbb{T}^n$ can be represented in terms of convolution: Let $u \coloneqq \chi_\Omega$, then $C_\Omega = u * \mathcal{I}u$, where $\mathcal{I}$ denotes the reflection operator and $*$ the convolution. Note that c_Ω is generally not a periodic function.

As alluded to in the the introduction, the Covariogram and therefore the Autocorrelation

Function have full space analogues. We will denote thesm by

$$\mathscr{C}_\Omega(z) \coloneqq |\Omega \cap (\Omega + z)|, \qquad \mathfrak{c}_\Omega(r) \coloneqq \int_{\mathbb{S}^{n-1}} \mathscr{C}_\Omega(rw)\,\mathrm{d}\mathscr{H}^{n-1}. \tag{4.8}$$

For a set $\Omega \subset \mathbb{T}^n$ with $\operatorname{diam}(\Omega) < 1$, there exists a representative $\hat{\Omega} \subset \mathbb{R}^n$. Due to the geometry of $\mathbb{T}^n$ and $\mathbb{R}^n$, we find

$$C_\Omega(x) = \mathscr{C}_{\hat{\Omega}}(x) \qquad \text{for all } x \in \mathbb{T}^n \text{ sufficiently close to 0,} \tag{4.9}$$

$$c_\Omega(r) = \mathfrak{c}_{\hat{\Omega}}(r) \qquad \text{for all } 0 < r \ll 1. \tag{4.10}$$

Most of the following results are inspired by [Gal11] (see also [KS23]) and carry over to $\mathscr{C}_\Omega$ and $\mathfrak{c}_\Omega$ analogously. For the theory, we will mostly consider the the Covariogram and Autcorrelation Function defined on $\mathbb{T}^n$ and get back to the full space analogues when it comes to explicit calculations in Section 4.4.

The following properties are immediate from the definition:

Proposition 4.2 Let $\Omega \subset \mathbb{T}^n$ be measurable. Then:

a) $0 \le C_\Omega(x) \le C_\Omega(0) = |\Omega|$ for all $x \in \mathbb{T}^n$.

b) $C_\Omega(x) = C_\Omega(-x)$ for all $x \in \mathbb{T}^n$.

c) $\|C_\Omega\|_{L^1(\mathbb{T}^n)} = |\Omega|^2$.

d) C_Ω is a uniformly continuous function.

Proof: a) follows from Hölders inequality and b) from a simple transformation. c) follows from the Theorem of Tonelli. To prove d), observe that for $x, y \in \mathbb{T}^n$ and $u \coloneqq \chi_\Omega$, we have

$$|C_\Omega(x) - C_\Omega(y)| \le \int_{\mathbb{T}^n} u(z)\,|u(z+x) - u(z+y)|\,\mathrm{d}z \tag{4.11}$$

$$\le \|u - u(\,\cdot\, + (x-y))\|_{L^1(\mathbb{T}^n)}. \tag{4.12}$$

The uniform continuity then follows from the fact, that $\|f - f(\,\cdot\, + h)\|_{L^1(\mathbb{T}^n)} \to 0$ as $h \to 0$ for every function $f \in L^1(\mathbb{T}^n)$. ■

Similar results are true for the Autocorelation Function:

Proposition 4.3 Let $\Omega \subset \mathbb{T}^n$ be measurable. Then:

a) $0 \le c_\Omega(r) \le c_\Omega(0) = |\Omega|$ for all $r \in \mathbb{R}$.

b) $c_\Omega(r) = c_\Omega(-r)$ for all $z \in \mathbb{T}^n$.

c) c_Ω is a uniformly continuous function.

Proof: Follows directly from the definition of c_Ω and Proposition 4.2. ■

The next lemma deals with trivial extensions of measurable sets and their effect on the Covariogram.

Lemma 4.4 Let $\Omega \subset \mathbb{T}^n$ be measurable. Let $\bar{\Omega} \coloneqq \Omega \times \mathbb{T}^k \subset \mathbb{T}^{n+k}$. Then

$$C_{\bar{\Omega}}(\bar{z}) = C_\Omega(z) \qquad \text{for all } \bar{z} = (z, z') \in \mathbb{T}^{n+k}. \tag{4.13}$$

Proof: We compute for all $z = (z, z') \in \mathbb{T}^{n+k}$ via Fubini

$$C_{\bar{\Omega}}(\bar{z}) = \int_{\mathbb{T}^{n+k}} \chi_{\Omega\times\mathbb{T}^k}(\bar{z}+\bar{x})\, \chi_{\Omega\times\mathbb{T}^k}(\bar{x})\, \mathrm{d}\bar{x} \tag{4.14}$$

$$= \int_{\mathbb{T}^{n+k}} \chi_\Omega(z+x)\, \chi_\Omega(x)\, \chi_{\mathbb{T}^k}(z'+x')\chi_{\mathbb{T}^k}(x')\, \mathrm{d}(x, x') \tag{4.15}$$

$$= \int_{\mathbb{T}^k} \int_{\mathbb{T}^n} \chi_\Omega(z+x)\, \chi_\Omega(x)\, \mathrm{d}x\, \mathrm{d}x' = C_\Omega(z), \tag{4.16}$$

as claimed. ■

4.2. Global Regularity Properties

In this section, we will take a closer look into the regularity of the function C_Ω and c_Ω and its connection to the geometry of Ω. In [MRS93] it was shown that under certain smoothness conditions of the boundary of a set, the covariogram $\mathscr{C}_\Omega$ of a convex body Ω is smooth, and they also present formulas for the first and second derivatives in this case. In [Gal11], the author showed that $\mathscr{C}_\Omega$ is Lipschitz if and only if Ω is a set of finite perimeter. In [KS23] this was also shown for C_Ω and c_Ω.

A formal argument to connect sets of finite perimeter and the Covariogram comes from the representation as convolution. In particular, as $C_\Omega = \chi_\Omega * \mathcal{I}\chi_\Omega$, we formally obtain

$$\nabla_w C_\Omega = \nabla_w \chi_\Omega * \mathcal{I}\chi_\Omega. \tag{4.17}$$

Young's Convolution Inequality now yields

$$\|\nabla_w C_\Omega\|_{L^1} \leq \|\nabla_w \chi_\Omega\|_{L^1} \|\chi_\Omega\|_{L^1} \leq \mathrm{Per}(\Omega), \tag{4.18}$$

formally obtaining a uniform bound of the gradient independent of $w \in \mathbb{S}^{n-1}$, and therefore Lipschitz continuity of C_Ω. The following proposition shows that the Lipschitz continuity of the Covariogram and the Autocorrelation Function only depends on the behaviour at the origin.

Proposition 4.5 Let $\Omega \subset \mathbb{T}^n$ be measurable. Then the following inequalities hold:

a) $|C_\Omega(x) - C_\Omega(y)| \leq C_\Omega(0) - C_\Omega(y-x)$ for all $x, y \in \mathbb{T}^n$.

b) $|c_\Omega(s) - c_\Omega(t)| \leq c_\Omega(0) - c_\Omega(s-t)$ for all $s, t \in \mathbb{R}$.

Proof: Let $x, y \in \mathbb{T}^n$. Without loss of generality we can assume that $C_\Omega(x) \geq C_\Omega(y)$. We use Lemma A.5 to obtain

$$\begin{aligned} C_\Omega(x) - C_\Omega(y) &= |\Omega \cap (\Omega + x)| - |\Omega \cap (\Omega + y)| && (4.19)\\ &\leq |\Omega + y| - |(x + \Omega) \cap (y + \Omega)| && (4.20)\\ &= |\Omega| - |\Omega \cap ((y-x) + \Omega)\,| = C_\Omega(0) - C_\Omega(y-x). && (4.21) \end{aligned}$$

Assertion b) then follows directly from a). ■

With the preceding proposition, we will focus now on the bahaviour at the origin. The following formula is due to Matheron [Mat86] (see also [Gal11]).

Lemma 4.6 Let $\Omega \subset \mathbb{T}^n$ be measurable. Then

$$C_\Omega(0) - C_\Omega(z) = \frac{1}{2} \int_{\mathbb{T}^n} |\chi_\Omega(x) - \chi_\Omega(x+z)|\,\mathrm{d}x \qquad \text{for every } z \in \mathbb{T}^n,$$

$$c_\Omega(0) - c_\Omega(r) = \frac{1}{2\sigma_n} \int_{\mathbb{S}^{n-1}} \int_{\mathbb{T}^n} |\chi_\Omega(x + rw) - \chi_\Omega(x)|\,\mathrm{d}x\,\mathrm{d}\mathscr{H}^{n-1}(w) \quad \text{for all } r \in \mathbb{R}.$$

Proof: Since the integrand only takes the values 0 and 1 we obtain

$$\begin{aligned} \int_{\mathbb{T}^n} |\chi_\Omega(x) - \chi_\Omega(x+z)|\,\mathrm{d}x &= \int_{\mathbb{T}^n} |\chi_\Omega(x) - \chi_\Omega(x+z)|^2\,\mathrm{d}x && (4.22)\\ &= C_\Omega(0) - 2C_\Omega(z) + C_\Omega(0), && (4.23) \end{aligned}$$

which was the first claim. The second assertion follows by definition of the Autocorrelation Function. ■

We recall that $\Omega \in BV_n$ if $\chi_\Omega \in BV(\mathbb{T}^n)$. The following theorem provides a characterisation of the space BV_n in terms of the Covariogram.

Theorem 4.7 Let $\Omega \subset \mathbb{T}^n$ be measurable. Then the following is equivalent:

a) $\Omega \in BV_n$.

b) $\lim\limits_{r \searrow 0} \dfrac{C_\Omega(rw) - C_\Omega(0)}{r}$ exists and is finite for all $w \in \mathbb{S}^{n-1}$.

c) C_Ω is a Lipschitz function.

In addition

$$\|\nabla C_\Omega\|_{L^\infty(\mathbb{T}^n, \mathbb{R}^n)} = \frac{1}{2} \sup_{w \in \mathbb{S}^{n-1}} V_w[\chi_\Omega] \leq \frac{1}{2} V[\chi_\Omega]. \tag{4.24}$$

Proof: Let $w \in \mathbb{S}^{n-1}$. Then we derive from Lemma 4.6 and Corollary 4.8

$$\lim_{r \searrow 0} \frac{C_\Omega(0) - C_\Omega(rw)}{r} = \frac{1}{2} \lim_{r \searrow 0} \int_{\mathbb{T}^n} \frac{|\chi_\Omega(x) - \chi_\Omega(x + rw)|}{r} \, \mathrm{d}x = \frac{1}{2} V_w[\chi_\Omega]. \tag{4.25}$$

So the limit exists and is finite for all $w \in \mathbb{S}^{n-1}$ if $V_w[\chi_\Omega]$ is finite for all $w \in \mathbb{S}^{n-1}$, which in turn is equivalent to Ω being a set of finite perimeter (see Corollary 4.8). This shows the equivalence of a) and b).

To show the equivalence to c), let $x, y \in \mathbb{T}^n$ such that $x \neq y$. Then we find $r > 0$ and $w \in \mathbb{S}^{n-1}$ such that $x - y = rw$ (or more precisely $x - y = \exp_0(rw)$). We compute

$$\begin{aligned}
|C_\Omega(x) - C_\Omega(y)| &\overset{4.5}{\leq} C_\Omega(0) - C_\Omega(y - x) && (4.26)\\
&\overset{4.6}{=} \frac{1}{2} \int_{\mathbb{T}^n} |\chi_\Omega(z) - \chi_\Omega(z + y - x)| \, \mathrm{d}z && (4.27)\\
&= \frac{r}{2} \int_{\mathbb{T}^n} \frac{|\chi_\Omega(z) - \chi_\Omega(z + rw)|}{r} \, \mathrm{d}z && (4.28)\\
&\overset{4.8}{\leq} \frac{r}{2} V_w[\chi_\Omega] \leq \frac{|x - y|}{2} \sup_{w \in \mathbb{S}^{n-1}} V_w[\chi_\Omega], && (4.29)
\end{aligned}$$

which shows that C_Ω is a Lipschitz function (see Corollary 2.12). The equivalence as well as the formula (4.24) then follow from (4.25). ■

We remark that the restriction to lines $C_\Omega^w \colon \mathbb{R} \longrightarrow \mathbb{R}$, which is given by $C_\Omega^w(r) \coloneqq C_\Omega(rw)$ for some fixed $w \in \mathbb{S}^{n-1}$, has Lipschitz constant $\frac{1}{2} V_w[\chi_\Omega]$, which is a byproduct of the proof of Theorem 4.7. Moreover, a combination of Theorem 4.7 and Rademacher's

Theorem shows that the Covariogram C_Ω (as well as the Autocorrelation Function c_Ω) are differentiable almost everywhere.

Since the Autocorrelation Function is an even function, we will treat it as a function defined on $\mathbb{R}_+$. If it comes to regularity properties we will denote

$$c'_\Omega(0) \coloneqq \lim_{r \searrow 0} \frac{c_\Omega(r) - c_\Omega(0)}{r} \tag{4.30}$$

as the right–derivative.

Corollary 4.8 Let $\Omega \subset \mathbb{T}^n$ be a set of finite perimeter. Then

a) $\lim\limits_{r \searrow 0} \dfrac{C_\Omega(rw) - C_\Omega(0)}{r} = -\dfrac{1}{2} V_w[\chi_\Omega]$ for all $w \in \mathbb{S}^{n-1}$.

b) $\|c'_\Omega\|_{L^\infty(\mathbb{R}_+)} = -c'_\Omega(0) = \dfrac{1}{n} \dfrac{\omega_{n-1}}{\omega_n} \operatorname{Per}(\Omega)$.

Proof: Assertion a) is shown in (4.25). Since c'_Ω exists almost everywhere, we obtain from Proposition 4.5 for almost every $r > 0$

$$|c'_\Omega(r)| = \lim_{h \searrow 0} \Big| \frac{c_\Omega(r+h) - c_\Omega(r)}{h} \Big| \leq \lim_{h \searrow 0} \frac{c_\Omega(0) - c_\Omega(h)}{h} = -c'_\Omega(0). \tag{4.31}$$

Thus it remains to calculate $c'_\Omega(0)$. We compute for $r > 0$

$$\begin{aligned} \frac{c_\Omega(r) - c_\Omega(0)}{r} &= \frac{1}{\sigma_n} \int_{\mathbb{S}^{n-1}} \frac{C_\Omega(rw) - C_\Omega(0)}{r} \, \mathrm{d}\mathscr{H}^{n-1}(w) && (4.32) \\ &\xrightarrow{r \searrow 0} -\frac{1}{2\sigma_n} \int_{\mathbb{S}^{n-1}} V_w[\chi_\Omega] \, \mathrm{d}\mathscr{H}^{n-1}(w) && (4.33) \\ &= -\frac{1}{n} \frac{\omega_{n-1}}{\omega_n} V[\chi_\Omega], && (4.34) \end{aligned}$$

where in the last line we used Corollary 4.8 and $\sigma_n = n\omega_n$. ■

We have seen that sets of finite perimeter imply Lipschitz regularity of the Covariogram. Formally, this was expected from the computations (4.17) and (4.18). We can expand these formal computations to obtain

$$\nabla_v \nabla_w C_\Omega = \nabla_w \chi_\Omega * \mathcal{I} \nabla_w \chi_\Omega \tag{4.35}$$

and again with Young's Convolution Inequality

$$\|\nabla_v \nabla_w C_\Omega\|_{L^1} \leq \|\nabla_w \chi_\Omega\|_{L^1} \|\nabla_v \chi_\Omega\|_{L^1} \lesssim \operatorname{Per}(\Omega)^2. \tag{4.36}$$

Therefore, the derivative of the Covariogram itself is expected to have a notion of weak differentiability. We end this section by proving that this is indeed the case.

Lemma 4.9 Let $\Omega \in BV_n$ and $w \in \mathbb{S}^{n-1}$. Then $\nabla_w C_\Omega \in BV(\mathbb{T}^n) \cap L^\infty(\mathbb{T}^n)$ and

$$\nabla_v \nabla_w C_\Omega = -\nabla_v \chi_\Omega * \mathcal{I} \nabla_w \chi_\Omega \qquad \text{for all } v \in \mathbb{S}^{n-1}, \tag{4.37}$$

where $\mathcal{I}$ denotes the reflection operator.

As a reminder, given two Borel measures $\mu, \nu \colon \mathscr{B}(\mathbb{T}^n) \longrightarrow [0, \infty]$, the convolution measure $\mu * \nu$ is defined via duality:

$$\int_{\mathbb{T}^n} \varphi \, \mathrm{d}(\mu * \nu) = \int_{\mathbb{T}^n} \varphi(x+y) \, \mathrm{d}\mu(x) \, \mathrm{d}\nu(y) \qquad \text{for all } \varphi \in L^\infty(\mathbb{T}^n). \tag{4.38}$$

Proof: Let $\varphi \in C^\infty(\mathbb{T}^n)$. Since Ω is a set of finite perimeter, we know from Theorem 4.7 that $\nabla_w C \in L^\infty(\mathbb{T}^n)$. We compute for $v \in \mathbb{S}^{n-1}$ with Corollary 2.7 and Fubini's Theorem

$$\begin{aligned}
\int_{\mathbb{T}^n} \nabla_w C_\Omega(x) \nabla_v \varphi(x) \, \mathrm{d}x &= -\int_{\mathbb{T}^n} \chi_\Omega(y) \int_{\mathbb{T}^n} \chi_\Omega(x+y) \, \nabla_v \nabla_w \varphi(x) \, \mathrm{d}x \, \mathrm{d}y && (4.39)\\
&= \int_{\mathbb{T}^n} \chi_\Omega(y) \int_{\mathbb{T}^n} \nabla_v \varphi(x-y) \, \mathrm{d}\nabla_w \chi_\Omega(x) \, \mathrm{d}y && (4.40)\\
&= -\int_{\mathbb{T}^n} \int_{\mathbb{T}^n} \varphi(x+y) \, \mathrm{d}\mathcal{I}\nabla_v \chi_\Omega(y) \, \mathrm{d}\nabla_w \chi_\Omega(x) && (4.41)\\
&= -\int_{\mathbb{T}^n} \varphi \, \mathrm{d}[\nabla_w \chi_\Omega * \mathcal{I} \nabla_v \chi_\Omega]. && (4.42)
\end{aligned}$$

By definition of the variation we obtain

$$V_v[\nabla_w C_\Omega] \overset{(4.41)}{\leq} V_w[\chi_\Omega] \, V_v[\chi_\Omega] \overset{2.12}{\leq} V[\chi_\Omega]^2 < \infty \qquad \text{for all } v \in \mathbb{S}^{n-1}. \tag{4.43}$$

Corollary 2.12 shows that $\nabla_w C_\Omega \in BV(\mathbb{T}^n)$ and formula (4.37) follows from the computations above. ■

We note that higher regularity cannot be expected globally as the Coavariogram and the Autocorrelation Function of a single laminate $S \coloneqq (0, \theta) \times \mathbb{T}^{n-1} \subset \mathbb{T}^n$ is not smooth, even though $S \in BV_2^\infty$ (see Section 4.4.3).

4.3. Local Regularity Properties

We will now focus on the case $n = 2$. As we have seen in Theorem 4.7 and Lemma 4.9, regularity of the set $\partial\Omega$ is connected to the regularity of the Covariogram and the

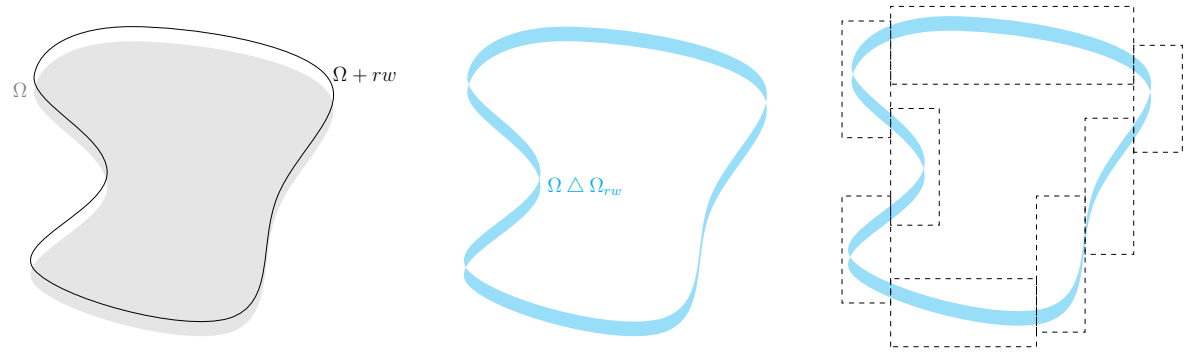

Figure 4.1.: Construction of the cuboids Q_i in Step 1 of the proof of Theorem 4.10.

Autocorrelation Function. We will now proceed by showing that they are smooth near the origin, if $\partial\Omega$ is sufficiently smooth. We will do so by localising the boundary in such a way that it is representable by a smooth graph. The Covariogram then is given by integrals of differences of smooth functions, which itself is smooth. As a reminder, we define (see Definition 2.17)

$$BV_2^\infty := \left\{\Omega \in BV_2 : \begin{smallmatrix}\Omega \text{ is open, } \partial\Omega \text{ is smooth, and } \nu^{-1}(\{w\}) \text{ has finitely} \\ \text{many connected components for all } w\in\mathbb{S}^1\end{smallmatrix}\right\}, \tag{4.44}$$

which is a dense class of sets in BV_2 (see Lemma 2.18).

Theorem 4.10 Let $\Omega \in BV_2^\infty$. Then there exists $R > 0$ such that $c_\Omega \in C^\infty((0, R])$.

Proof: We denote $\Omega_z := \Omega + z$. Then we have $C_\Omega(z) = |\Omega \cap \Omega_z|$. Let $r > 0$ and $w \in \mathbb{S}^1$. Then

$$C_\Omega(0) - C_\Omega(rw) = |\Omega_{rw} \setminus \Omega| = |\Omega \setminus \Omega_{rw}| = \frac{1}{2}|\Omega \triangle \Omega_{rw}|, \tag{4.45}$$

where $\triangle$ denotes the symmetric difference. Since $C_\Omega(0) = |\Omega|$ by Proposition 4.2 it hence remains to calculate $|\Omega \triangle \Omega_{rw}|$ and its dependence on r. We will do this is multiple steps:

Step 1: Localisation. Since Ω has a smooth boundary, for every $x \in \partial\Omega$ there exists $r_x > 0$, such that (possibly after rotation) $\partial\Omega \cap B_{4r_x}(x)$ is representable as a graph of a smooth function. So we find an open covering

$$\partial\Omega = \bigcup_{x\in\partial\Omega} \partial\Omega \cap Q_{3r_x}(x). \tag{4.46}$$

Since $\partial\Omega$ is compact, we find a finite subcovering, i.e. $N \in \mathbb{N}$, $x_i \in \partial\Omega$ and $r_i > 0$ such that

$$\partial\Omega = \bigcup_{i=1}^{N} \partial\Omega \cap Q_{3r_i}(x_i), \tag{4.47}$$

where $Q_t(y)$ denotes a cube of sidelength t with centre y. We define $Q_i := Q_{r_i}(x_i)$. Let

$U_i \subset \mathbb{R}$ open and $f_i \in C^\infty(U_i)$ such that (possibly after rotation) we have $\partial\Omega \cap Q_i = \operatorname{graph}(f_i)$. Without loss of generality we can assume $f_i \geq 1$, f_i' is a monotone function (due to the assumption on ν as $\Omega \in BV_2^\infty$), and $U_i = [-R_i, R_i]$. Also, after refining and changing from cubes to cuboids, without loss of generality we can assume that the family of cuboids $\{Q_i\}_i$ is pairwise essentially disjoint (see Figure 4.1). We define $R \coloneqq \frac{1}{4}\min\{r_1, \dots, r_N, \frac{1}{8}\}$.

We note that $\Omega \triangle \Omega_{rw} \subset \bigcup Q_{r_i}(x_i)$ for all $0 < r < R$. To see this, we first observe that for every $x \in \partial\Omega_{rw}$ there exists $\bar{x} \in \partial\Omega$, such that $x = \bar{x} + rw$. Thus, $x \in B_r(\bar{x}) \subset B_{\frac{R}{2}}(\bar{x})$. Likewise, for every $y \in \partial\Omega$ there exists $\bar{y} \in \partial\Omega_{rw}$ such that $y \in B_{\frac{R}{2}}(\bar{y})$. Now, let $x \in \Omega \triangle \Omega_{rw}$ and define $R_x \coloneqq \sup\{r > 0 : B_r(x) \subset \Omega \triangle \Omega_{rw}\}$. Using the above arguments, we have $R_x < R$ for all $x \in \Omega \triangle \Omega_{rw}$. Thus

$$\Omega \triangle \Omega_{rw} \subset (\partial\Omega + B_R(0)) \cup (\partial\Omega_{rw} + B_R(0)) \subset \bigcup_{i=1}^{N} Q_{r_i}(x_i), \tag{4.48}$$

as claimed. Thus, we find

$$|\Omega \triangle \Omega_{rw}| = \big|(\Omega \triangle \Omega_{rw}) \cap \bigcup_{i=1}^{N} Q_i\big| = \big|\bigcup_{i=1}^{N} (\Omega \triangle \Omega_{rw}) \cap Q_i\,\big| = \sum_{i=1}^{N} |(\Omega \triangle \Omega_{rw}) \cap Q_i|. \tag{4.49}$$

Step 2: Regularity via Graph representation. We will now focus on a fixed cube Q_i. By definition, $\Omega_{rw} \in BV_2^\infty$ and by construction we have $\partial\Omega_{rw} \cap Q_i = \operatorname{graph}(f_i^{(rw)})$, where

$$f_i^{(rw)}(x) \coloneqq \begin{cases} f_i(x + rw_1) + rw_2 & \text{if no rotation is needed,} \\ f_i(x + rw_2) + rw_1 & \text{if clockwise rotated,} \\ f_i(x - rw_2) + rw_1 & \text{if counter clockwise rotated,} \end{cases} \qquad \text{for all } x \in U_i.$$

We note that by definition of R, the functions $f^{(rw)}$ are also defined on $[-R_i, R_i]$ since the domain of f_i is at least $[-2R_i, 2R_i]$ (see (4.46)). Depending on w, we find the following possible cases:

- $f_i^{(rw)} < f_i$ in U_i. Then we compute (see Figure 4.2 b))

$$|(\Omega \triangle \Omega_{rw}) \cap Q_i| = \int_{-R_i}^{R_i} f_i(x) - f_i^{(rw)}(x)\,\mathrm{d}x. \tag{4.50}$$

- $f_i^{(rw)} > f_i$ in U_i. Then we compute (see Figure 4.2 b))

$$|(\Omega \triangle \Omega_{rw}) \cap Q_i| = \int_{-R_i}^{R_i} f_i^{(rw)}(x) - f_i(x)\,\mathrm{d}x. \tag{4.51}$$

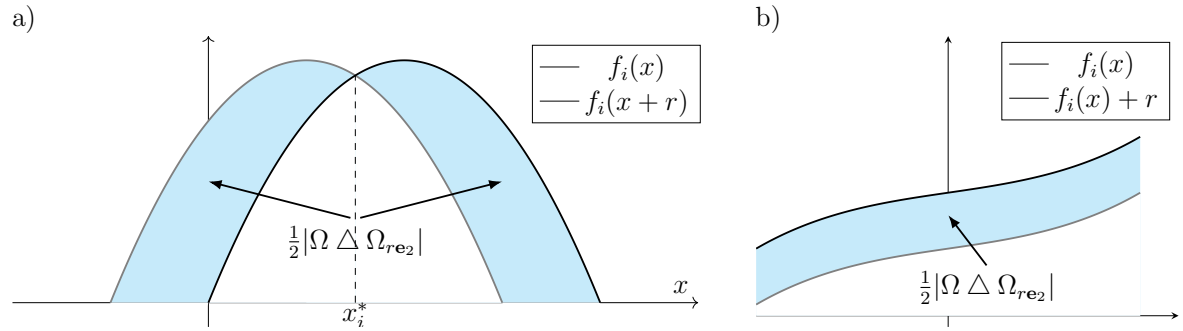

Figure 4.2.: Covariogram localised in in Q_i. a) shows horizontal displacement, b) shows vertical displacement.

- There exists $x_{i*}(rw), x_i^*(rw) \in U_i$, such that $x_{i*}(rw) < x_i^*(rw)$, $f_i(x) < f_i^{(rw)}(x)$ for all $x \in [-R_i, x_{i*}(rw)]$ and $f_i^{(rw)}(x) < f_i(x)$ for all $x \in [x_i^*(rw), R_i]$. Then we compute (see Figure 4.2 a))

$$|(\Omega \triangle \Omega_{rw}) \cap Q_i| = \int_{-R_i}^{x_{i*}(rw)} f_i^{(rw)}(x) - f_i(x)\,\mathrm{d}x \tag{4.52}$$

$$+ \int_{x_i^*(rw)}^{R_i} f_i(x) - f_i^{(rw)}(x)\,\mathrm{d}x. \tag{4.53}$$

- There exists $x_{i*}(rw), x_i^*(rw) \in U_i$, such that $x_{i*}(rw) < x_i^*(rw)$, $f_i^{(rw)}(x) < f_i(x)$ for all $x \in [-R_i, x_{i*}(rw)]$ and $f_i(x) < f_i^{(rw)}(x)$ for all $x \in [x_i^*(rw), R_i]$. Then we compute (see Figure 4.2 a))

$$|(\Omega \triangle \Omega_{rw}) \cap Q_i| = \int_{-R_i}^{x_{i*}(rw)} f_i(x) - f_i^{(rw)}(x)\,\mathrm{d}x \tag{4.54}$$

$$+ \int_{x_i^*(rw)}^{R_i} f_i^{(rw)}(x) - f_i(x)\,\mathrm{d}x. \tag{4.55}$$

The number of $w \in \mathbb{S}^1$ for which $x_{i*}(rw) < x_i^*(rw)$ are finite. This can only happen if there exists an open interval in U_i such that f_i' is constant in that interval (in other words, the part of $\partial\Omega$ described by f_i is flat).

Moreover, these values are characterised by the equation $f_i(x + rw_1) + rw_2 = f_i(x)$. Using the Implicit Function Theorem, $x_{i*}(rw)$ depends smoothly on rw. Thus the right-hand side depends smoothly on r and w in every case (4.50) – (4.54).

Step 3: Conclusion. Using the four cases in the previous step, we find four corresponding regimes in $\mathbb{S}^1$:

$$S_{i1} \coloneqq \{w \in \mathbb{S}^1 : (4.50) \text{ holds}\}, \qquad S_{i2} \coloneqq \{w \in \mathbb{S}^1 : (4.51) \text{ holds}\}, \tag{4.56}$$

$$S_{i3} \coloneqq \{w \in \mathbb{S}^1 : (4.52) \text{ holds}\}, \qquad S_{i4} \coloneqq \{w \in \mathbb{S}^1 : (4.54) \text{ holds}\}. \tag{4.57}$$

We note that $S_{i1}, \dots, S_{i4}$ are independent of r for all $0 < r < R$. Indeed, in case (4.50) we find that

$$f_i(x + rw_1) + rw_2 < f_i(x) \qquad \text{for all } x \in [-R_i, R_i]. \tag{4.58}$$

Using the Mean Value Theorem, we that (4.58) is equivalent to

$$f_i'(\zeta_r(x)) < -\frac{w_2}{w_1} \qquad \text{for all } x \in [-R_i, R_i], \tag{4.59}$$

where $\zeta_r(x) \in [-R_i, R_i]$. Due to the monotonicity of f_i', it suffices that either $f_i'(-R_i)$ or $f_i'(R_i)$ satisfies this condition, which is now independent of r. Thus S_{i1} is independent of r. Similarly, this holds for S_{i2} (with reversed sign in (4.58)).

In case (4.52), we first note that by the Implicit Function Theorem $x_{i*}(rw) = x_i^*(rw)$ for almost all $0 < r < R$ and $w \in \mathbb{S}^1$ and x_{i*} is a smooth function of r and w (inequality only occurs for flat parts of $\partial\Omega$). Moreover, as solution to the equation $f(x+rw_1)+rw_2 = f(x)$, we compute using the Implicit Function Theorem

$$x_{i*}'(rw) = -\frac{f_i'(x_{i*}(rw) + rw_1) + w_2}{f_i'(x_{i*}(rw) + rw_1) - f_i'(x_{i*}(rw))} \qquad \text{for all } 0 < r < R. \tag{4.60}$$

Due to the monotonicity of f_i', the function $r \longmapsto x_{i*}(rw)$ is monotonic and using Lemma A.16 also convergent as $r \to 0$. Thus, the set S_{i3} is independent of r. Similar reasoning shows that S_{i4} is independent of r.

In summary we obtain

$$\begin{aligned} c_\Omega(r) - c_\Omega(0) &= \fint_{\mathbb{S}^1} C_\Omega(rw) - C_\Omega(0) \,\mathrm{d}\mathscr{H}^1(w) && (4.61)\\ &= \frac{1}{2} \fint_{\mathbb{S}^1} \sum_{i=1}^{N} |(\Omega \triangle \Omega_{rw}) \cap Q_i| \,\mathrm{d}\mathscr{H}^1(w) && (4.62)\\ &= \frac{1}{2\sigma_2} \sum_{i=1}^{N} \sum_{j=1}^{4} \int_{S_{ij}} |(\Omega \triangle \Omega_{rw}) \cap Q_i| \,\mathrm{d}\mathscr{H}^1(w). && (4.63) \end{aligned}$$

Since the right-hand side is smooth for $0 < r < R$, we find that c_Ω is smooth. ■

We improve on the argument before to show the following:

Lemma 4.11 Let $\Omega \in BV_2^\infty$ and $w \in \mathbb{S}^1$. Then

$$\left(\frac{\mathrm{d}}{\mathrm{d}r}\right)^2 C_\Omega(rw)\Big|_{r=0} = 0. \tag{4.64}$$

Proof: Without loss of generality we choose $w = \mathbf{e}_2$. We use the notation as in the proof of Theorem 4.10. As before, we write

$$C_\Omega(r\mathbf{e}_2) - C_\Omega(0) = \frac{1}{2}|\Omega \triangle \Omega_{r\mathbf{e}_2}| = \frac{1}{2}\sum_{i=1}^{N} |(\Omega \triangle \Omega_{r\mathbf{e}_2}) \cap Q_i|, \tag{4.65}$$

We first note that the only cases $i \in \{1, \dots, N\}$ that contribute to $(\frac{\mathrm{d}}{\mathrm{d}r})^2 C_\Omega(rw)$ are those which need rotation for a graph representation. Indeed, if the graph representation does not need rotation, we compute (see Figure 4.2 b))

$$|(\Omega \triangle \Omega_{r\mathbf{e}_2}) \cap Q_i| = \Big| \int_{U_i} f_i(y) + r - f_i(y)\,\mathrm{d}y \Big| = r|U_i|. \tag{4.66}$$

Deriving twice with respect to r yields a trivial contribution.

We note that the graph representation requires rotation if and only if there exists $x \in \partial\Omega \cap Q_i$, such that $x \in \nu^{-1}(\pm\mathbf{e}_1)$, or equivalently $x \in (\nu^\perp)^{-1}(\{\pm\mathbf{e}_2\})$. Using the assumption $\Omega \in BV_2^\infty$, we know that there exist only finitely many such cubes Q_i independently of r. In this situation we have the following cases to consider:

Case 1: $f_i' = 0$. This means this section of $\partial\Omega$ is flat. Thus we compute $|(\Omega \triangle \Omega_{r\mathbf{e}_2}) \cap Q_i| = 0$.

Case 2: f_i' does not change sign. This means that f_i is either strictly increasing, or strictly decreasing. If f_i is strictly increasing, then $f_i(x) < f_i(x+r)$ for any $x \in U_i$. We compute

$$\begin{aligned}
|(\Omega \triangle \Omega_{r\mathbf{e}_2}) \cap Q_i| &= \int_{-R_i-r}^{R_i} f_i(y+r)\,\mathrm{d}y + \int_{-R_i}^{R_i-r} f_i(y+r) - f_i(y)\,\mathrm{d}y && (4.67)\\
&\quad + \int_{R_i-r}^{R_i} f_i\big((R_i - r) + r\big) - f(y)\,\mathrm{d}y && (4.68)\\
&= \int_{-R_i-r}^{R_i-r} f_i(y+r)\,\mathrm{d}y - \int_{-R_i}^{R_i} f_i(y)\,\mathrm{d}y + r f_i(R_i) && (4.69)\\
&= r f_i(R_i). && (4.70)
\end{aligned}$$

Deriving twice with respect to r gives a trivial contribution for right shift. For left shifts we note that $f_i(x-r) < f_i(x)$ for any $x \in U_i$. We compute

$$\begin{aligned}
|(\Omega \triangle \Omega_{r\mathbf{e}_2}) \cap Q_i| &= \int_{-R_i}^{-R_i+r} f_i(y)\,\mathrm{d}y + \int_{-R_i+r}^{R_i} f_i(y) - f_i(y-r)\,\mathrm{d}y && (4.71)\\
&\quad + \int_{R_i}^{R_i+r} f_i(R_i) - f(y-r)\,\mathrm{d}y && (4.72)\\
&= \int_{-R_i}^{R_i} f_i(y)\,\mathrm{d}y - \int_{-R_i+r}^{R_i+r} f_i(y-r)\,\mathrm{d}y + r f_i(R_i) && (4.73)\\
&= r f_i(R_i). && (4.74)
\end{aligned}$$

Deriving twice with respect to r gives a trivial contribution for left shifts. In the situation in which f_i is strictly decreasing, the overall signs in the computations above change and again, deriving twice yields a trivial contribution.

Case 3: f_i' changes sign. Since f_i' is assumed to be monotone, that means either f_i is strictly convex or strictly concave. We note that there exists a unique $\bar{x}_i \in U_i$ such that $f_i'(\bar{x}_i) = 0$. This value corresponds to the value $X_i \in (\nu^\perp)^{-1}(\{\pm \mathbf{e}_2\})$, where $\bullet^\perp$ denotes counter clockwise rotation.

As the curvature κ is extrinsic (meaning it depends on the orientation of $\mathbb{T}^2$), we need to be careful about the rotations to obtain the graph representation. Without loss of generality, we assume that all representations in terms of graphs are obtained by counter-clockwise rotations. In that case, the Covariogram is always computed by a left shift. In addition, we note the following:

- If $\kappa(X_i) > 0$ and $X_i \in (\nu^\perp)^{-1}(\{+\mathbf{e}_2\})$, then f_i is concave and thus $f_i''(\bar{x}_i) < 0$.
- If $\kappa(X_i) > 0$ and $X_i \in (\nu^\perp)^{-1}(\{-\mathbf{e}_2\})$, then f_i is convex and thus $f_i''(\bar{x}_i) > 0$.
- If $\kappa(X_i) < 0$ and $X_i \in (\nu^\perp)^{-1}(\{+\mathbf{e}_2\})$, then f_i is convex and thus $f_i''(\bar{x}_i) > 0$.
- If $\kappa(X_i) < 0$ and $X_i \in (\nu^\perp)^{-1}(\{-\mathbf{e}_2\})$, then f_i is concave and thus $f_i''(\bar{x}_i) < 0$.

Using the Implicit Function Theorem we find $x_i \in C^\infty(U_i)$ such that $f_i(x_i(r) + r) = f_i(x_i(r))$. Assume f_i is concave, we compute (see Figure 4.2 a))

$$|(\Omega \triangle \Omega_{r\mathbf{e}_2}) \cap Q_i| = \int_{-R_i - r}^{x_i^*(r)} f_i(y + r)\,\mathrm{d}y - \int_{-R_i}^{x_i^*(r)} f_i(y)\,\mathrm{d}y \tag{4.75}$$

$$+ \int_{x_i^*(r)}^{R_i} f_i(y)\,\mathrm{d}y - \int_{x_i^*(r)}^{R_i - r} f_i(y + r)\,\mathrm{d}y \tag{4.76}$$

$$= \int_{-R_i}^{x_i^*(r)+r} f(y)\,\mathrm{d}y - \int_{-R_i}^{x_i^*(r)} f(y)\,\mathrm{d}y \tag{4.77}$$

$$+ \int_{x_i^*(r)}^{R_i} f(y)\,\mathrm{d}y - \int_{x_i^*(r)+r}^{R_i} f(y)\,\mathrm{d}y \tag{4.78}$$

$$= 2\int_{x_i^*(r)}^{x_i^*(r)+r} f(y)\,\mathrm{d}y. \tag{4.79}$$

Deriving twice yields and using Lemma A.18 yields

$$\left(\frac{\mathrm{d}}{\mathrm{d}r}\right)^2 |(\Omega \triangle \Omega_{r\mathbf{e}_2}) \cap Q_i| \xrightarrow{r \searrow 0} 0, \tag{4.80}$$

In the case when f_i is convex, we find with a similar computation

$$|(\Omega \triangle \Omega_{r\mathbf{e}_2}) \cap Q_i| = -2\int_{x_i^*(r)}^{x_i^*(r)+r} f(y)\,\mathrm{d}y, \tag{4.81}$$

and as before a trivial contribution to the second derivative.

Thus, in all cases, the contribution to the second derivative of the Covariogram C_Ω are trivial in the limit $r \searrow 0$ and the claim follows. ■

Corollary 4.12 Let $\Omega \in BV_2^\infty$. Then $c''_\Omega(0) = 0$.

Proof: Using Theorem 4.10 we know c_Ω is smooth near the origin. Using Lemma 4.11 and the Dominated Convergence Theorem we find for $r \to 0$

$$c''_\Omega(r) = \frac{1}{\sigma_2} \int_{\mathbb{S}^1} \left(\frac{\mathrm{d}}{\mathrm{d}r}\right)^2 C_\Omega(rw)\, \mathrm{d}\mathscr{H}^1(w) \xrightarrow{r\to 0} 0, \tag{4.82}$$

which concludes the proof. ■

Third derivative of the Autocorrelation function In what follows we compute the third derivative of the Autocorrelation Function for smooth sets. As we have seen in the section before, the only contributions to the derivatives of the Autocorelation Function is at points tangential to the normal vector, i.e. elements of $(\nu^\perp)^{-1}(\{w\})$. We use the same procedure to obtain the following result:

Lemma 4.13 Let $\Omega \in BV^\infty$ and $w \in \mathbb{S}^1$. Then

$$\left(\frac{\mathrm{d}}{\mathrm{d}r}\right)^3 C_\Omega(rw)\Big|_{r=0} = \frac{1}{2} \int_{(\nu^\perp)^{-1}(\{w\})} |\kappa|\, \mathrm{d}\mathscr{H}^0, \tag{4.83}$$

where $\nu : \partial\Omega \longrightarrow \mathbb{S}^1$ denotes the Gauß map and $\kappa \colon \partial\Omega \longrightarrow \mathbb{R}$ denotes the curvature.

Proof: Without loss of generality we choose $w = \mathbf{e}_2$. We use the notation as in the proof of Theorem 4.10 and Lemma 4.11. As we have seen in the proof of Lemma 4.11, the only cases that have a non-trivial contribution to the third derivative are $\nu = \pm\mathbf{e}_1$ (i.e. $w \in (\nu^\perp)^{-1}(\mathbf{e}_2)$). Thus, we need to analyse the contributions of the form

$$|(\Omega \triangle \Omega_{r\mathbf{e}_2}) \cap Q_i| = 2 \int_{x_i^*(r)}^{x_i^*(r)+r} f_i(y)\, \mathrm{d}y \qquad \text{if } f_i \text{ is concave,} \tag{4.84}$$

$$|(\Omega \triangle \Omega_{r\mathbf{e}_2}) \cap Q_i| = -2 \int_{x_i^*(r)}^{x_i^*(r)+r} f_i(y)\, \mathrm{d}y \qquad \text{if } f_i \text{ is convex,} \tag{4.85}$$

where $x_i^* \in C^\infty(U_i)$ such that $f_i(x_i^*(r)+r) = f_i(x_i^*(r))$. We note that there exists a unique $\bar{x}_i \in U_i$ such that $f_i'(\bar{x}_i) = 0$ (since flat parts of the boundary have already been dealt

with in the first case of the proof of Lemma 4.11). Thus, using Lemma A.19, we obtain

$$\Big(\frac{\mathrm{d}}{\mathrm{d}r}\Big)^3 |(\Omega \triangle \Omega_{r\mathbf{e}_2}) \cap Q_i| \xrightarrow{r\to 0} -\frac{1}{2} f_i''(\bar{x}_i) \qquad \text{if } f_i \text{ is concave,} \tag{4.86}$$

$$\Big(\frac{\mathrm{d}}{\mathrm{d}r}\Big)^3 |(\Omega \triangle \Omega_{r\mathbf{e}_2}) \cap Q_i| \xrightarrow{r\to 0} \frac{1}{2} f_i''(\bar{x}_i) \qquad \text{if } f_i \text{ is convex.} \tag{4.87}$$

Since $f_i'(\bar{x}_i) = 0$, we have $\kappa = f''(\bar{x}_i)$. As described in the proof of Lemma 4.11 in Case 3, we therefore obtain

$$\Big(\frac{\mathrm{d}}{\mathrm{d}r}\Big)^3 |(\Omega \triangle \Omega_{r\mathbf{e}_2}) \cap Q_i| \xrightarrow{r\to 0} -\frac{1}{2}|\kappa|, \tag{4.88}$$

from which the claim follows. Note that the negative sign comes from the difference $C_\Omega(0) - C_\Omega(rw)$ in (4.45). ■

To derive the quantity $c_\Omega'''(0)$ from Lemma 4.13, we integrate over all directions $w \in \mathbb{S}^1$ and we aim to use the Coarea Formula to relate integrals over $(\nu^\perp)^{-1}(\{w\})$ and $\mathbb{S}^1$ back to Ω. For this reason, we need the Jacobian of the outer unit vector ν. As a reminder, given a smooth map $f\colon M \longrightarrow N$ between two smooth manifolds, the Jacobian $\mathrm{Jac}_f(x)\colon M \longrightarrow \mathbb{R}$ is defined via

$$\mathrm{Jac}_f(x) \coloneqq \det(\mathrm{D}_x f\, \mathrm{D}_x f^*)^{\frac{1}{2}} \qquad \text{for all } x \in M, \tag{4.89}$$

where $\mathrm{D}_x f\colon \mathsf{T}_x M \longrightarrow \mathsf{T}_{f(x)} N$ denotes the differential map and $\bullet^*$ the adjoint.

Lemma 4.14 Let $\Omega \subset \mathbb{T}^2$ be smooth and let $\nu\colon \partial\Omega \longrightarrow \mathbb{S}^1$ be the outward normal vector. Then

$$\mathrm{Jac}_\nu(x) = \mathrm{Jac}_{\nu^\perp}(x) = |\kappa(x)| \qquad \text{for all } x \in \partial\Omega. \tag{4.90}$$

Proof: By definition, the curvature $\kappa\colon \partial\Omega \longrightarrow \mathbb{R}$ is defined as the unique constant such that (see Definition 2.3)

$$\ddot{\gamma}(0) = \kappa(x)\, \nu^\perp(x), \tag{4.91}$$

where $\gamma \in C^\infty((-\varepsilon, \varepsilon), \partial\Omega)$ is a parametrisation of $\partial\Omega$ around x for some $\varepsilon > 0$ sufficiently small, i.e. $\gamma(0) = x$ and $|\dot{\gamma}| = 1$. We note that without loss of generality $\dot{\gamma}(0) = \nu^\perp(x)$. For details, see Section 2.1.1. Using the Chain Rule we find

$$\kappa(x)\, \nu^\perp(x) = \kappa(\gamma(0))\, \nu(\gamma(0))^\perp = (\mathrm{D}_0 \dot{\gamma})(\partial_t) \tag{4.92}$$

$$= \mathrm{D}_0(\nu^\perp \circ \gamma)(\partial_t) = (\mathrm{D}_{\gamma(0)} \nu^\perp)(\mathrm{D}_0 \gamma(\partial_t)) \tag{4.93}$$

$$= (\mathrm{D}_x \nu^\perp)(\dot{\gamma}(0)) = (\mathrm{D}_x \nu^\perp)(\nu^\perp(x)). \tag{4.94}$$

Thus, we find that $\nu(x)^\perp$ is an eigenvector of $\mathrm{D}_x\nu^\perp$ with eigenvalue $\kappa(x)$ and thus

$$\mathrm{Jac}_{\nu^\perp}(x)^2 = \kappa(x)^2 \tag{4.95}$$

as claimed. Since the inverse operator to $\bullet^\perp$ is given by $-\bullet^\perp$ we find

$$\mathrm{Jac}_{\nu}(x)^2 = \det(\mathrm{D}_x\nu\,\mathrm{D}_x\nu^*) = \det(\mathrm{D}_x\nu^\perp \mathrm{D}_x\nu^{\perp *}) = \mathrm{Jac}_{\nu^\perp}(x)^2 \tag{4.96}$$

as claimed. ■.

With this formula at hand, we are able to obtain the following result concerning the third derivative of the Autocorrelation Function.

Corollary 4.15 Let $\Omega \in BV_2^\infty$. Then

$$c_\Omega'''(0) = \frac{1}{4\pi}\int_{\partial\Omega} \kappa^2 \,\mathrm{d}\mathscr{H}^1, \tag{4.97}$$

where $\kappa\colon \partial\Omega \longrightarrow \mathbb{R}$ denotes the curvature.

Proof: Using Lemma 4.13 we find

$$\begin{aligned}
c_\Omega'''(r) &= \frac{1}{\sigma_2}\int_{\mathbb{S}^1} \left(\frac{\mathrm{d}}{\mathrm{d}r}\right)^3 C_\Omega(rw)\,\mathrm{d}\mathscr{H}^1(w) && (4.98)\\
&\xrightarrow{r\searrow 0} \frac{1}{\sigma_2}\int_{\mathbb{S}^1} \left(\frac{\mathrm{d}}{\mathrm{d}r}\right)^3 C_\Omega(0)\,\mathrm{d}\mathscr{H}^1(w) && (4.99)\\
&= \frac{1}{2\sigma_2}\int_{\mathbb{S}^1}\int_{\nu^{-1}(\{w\})} \kappa(x)\,\mathrm{d}\mathscr{H}^0(x)\,\mathrm{d}\mathscr{H}^1(w) && (4.100)\\
&= \frac{1}{2\sigma_2}\int_{\partial\Omega} |\kappa(x)|\,\mathrm{Jac}_{\nu^\perp}(x)\,\mathrm{d}\mathscr{H}^1(x) && (4.101)\\
&= \frac{1}{4\pi}\int_{\partial\Omega} \kappa^2\,\mathrm{d}\mathscr{H}^1, && (4.102)
\end{aligned}$$

where we used the Coarea Formula (see Theorem A.9), Lemma 4.14 and $\sigma_2 = 2\pi$. ■

We note two interesting facts about this formula. First, in Lemma 4.17 it is shown that for a polytope $\Omega \subset \mathbb{T}^2$ there exist $a \geq 0$ and $b, d > 0$ such that

$$c_\Omega(r) = ar^2 - br + d \qquad \text{for all } 0 < r \ll 1. \tag{4.103}$$

Deriving three times we obtain $c_\Omega'''(0) = 0$, matching the result of Corollary 4.15 even though $\Omega \notin BV_2^\infty$. However, in Section 4.4.5 it is shown that $c'''_{\Omega_{2R,R}}(0)$ does not exist for

n	$\mathfrak{c}_{B_R(0)}(r)$
2	$2R^2 \arccos(\frac{r}{2R}) - \frac{r}{2}\sqrt{4R^2 - r^2}$
3	$\frac{\pi}{12}(4R + r)(2R - r)^2$
4	$2\pi R^4 \operatorname{arccot}\left(\frac{2R+r}{\sqrt{4R^2-r^2}}\right) - \frac{\pi}{24} r\sqrt{4R^2 - r^2}(10R^2 - r^2)$
5	$\frac{\pi^2}{480}(2R - r)^3(3r^2 + 18rR + 32R^2)$

Figure 4.3.: Explicit expressions of the Autocorrelation Funtion of B_R for $0 < r < 2R$ for dimensions $2 \leq n \leq 5$.

the cusp domain $\Omega_{2R,R} \coloneqq B_R(-R\mathbf{e}_1) \cup B_R(R\mathbf{e}_2)$, even though there only exists one point on $\partial\Omega_{2R,R}$ which has a cusp. Moreover, the quantity

$$\int_{\partial\Omega_{2R,R}} \kappa^2 \,\mathrm{d}\mathscr{H}^1 = \frac{4\pi}{R} \tag{4.104}$$

exists and is finite but does not match $c'''_{\Omega_{2R,R}}(0)$.

4.4. Examples

We will now discuss some explicit examples of Autocorrelation Functions. We note that in most cases, we cannot compute $c_\Omega(r)$ for all $r > 0$ since the symmetrisation for large r is too complicated to compute. Thus, some sections will compute $\mathfrak{c}_\Omega$, knowing that in most cases $\mathfrak{c}_\Omega(r) = c_\Omega(r)$ for $0 < r \ll 1$ (see (4.9)).

4.4.1. Single Ball

In this section, we will compute the autocorrelation function of a single ball of radius $R > 0$. Due to symmetry we have $\mathfrak{c}_{B_R(0)}(r) = \mathscr{C}_{B_R(0)}(r\mathbf{e}_n)$. We compute for $0 < r < 2R$ via Tonelli's Theorem

$$\mathfrak{c}_{B_R(0)}(r) = |B_R(0) \cap B_R(r\mathbf{e}_n)| = \left| \left\{ \begin{array}{l} |x'|^2 \leq R^2 - x_n^2 \\ |x'|^2 \leq R^2 - (x_n - r)^2 \end{array} \right\} \right| \tag{4.105}$$

$$= \int_{r-R}^{\frac{r}{2}} |B^{n-1}_{\sqrt{R^2-(x_n-r)^2}}(0)| \,\mathrm{d}x_n + \int_{\frac{r}{2}}^{R} |B^{n-1}_{\sqrt{R^2-x_n^2}}(0)| \,\mathrm{d}x_n \tag{4.106}$$

$$= 2\int_{\frac{r}{2}}^{R} |B^{n-1}_{\sqrt{R^2-x_n^2}}(0)| \,\mathrm{d}x_n \tag{4.107}$$

$$= 2\omega_{n-1} \int_{\frac{r}{2}}^{R} (R^2 - x_n)^{\frac{n-1}{2}} \, \mathrm{d}x_n \tag{4.108}$$

$$= 2\omega_{n-1} R^n \int_{\frac{r}{2R}}^{1} (1 - t^2)^{\frac{n-1}{2}} \, \mathrm{d}t, \tag{4.109}$$

where $B_\rho^{n-1}(0) \coloneqq \{x' \in \mathbb{R}^{n-1} : |x'| < \rho\}$. Solving this integral involves the Hypergeometric Function ${}_2F_1$. However, higher derivatives can be computed explicitly: for $0 < r < 2R$ we have

$$\mathfrak{c}'_{B_R(0)}(r) = -2^{1-n}\omega_{n-1}(4R^2 - r^2)^{\frac{n-1}{2}} \tag{4.110}$$

$$\mathfrak{c}''_{B_R(0)}(r) = 2^{1-n}(n-1)\omega_{n-1} r (4R^2 - r^2)^{\frac{n-3}{2}} \tag{4.111}$$

$$\mathfrak{c}'''_{B_R(0)}(r) = 2^{1-n}(n-1)\omega_{n-1}(4R^2 - r^2)^{\frac{n-5}{2}}(4R^2 - (n-2)r^2) \tag{4.112}$$

$$\mathfrak{c}^{(iv)}_{B_R(0)}(r) = 2^{1-n}(n-3)(n-1)\omega_{n-1} r((n-2)r^2 - 12R^2)(4R^2 - r^2)^{\frac{n-7}{2}} \tag{4.113}$$

$$\mathfrak{c}^{(v)}_{B_R(0)}(r) = -2^{1-n}(n-3)(n-1)\omega_{n-1}(4R^2 - r^2)^{\frac{n-9}{2}} \tag{4.114}$$

$$\times ((n-4)(n-2)r^4 - 24(n-4)r^2R^2 + 48R^4) \tag{4.115}$$

We note that the Autocorrelation Function is a polynomial of degree n for odd dimensions $n \in 2\mathbb{N} + 1$.

4.4.2. Annulus

In this section, we compute the Autocorrelation Function of an annulus. For this purpose, let $0 < \rho < R$ be fixed and define $A_{\rho,R} \coloneqq B_R(0) \setminus B_\rho(0) \subset \mathbb{R}^n$. Similar to the previous section, we will stick to the Euclidean case and since annulli are radially symmetric, we have $\mathfrak{c}_{A_{\rho,R}}(r) = \mathscr{C}_{A_{\rho,R}}(r\mathbf{e}_1)$. As two balls with different radii are interacting now, we need to compute different lense segments along r. Thus, we recall the volume for a lense element

n	$\mathfrak{c}_{B_R(0)}(0)$	$\mathfrak{c}'_{B_R(0)}(0)$	$\mathfrak{c}''_{B_R(0)}(0)$	$\mathfrak{c}'''_{B_R(0)}(0)$	$\mathfrak{c}^{(iv)}_{B_R(0)}(0)$	$\mathfrak{c}^{(v)}_{B_R(0)}(0)$
2	πR^2	$-2R$	0	$\frac{1}{2R}$	0	$-\frac{3}{8R^3}$
3	$\frac{4}{3}\pi R^3$	$-\pi R^2$	0	$\frac{\pi}{2}$	0	0
4	$\frac{1}{2}\pi^2 R^4$	$-\frac{4\pi}{3}R^3$	0	πR	0	$-\frac{3\pi}{4R}$
5	$\frac{8}{15}\pi^2 R^5$	$-\frac{\pi^2}{2}R^4$	0	$\frac{\pi^2}{2}R^2$	0	$\frac{-3\pi^2}{4}$

Figure 4.4.: Higher derivatives of the autocorrelation of balls of radius R for $0 < r < 2R$ for dimensions $2 \leq n \leq 5$ evaluated at 0.

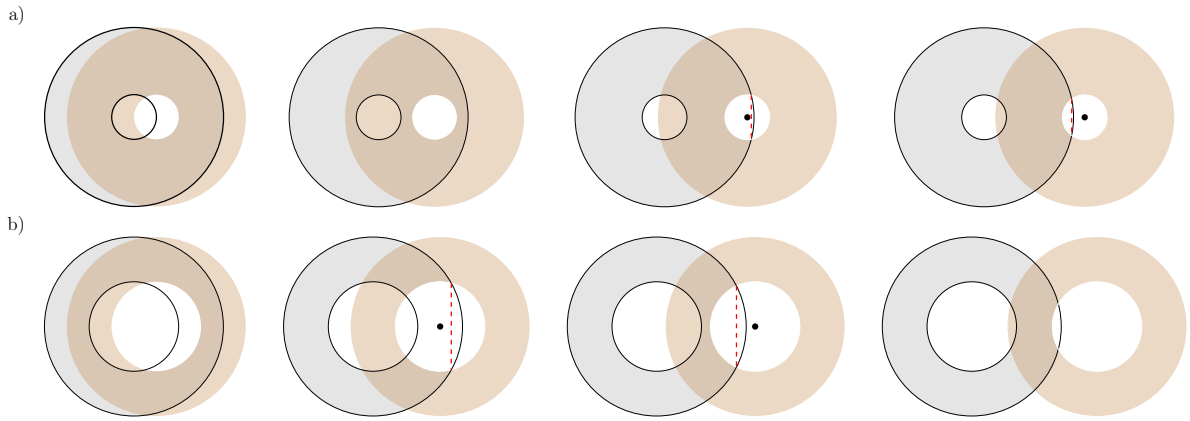

Figure 4.5.: Setup of Annulus for different ratios of the radii. The point represents $r\mathbf{e}_1$ and the red line is at $x = \sqrt{R^2 - \rho^2}$. a) shows $2\rho < R$, b) shows $2\rho > R$.

of a circle with radius R and triangular height d (see (4.109))

$$L(R, d) = \omega_{n-1} R^n \int_{\frac{d}{R}}^{1} (1 - t^2)^{\frac{n-1}{2}} \, \mathrm{d}t \qquad \text{for all } 0 < d < R. \tag{4.116}$$

There are two cases to consider based on the ratio of the two circles. A big ratio assures that the inner circle of $A_{\rho,R} + r\mathbf{e}_1$ is not crossing both components of $\partial A_{\rho,R}$ at the same time.

The case $R > 2\rho$: In this situation, the inner circle of $A_{\rho,R} + r\mathbf{e}_1$ is not crossing both components of $\partial A_{\rho,R}$ at the same time. We have the following cases:

- For $0 < r < 2\rho$ we have (see the first picture of Figure 4.5 a))

$$\mathfrak{c}_{A_{\rho,R}}(r) = \mathfrak{c}_{B_R}(r) - |B_\rho(0)| - |B_\rho(r\mathbf{e}_1)| + \mathfrak{c}_{B_\rho}(r) = \mathfrak{c}_{B_R}(r) + \mathfrak{c}_{B_\rho}(r) - 2|B_\rho|. \tag{4.117}$$

- For $2\rho < r < R - \rho$ we have (see the second picture of Figure 4.5 a))

$$\mathfrak{c}_{A_{\rho,R}}(r) = \mathfrak{c}_{B_R}(r) - |B_\rho(0)| - |B_\rho(r\mathbf{e}_1)| = \mathfrak{c}_{B_R}(r) - 2|B_\rho|. \tag{4.118}$$

- For $R - \rho < r < \sqrt{R^2 - \rho^2}$, we have (see the third picture of Figure 4.5 a))

$$\mathfrak{c}_{A_{\rho,R}}(r) = \mathfrak{c}_{B_R}(r) - 2\big(|B_\rho(0)| - L(\rho, \tfrac{R^2-\rho^2+r^2}{2r} - r) + L(R, \tfrac{R^2-\rho^2+r^2}{2r})\big). \tag{4.119}$$

  The conditions on r ensure that the centre of the translated annulus is to the left of the red line (see the third picture of Figure 4.5 a)).

- For $\sqrt{R^2 - \rho^2} < r < R + \rho$, we have (see the fourth picture of Figure 4.5 a))

$$\mathfrak{c}_{A_{\rho,R}}(r) = \mathfrak{c}_{B_R}(r) - 2\big(L(\rho, r - \tfrac{R^2-\rho^2+r^2}{2r}) + L(R, \tfrac{R^2-\rho^2+r^2}{2r})\big). \tag{4.120}$$

The conditions on r ensure that the centre of the translated annulus is to the right of the red line (see the fourth picture of Figure 4.5 a)).

- For $r > R + \rho$ we have

$$\mathfrak{c}_{A_{\rho,R}}(r) = \mathfrak{c}_{B_R}(r). \tag{4.121}$$

The case $R < 2\rho$: This situation is more complicated to compute as the inner circle of $A_{\rho,R} + r\mathbf{e}_1$ is crossing both components of $\partial A_{\rho,R}$ at the same time.

- For $0 < r < R - \rho$ we have (see the first picture of Figure 4.5 b))

$$\mathfrak{c}_{A_{\rho,R}}(r) = \mathfrak{c}_{B_R}(r) - |B_\rho(0)| - |B_\rho(r\mathbf{e}_1)| + \mathfrak{c}_{B_\rho}(r) = \mathfrak{c}_{B_R}(r) + \mathfrak{c}_{B_\rho}(r) - 2|B_\rho|. \tag{4.122}$$

- For $R - \rho < r < \sqrt{R^2 - \rho^2}$ we have (see the second picture of Figure 4.5 b))

$$\mathfrak{c}_{A_{\rho,R}}(r) = \mathfrak{c}_{B_R}(r) + \mathfrak{c}_{B_\rho}(r) - |B_\rho(0)| + 2L(\rho, \tfrac{R^2-\rho^2+r^2}{2r} - r) - 2L(R, \tfrac{R^2-\rho^2+r^2}{2r}) \tag{4.123}$$

The conditions on r ensure that the centre of the translated annulus is to the left of the red line (see the second picture of Figure 4.5 b)).

- For $\sqrt{R^2 - \rho^2} < r < 2\rho$, we have (see the third picture of Figure 4.5 b))

$$\mathfrak{c}_{A_{\rho,R}}(r) = \mathfrak{c}_{B_R}(r) + \mathfrak{c}_{B_\rho}(r) - 2L(\rho, r - \tfrac{R^2-\rho^2+r^2}{2r}) - 2L(R, \tfrac{R^2-\rho^2+r^2}{2r})\big). \tag{4.124}$$

The conditions on r ensure that the centre of the translated annulus is to the right of the red line (see the third picture of Figure 4.5 b)).

- For $2\rho < r < R + \rho$, we have (see the fourth picture of Figure 4.5 b))

$$\mathfrak{c}_{A_{\rho,R}}(r) = \mathfrak{c}_{B_R}(r) - 2\big(L(\rho, r - \tfrac{R^2-\rho^2+r^2}{2r}) + L(R, \tfrac{R^2-\rho^2+r^2}{2r})\big). \tag{4.125}$$

- For $R + \rho < r < 2R$ we have

$$\mathfrak{c}_{A_{\rho,R}}(r) = \mathfrak{c}_{B_R}(r). \tag{4.126}$$

4.4.3. Laminate

In this section, we will compute the autocorrelation function of a laminate on the torus, since laminates are no sets of finite perimeter in $\mathbb{R}^n$. Let $0 < \theta < 1$ and define $S \coloneqq \mathbb{T}^{n-1} \times (0, \theta) \subset \mathbb{T}^n$. We remark that in order to compute c_Ω, we can assume $0 < \theta < \frac{1}{2}$ since $c_{S^c}(r) = 1 - 2\theta + c_S(r)$.

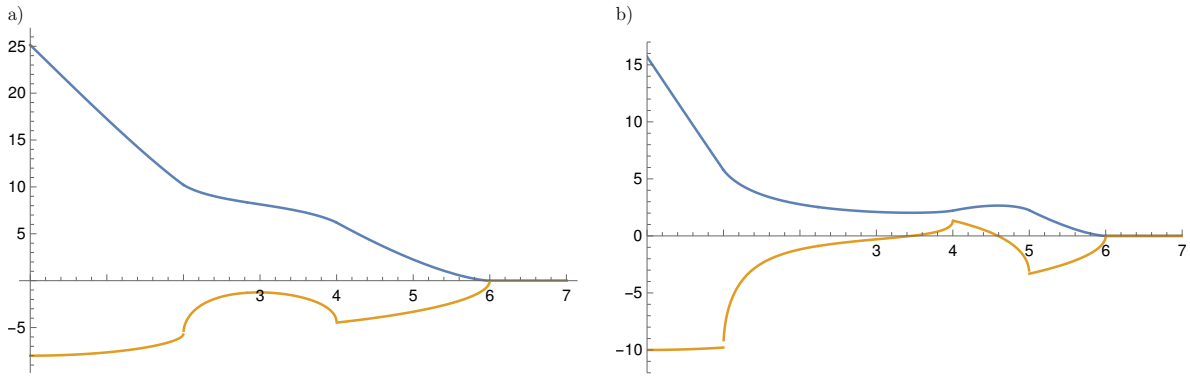

Figure 4.6.: Graphs of $c_{A_{\rho,R}}$ (blue) and $c'_{A_{\rho,R}}$ (orange) with $R = 3$ and a) $\rho = 1$, b) $\rho = 2$.

We first observe that by definition of S we have $C_S(z) = C_S(z_n)$ for all $z \in \mathbb{T}^n$. Thus, in order to compute $c_S(r)$, we only need to compute $C_S(r\mathbf{e}_n)$, which is given by

$$C_S(r\mathbf{e}_n) = \begin{cases} \theta - r & \text{for all } 0 < r - \lfloor r \rfloor < \theta, \\ 0 & \text{for all } \theta < r - \lfloor r \rfloor < 1 - \theta, \\ r - (1-\theta) & \text{for all } 1 - \theta < r - \lfloor r \rfloor < 1, \end{cases} \tag{4.127}$$

We define $g\colon B_1^{n-1} \longrightarrow \mathbb{S}^{n-1} \cap \mathbb{H}^n_+$ via $g(\xi) \coloneqq \sqrt{1 - |\xi|^2}$. Using the symmetry $C_S(z) = C_S(-z)$ (see Proposition 4.2) and the formula for integration over graphs, we obtain

$$c_S(r) = \frac{1}{\sigma_n} \int_{\mathbb{S}^{n-1}} C_S(rw) \, \mathrm{d}\mathscr{H}^{n-1}(w) \tag{4.128}$$

$$= \frac{2}{\sigma_n} \int_{\mathbb{S}^{n-1} \cap \mathbb{H}^n_+} C_S(rw) \, \mathrm{d}\mathscr{H}^{n-1}(w) \tag{4.129}$$

$$= \frac{2}{\sigma_n} \int_{B_1^{n-1}} \frac{C_S(r\xi, r\sqrt{1 - |\xi|^2})}{\sqrt{1 - |\xi|^2}} \, \mathrm{d}\xi. \tag{4.130}$$

Since $C_S(z) = C_S(z_n)$ for all $z \in \mathbb{T}^n$, we derive from the radial symmetry

$$c_S(r) = \frac{2\sigma_{n-1}}{\sigma_n} \int_0^1 \rho^{n-2} \frac{C_S(r\sqrt{1-\rho^2}\mathbf{e}_n)}{\sqrt{1-\rho^2}} \, \mathrm{d}\rho \tag{4.131}$$

$$= \frac{2\sigma_{n-1}}{\sigma_n} \int_0^{\frac{\pi}{2}} \sin^{n-2}(\alpha) \, C_S(r\cos(\alpha)\mathbf{e}_n) \, \mathrm{d}\alpha. \tag{4.132}$$

We will now turn to the explicit computation regarding $C_S(r\cos(\alpha)\mathbf{e}_n)$.

$$\int_0^{\frac{\pi}{2}} \sin^{n-2}(\alpha)\, C_S(r\cos(\alpha)\mathbf{e}_n)\,\mathrm{d}\alpha \tag{4.133}$$

$$= \mathrm{Rem}_\theta(r) + \sum_{k=0}^{\lfloor r\rfloor -1} \int_{\mathrm{acos}(\frac{k+\theta}{r})}^{\mathrm{acos}(\frac{k}{r})} \sin^{n-2}(\alpha)(\theta - r\cos(\alpha))\,\mathrm{d}\alpha \tag{4.134}$$

$$+ \sum_{k=0}^{\lfloor r\rfloor -1} \int_{\mathrm{acos}(\frac{k+1}{r})}^{\mathrm{acos}(\frac{k+1-\theta}{r})} \sin^{n-2}(\alpha)(r\cos(\alpha) - (1-\theta))\,\mathrm{d}\alpha \tag{4.135}$$

where we introduced

$$\mathrm{Rem}_\theta(r) \coloneqq \begin{cases} \displaystyle\int_0^{\mathrm{acos}(\frac{\lfloor r\rfloor}{r})} \sin^{n-2}(\alpha)(\theta - r\cos(\alpha))\,\mathrm{d}\alpha & \text{for all } 0 < r - \lfloor r\rfloor < \theta, \\ \displaystyle\int_{\mathrm{acos}(\frac{\lfloor r\rfloor+\theta}{r})}^{\mathrm{acos}(\frac{\lfloor r\rfloor}{r})} \sin^{n-2}(\alpha)(\theta - r\cos(\alpha))\,\mathrm{d}\alpha & \text{for all } \theta < r - \lfloor r\rfloor < 1-\theta, \\ \displaystyle\int_{\mathrm{acos}(\frac{\lfloor r\rfloor+\theta}{r})}^{\mathrm{acos}(\frac{\lfloor r\rfloor}{r})} \sin^{n-2}(\alpha)(\theta - r\cos(\alpha))\,\mathrm{d}\alpha & \\ \quad + r\displaystyle\int_0^{\mathrm{acos}(\frac{\lfloor r\rfloor+1-\theta}{r})} \sin^{n-2}(\alpha)\cos(\alpha)\,\mathrm{d}\alpha & \text{for all } 1-\theta < r - \lfloor r\rfloor. \\ \quad -(1-\theta)\displaystyle\int_0^{\mathrm{acos}(\frac{\lfloor r\rfloor+1-\theta}{r})} \sin^{n-2}(\alpha)\,\mathrm{d}\alpha & \end{cases}$$

Solving these integrals explicitly involves the Hypergeometric Function ${}_2F_1$ (different representations of these integrals are given in Lemma A.11 and Lemma A.12). However, we see that c_S is an affine linear function near the origin, i.e. for all $0 < r < \theta$ we compute

$$c_S(r) = \mathrm{Rem}_\theta(r) = \frac{2\sigma_{n-1}}{\sigma_n} \int_0^{\frac{\pi}{2}} \sin^{n-2}(\alpha)\, C_S(r\cos(\alpha)\mathbf{e}_n)\,\mathrm{d}\alpha \tag{4.136}$$

$$= \frac{2\sigma_{n-1}}{\sigma_n} \int_0^{\frac{\pi}{2}} \sin^{n-2}(\alpha)\,(\theta - r\cos(\alpha))\,\mathrm{d}\alpha \tag{4.137}$$

$$= \theta - r\frac{2\sigma_{n-1}}{\sigma_n} \int_0^{\frac{\pi}{2}} \sin^{n-2}(\alpha)\,\cos(\alpha)\,\mathrm{d}\alpha \tag{4.138}$$

$$= \theta - \frac{2\sigma_{n-1}}{\sigma_n(n-1)} = \theta - 2\frac{\omega_{n-1}}{n\omega_n}, \tag{4.139}$$

where in the last line we used the identity $n\omega_n = \sigma_n$. As $n = 2$ is the physical relevant dimension in the modelling in Chapter 3, we explicitly write down the autocorrelation function for the derivative c_S'. We remark that c_S is smooth except for $r \in \mathbb{N} \cup (\theta + \mathbb{N}) \cup ((1-\theta) + \mathbb{N})$.

Lemma 4.16 Let $0 < \theta < 1$ and $S := (0, \theta) \times \mathbb{T}^{n-1}$. Then $c_S \in C^{0,1}(\mathbb{R}_+)$ and for almost all $r > 0$:

$$\frac{\pi}{2} c_S'(r) = \mathrm{Rem}_\theta'(r) + \frac{\theta}{r}\left(\frac{1}{r} - \frac{\lfloor r \rfloor}{\sqrt{r^2 - \lfloor r \rfloor^2}}\right)$$

$$+ \frac{1}{r} \sum_{k=0}^{\lfloor r \rfloor - 1} -\sqrt{r^2 - k^2} - \sqrt{r^2 - (k+1)^2} + \sqrt{r^2 - (k+\theta)^2} + \sqrt{r^2 - (k+1-\theta)^2},$$

where

$$\mathrm{Rem}_\theta'(r) := \frac{1}{r} \begin{cases} \frac{\theta \lfloor r \rfloor}{\sqrt{r^2 - \lfloor r \rfloor^2}} - \sqrt{r^2 - \lfloor r \rfloor^2} & \text{for all } 0 < r - \lfloor r \rfloor < \theta, \\ \frac{\theta \lfloor r \rfloor}{\sqrt{r^2 - \lfloor r \rfloor^2}} - \sqrt{r^2 - \lfloor r \rfloor^2} & \\ \quad + \sqrt{r^2 - (\lfloor r \rfloor + \theta)^2} & \text{for all } \theta < r - \lfloor r \rfloor < 1 - \theta, \\ \frac{\theta \lfloor r \rfloor}{\sqrt{r^2 - \lfloor r \rfloor^2}} - \sqrt{r^2 - \lfloor r \rfloor^2} & \\ \quad + \sqrt{r^2 - (\lfloor r \rfloor + \theta)^2} & \text{for all } 1 - \theta < r - \lfloor r \rfloor < 1. \\ \quad + \sqrt{r^2 - (\lfloor r \rfloor + 1 - \theta)^2} & \end{cases}$$

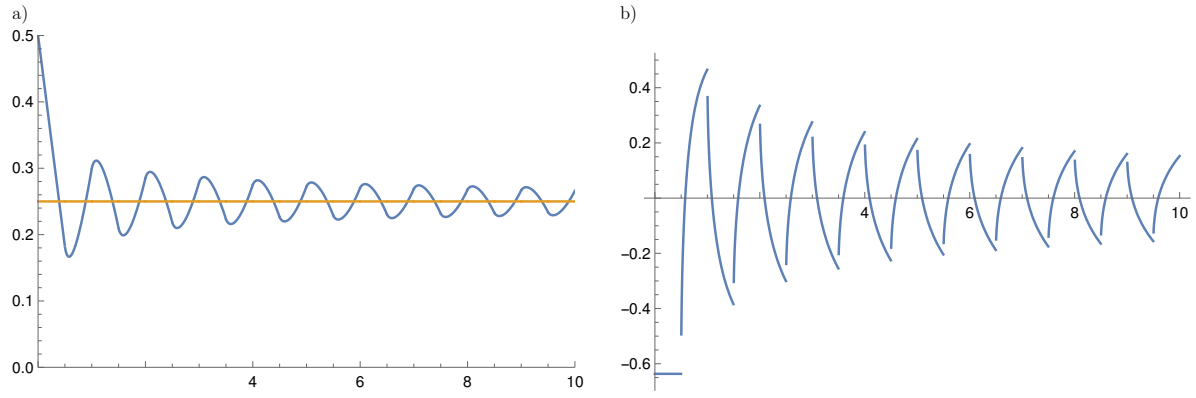

Figure 4.7.: Graphs of a) c_S and b) c_S' with $n = 2$ and $\theta = \frac{1}{2}$. The asymptote in a) is θ^2.

4.4.4. Polytopes

In this section, we will analyse the behaviour of the autocorrelation function of polyhedral domains in $\mathbb{R}^n$ and $\mathbb{T}^n$ near the origin. In fact, we will see that for a polyhedral domain $P \subset \mathbb{R}^n$, the autocorrelation functions $\mathfrak{c}_P$ is a polynomial of at most degree n near the

origin. Likewise, for a polyhedral domain $P \subset \mathbb{T}^n$ we will see that c_P is a polynomial of at most degree n. The following result is known in the full space setting for convex polytopes in dimensions $n = 2$ (see [Nag93, GZ98, EL11]) and was proven in [BKMC23, Lemma 3.3]. As a reminder, a closed set $\Omega \subset \mathbb{T}^n$ is said to be a polytope, if the restriction of its canonical embedding to $\mathcal{Q}^n$ is a polytope in $\mathbb{R}^n$.

Lemma 4.17 (Autocorrelation function for polytopes) Let $\Omega \subset \mathbb{T}^n$ be a polytope. Then there exists $0 < R < 1$ and $a_2, \dots, a_n \in \mathbb{R}$ with $a_2 \geq 0$ such that

$$c_\Omega(r) = |\Omega| - r\frac{\omega_{n-1}}{n\omega_n} V[\chi_\Omega] + \sum_{j=2}^{n} a_j r^j \qquad \text{for all } 0 \leq r < R. \tag{4.140}$$

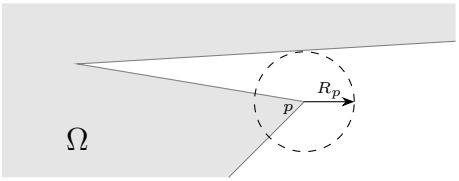

Figure 4.8.: The quantity R_p (and therefore R) ensures that the vertices of $\Omega \triangle \Omega_{rw}$ do not intersect faces which are not adjacent to them.

Proof: In the previous section we have shown that (4.140) holds for laminates with $a_2, \dots, a_n = 0$. Since the only polytopes which do not have corners are trivial extensions of polytopes, we can without loss of generality assume that Ω has at least one corner (see Lemma 4.4). We denote the set of corners of Ω by $\mathcal{C}$. We define

$$R \coloneqq \frac{1}{2} \min \left\{ \min_{p \in \mathcal{C}} R_p, \min_{\substack{p,q \in \mathcal{C} \\ p \neq q}} \operatorname{dist}(p, q) \right\} > 0, \tag{4.141}$$

where for any $p \in \mathcal{C}$ we set

$$R_p \coloneqq \sup \left\{ \varrho > 0 : \begin{smallmatrix} B_\varrho(p) \cap \Omega \text{ and } B_\varrho(p) \cap \Omega^c \text{ have} \\ \text{only one connected component} \end{smallmatrix} \right\} > 0. \tag{4.142}$$

Let $r > 0$, $w \in \mathbb{S}^{n-1}$ and let $\Omega_{rw} \coloneqq \Omega + rw$. Then

$$C_\Omega(0) - C_\Omega(rw) = |\Omega_{rw} \setminus \Omega| = |\Omega \setminus \Omega_{rw}| = \frac{1}{2}|\Omega \triangle \Omega_{rw}|, \tag{4.143}$$

where $\triangle$ denotes the symmetric difference. Since $C_\Omega(0) = |\Omega|$ by Proposition 4.2 it hence remains to calculate $|\Omega \triangle \Omega_{rw}|$ and its dependence on r.

We assume that $w \notin \mathcal{S}$, where $\mathcal{S} \subset \mathbb{S}^{n-1}$ is the negligible set of vectors which are tangential to any of the (finitely many) faces of Ω. By the choice of R, the number of faces N of

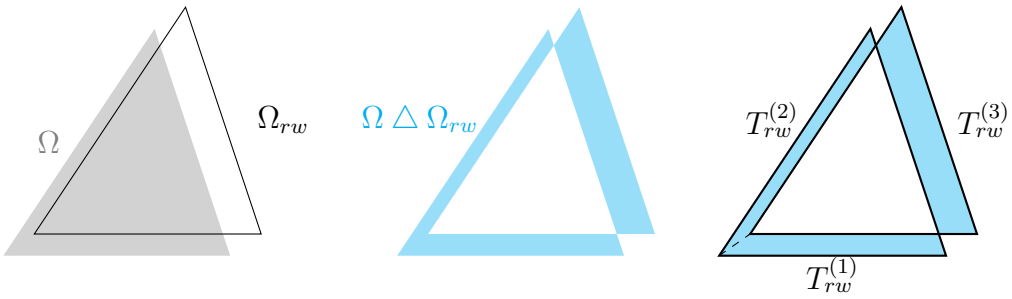

Figure 4.9.: Construction of the trapezoids $T_{rw}^{(i)}$.

$\Omega \triangle \Omega_{rw}$ is then is independent of $r \in (0, R)$ and independent of w. Furthermore, since a face of Ω and the corresponding face of Ω_{rw} are parallel, there exist convex trapezoids $T_{rw}^{(1)}, \dots T_{rw}^{(N)} \subset \mathbb{T}^n$ with pairwise disjoint interiors such that (see Figure 4.9)

$$\Omega \triangle \Omega_{rw} = \bigcup_{i=1}^{N} T_{rw}^{(i)} \qquad \text{for all } 0 < r < R,\ w \in \mathbb{S}^{n-1} \setminus \mathcal{S}. \tag{4.144}$$

Each of these convex trapezoids $T_{rw}^{(i)}$, $i \in \{1, \dots, N\}$ is determined by a system of linear inequalities

$$T_{rw}^{(i)} = \{x \in \mathbb{T}^n : A^{(i)}[x] \leq b^{(i)},\ A^{(i)}[x + rw] \leq b^{(i)}\}, \tag{4.145}$$

where for $x, y \in \mathbb{T}^n$ we denote $x \leq y$ if and only if $x_j \leq y_j \mod 1$ for every $j \in \{1, \dots, n\}$ and for some matrices $A^{(i)} \in \mathbb{R}^{2N \times n}$ and vectors $b^{(i)} \in \mathbb{T}^{2N}$. By a slicing argument there exist $d_1^{(i)}(w), \dots, d_n^{(i)}(w) \in \mathbb{R}$ such that (see Figure 4.9)

$$|T_{rw}^{(i)}| = \sum_{k=1}^{n} d_k^{(i)}(w)\, r^k. \tag{4.146}$$

More precisely, for $x = (x_1, x')$, due to the linear systems defining $T_{rw}^{(i)}$ in (4.145), there exist at most $2N$ intervals $I_{m_1} = [q_{m_1}^{\text{left}}(x', rw), q_{m_1}^{\text{right}}(x', rw)]$, where $q_{m_1}^{\text{left}}$ and $q_{m_1}^{\text{right}}$ depend in an affine way on x' and rw, and convex polytopes $K_{m_1} \subset \mathbb{T}^{n-1}$ such that

$$|T_{rw}^{i}| = \sum_{m_1=1}^{2N} \int_{K_{m_1}} \int_{I_{m_1}} \mathrm{d}x_1\, \mathrm{d}x' = \sum_{m_1=1}^{2N} \int_{K_{m_1}} q_{m_1}^{\text{right}}(x', rw) - q_{m_1}^{\text{left}}(x', rw)\, \mathrm{d}x'. \tag{4.147}$$

The integrand is now a polynomial in r of degree 1 and the set of integration is again a convex polytope of the form (4.145) (reduced in dimension, with different matrices $A^{(i)}$ and $b^{(i)}$). Iteratively, we obtain in the l-th step convex polytopes $K_{m_1,\dots,m_l}$ and a polynomial $p_{m_1,\dots,m_l}$ of degree l such that

$$|T_{rw}^{i}| = \sum_{m_1=1}^{2N} \cdots \sum_{m_l=1}^{2N} \int_{K_{m_1,\dots,m_l}} p_{m_1,\dots,m_l}(x_{l+1}, \dots, x_n, rw)\, \mathrm{d}(x_{l+1}, \dots, x_n). \tag{4.148}$$

The algorithm terminates after n steps and leaves a polynomial in r of degree n as described in (4.146). Combining the above identities we obtain

$$C_\Omega(rw) \overset{(4.143)}{=} C_\Omega(0) - \frac{1}{2}|\Omega \triangle \Omega_{rw}| \tag{4.149}$$

$$= |\Omega| - \frac{1}{2}\sum_{i=1}^{N} |T_{rw}^{(i)}| = |\Omega| - \frac{1}{2}\sum_{i=1}^{N}\sum_{k=1}^{n} d_k^{(i)}(w) r^k \tag{4.150}$$

for all $r \in (0, R)$. Averaging with respect to w then yields

$$c_\Omega(r) = |\Omega| + \sum_{j=1}^{n} a_j r^j \qquad \text{for all } 0 \leq r < R \tag{4.151}$$

for some $a_1, \ldots, a_n \in \mathbb{R}$. Corollary 4.8 shows that $a_1 = -\frac{\omega_{n-1}}{n\omega_n}\operatorname{Per}(\Omega)$. To obtain the estimate of the coefficient a_2, we observe that $c_\Omega''(0) = 2a_2$. Corollary 4.8 now yields

$$2a_2 = c_\Omega''(0) = \lim_{h \searrow 0} \frac{c'(h) - c'(0)}{h} \geq 0 \tag{4.152}$$

as claimed. ■

As the proof of Lemma 4.17 only involves local arguments, the statement is also true in the full space setting. Meaning that $\mathfrak{c}_\Omega$ is a polynomial of degree at most n for polytopes $\Omega \subset \mathbb{R}^n$. However, the reverse of statement is not true, since the Autocorrelation Function of e.g. balls in odd dimensions is also a polynomial of degree n.

In the case $n = 2$, the coefficient a_2 in Lemma 4.17 can be determined explicitly. We note that the coefficient a_2 for convex polytopes was considered in [EL11]. With our methods, we are able to compute a_2 for simple polytopes. Reducing the computation of the Autocorrelation Functions of (generally non-convex) polygons to convex trapeziums (or in other words, from the vertices to the edges) allows us to compute the coefficient $c_\Omega''(0) = 2a_2$ in this generality. As a reminder, a polygon is called *simple*, if the boundary does not intersect itself.

Corollary 4.18 Let $\Omega \subset \mathbb{T}^2$ be a simple polygon. Let $\{\vartheta_1^{(i)}, \ldots \vartheta_{N_i}^{(i)}\} \subset (0, 2\pi)$ be the interior angles. Then

$$c_\Omega''(0) = \frac{1}{2\pi}\sum_{i=1}^{N}\sum_{j=1}^{N_i} 1 + (\pi - \vartheta_j^{(i)})\cot(\vartheta_j^{(i)}). \tag{4.153}$$

Proof: We adapt the notation as in the proof of Lemma 4.17 and write $w = (w_1, w_2) =$

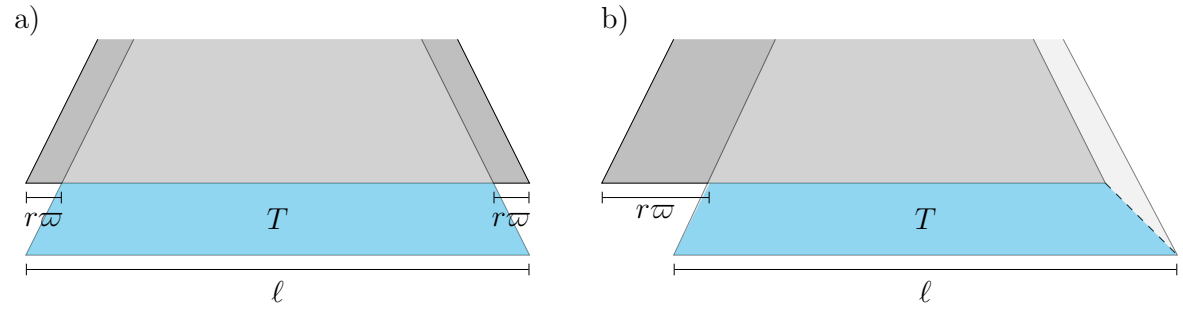

Figure 4.10.: Setup and notation for the deficit ϖ.

$(\cos(\alpha), \sin(\alpha))$. In particular, we find that

$$C_\Omega(rw) = |\Omega| - \frac{1}{2}\sum_{i=1}^{N} |T_{rw}^{(i)}|. \tag{4.154}$$

In order to compute the desired quantity, we thus have to compute the volume of the trapeziums $T_i^{(rw)}$ in (4.154). Let $i \in \{1, \dots, N\}$. The edge corresponding to $T_i^{(rw)}$ has two interior angles $\vartheta_i^{(l)}, \vartheta_i^{(r)} \in (0, 2\pi)$. Since Ω is assumed to be simple, these angles do not change with α. In the following, we will omit the index notation and just denote

$$T \coloneqq T_i^{(rw)}, \qquad \vartheta_l \coloneqq \vartheta_i^{(l)}, \qquad \vartheta_r \coloneqq \vartheta_i^{(r)}. \tag{4.155}$$

We compute (see Figure 4.10 b))

$$|T| = |rw_2| \frac{\ell + (\ell - r\varpi(\alpha, \vartheta_l, \vartheta_r))}{2} = r\ell|w_2| - \frac{r^2}{2}|w_2|\varpi(\alpha, \vartheta_l, \vartheta_r), \tag{4.156}$$

where ℓ denotes the length of the base edge and ϖ is the deficit of the side length of the base line. Depending on ϑ_l and ϑ_r there are multiple cases to consider. We compute these cases in the Appendix. Using Lemma A.6 we find that

$$\frac{1}{2\pi}\int_0^{2\pi} |w_2|\varpi(\alpha, \vartheta_r, \vartheta_l)\,\mathrm{d}\alpha = \frac{1}{2\pi}(1 + (\pi - \vartheta_r)\cot(\vartheta_r)) \tag{4.157}$$

$$+ \frac{1}{2\pi}(1 + (\pi - \vartheta_r)\cot(\vartheta_l)). \tag{4.158}$$

Plugging into (4.154) and (4.156) proves the claim. ■

As with Lemma 4.17, the formula presented in Corollary 4.18 is also true for the full space analogue $\mathfrak{c}_\Omega$, since the proof only involved local arguments. Using Lemma 4.17 and Corollary 4.18 we can explicitly compute the Autocorrelation Function for polytopes near the origin for $n = 2$. As with previous examples, we will use the full space analogue $\mathfrak{c}_\Omega$ (see (4.9)).

Rectangles and non-simple polygons Given a rectangle $P_{a,b} = (0,a) \times (0,b) \subset \mathbb{R}^2$, we compute

$$|P_{a,b}| = ab, \qquad \mathrm{Per}(P) = 2(a+b), \qquad \vartheta = \frac{3\pi}{2}, \tag{4.159}$$

and thus

$$\mathfrak{c}_{P_{a,b}}(r) = ab - \frac{2}{\pi}(a+b)r + \frac{1}{\pi}r^2 \qquad \text{for all } 0 < r \ll 1. \tag{4.160}$$

This can be verified geometrically as

$$\mathscr{C}_{P_{a,b}}(rw) = (a - rw_1)(b - rw_2) \tag{4.161}$$

$$= ab - (bw_1 + aw_2)r + w_1 w_2 r^2 \qquad \text{for all } 0 < r \ll 1, 0 < \alpha < \frac{\pi}{2}. \tag{4.162}$$

where $w = (w_1, w_2) = (\cos(\alpha), \sin(\alpha))$. Integrating with respect to α and using the symmetry of $P_{a,b}$ yields (4.160).

An example of a non-simple polytope is given by $\tilde{P}_{a,b} \coloneqq P_{a,b} \cup (P_{a,b} + (a,b))$. A simple geometric verification shows that

$$\mathscr{C}_{\tilde{P}_{a,b}}(rw) = 2\mathscr{C}_{P_{a,b}}(rw) + r^2 w_1 w_2 \qquad \text{for all } 0 < r \ll 1, 0 < \alpha < \frac{\pi}{2}, \tag{4.163}$$

where $w = (w_1, w_2) = (\cos(\alpha), \sin(\alpha))$. Thus we obtain

$$\mathfrak{c}_{\tilde{P}}(r) = 2\mathfrak{c}_{P_{a,b}}(r) + \frac{2}{2\pi}\int_0^{\frac{\pi}{2}} r^2 \sin(\alpha)\cos(\alpha)\,\mathrm{d}\alpha \tag{4.164}$$

$$= 2ab - \frac{4}{\pi}(a+b)r + \frac{2}{\pi}r^2 + \frac{1}{\pi}r^2 \tag{4.165}$$

$$= 2ab - \frac{4}{\pi}(a+b)r + \frac{3}{\pi}r^2, \tag{4.166}$$

which is not in accordance with the formula given in Corollary 4.18.

Regular polytopes For a regular polytope $\Xi_N \subset \mathbb{R}^2$ with N edges the, interior angles are given by $\vartheta = \pi\frac{N-2}{N}$. Using Lemma 4.18 we compute

$$\mathfrak{c}''_{\Xi_N}(0) = \frac{1}{2\pi}\sum_{j=1}^{N} 1 + (\pi - \pi\tfrac{N-2}{N})\cot(\pi\tfrac{N-2}{N}) = \frac{N}{2\pi} + \cot(\pi(1 - \tfrac{2}{N})) \tag{4.167}$$

$$= \frac{N}{2\pi} - \frac{N}{2\pi} + \frac{2\pi}{3N} + \mathcal{O}(\tfrac{1}{N^3}) = \frac{2\pi}{3N} + \mathcal{O}(\tfrac{1}{N^3}) \tag{4.168}$$

where we used the Laurent expansion

$$\cot(\pi(1-x)) = -\frac{1}{\pi x} + \frac{\pi x}{3} + \mathcal{O}(x^3). \tag{4.169}$$

Thus, for $N \to \infty$ we obtain

$$c''_{\Xi_N}(0) \xrightarrow{N\to\infty} 0. \tag{4.170}$$

Semicontinuity of the second derivative In what follows, we show that the mapping $\Omega \longmapsto c''_\Omega(0)$ is neither lower-, nor upper semi continuous with respect to L^1–convergence. We are now in the position to do so due to the insights obtained in this section. The lack of semi-continuity for the second derivative is different to lower order derivatives, as $\Omega \longmapsto c_\Omega(0)$ is continuous, and $\Omega \longmapsto c'_\Omega(0)$ is upper semi continuous with respect to L^1–convergence.

Lemma 4.19

a) There exist $\Omega_k, \Omega \in BV_n$ such that $|\Omega_k| = |\Omega|$ and

$$\liminf_{k\to\infty} c''_{\Omega_k}(0) < c''_\Omega(0). \tag{4.171}$$

b) There exist $\Omega_k, \Omega \in BV_n$ such that $|\Omega_k| = |\Omega|$ and

$$c''_\Omega(0) < \limsup_{k\to\infty} c''_{\Omega_k}(0). \tag{4.172}$$

Proof: Using Lemma 4.4, it suffices to show the statement for $n = 2$.

To disprove lower semi continuity, let $\Omega \coloneqq P_{a,b} = (0,a) \times (0,b)$. Then $P_{a,b} \in BV_2$ and (4.160) yields $c''_{P_{a,b}}(0) = \frac{2}{\pi}$. Using Lemma 2.18, we find $P_k \in BV_2^\infty$ such that $|P_k| = |P|$ and $\mathrm{Per}(P_k) \xrightarrow{k\to\infty} \mathrm{Per}(P)$. Using Corollary 4.12 we find that $c''_{P_k}(0) = 0$ and thus

$$c''_P(0) = \frac{2}{\pi} > 0 = \liminf_{k\to\infty} c''_{P_k}(0). \tag{4.173}$$

To disprove upper semi continuity, we choose the laminate $\Omega \coloneqq S = (0, \frac{1}{2}) \times (0,1)$ and $\Omega_k \coloneqq (0, \frac{1}{2} - \frac{1}{k}) \times (0, \frac{1}{2}(\frac{1}{2} - \frac{1}{k})^{-1})$. Then $|\Omega_k| = |\Omega|$ and using (4.160) and Lemma 4.16 we obtain

$$\limsup_{k\to\infty} c''_{P_k}(0) = \frac{2}{\pi} > 0 = c''_S(0). \tag{4.174}$$

Altogether, the claim follows. ■

4.4.5. Two Balls

In this section, we will take a look at the set $\Omega_{d,R} \coloneqq B_R(-\frac{d}{2}\mathbf{e}_1) \cup B_R(\frac{d}{2}\mathbf{e}_1) \subset \mathbb{R}^2$, where $R, d > 0$. We aim to compute $\mathscr{C}_{\Omega_{d,R}}$ and $\mathfrak{c}_{\Omega_{d,R}}$ for the whole parameter range $d \geq 2R$, as

- $\Omega_{d,R}$ has a smooth boundary for $d > 2R$,
- $\Omega_{d,R}$ has a cusp at the origin for $d = 2R$,

As we will see, the regularity of the autocorrelation function is linked to the regularity of the boundary. Singular points such as cusps and corners will show an effect on the second and third derivative. We recall the volume for a lense element of a circle with radius R and triangular height z (see (4.109))

$$L(R,z) = \omega_{n-1} R^n \int_{\frac{z}{R}}^1 (1-t^2)^{\frac{n-1}{2}} \,\mathrm{d}t \tag{4.175}$$

$$\overset{n=2}{=} R^2 \arccos(\tfrac{z}{R}) - z\sqrt{R^2 - z^2} \qquad \text{for all } 0 < z < R. \tag{4.176}$$

The triangular height z in our scenario can be computed from the Cosine Theorem for Triangles and is given by (see Figure 4.11)

$$z = \frac{\sqrt{r^2 + d^2 - 2drw_1}}{2}. \tag{4.177}$$

The ratio of d and R will determine for what range of r the lense segment will be included in $\mathscr{C}_{\Omega_{d,R}}$ and $\mathfrak{c}_{\Omega_{d,R}}$. We write $w = (w_1, w_2) = (\cos(\alpha), \sin(\alpha)) \in \mathbb{S}^1$. Due to the symmetry of $\Omega_{d,R}$ we can reduce the computation to the range $0 < \alpha < \frac{\pi}{2}$. Further, we find that

$$C_{\Omega_{d,R}}(rw) = 2\mathscr{C}_{B_R(0)}(rw) \qquad \text{for all } \arccos(\tfrac{r^2+d^2-4R^2}{2rd}) < \alpha < \frac{\pi}{2}. \tag{4.178}$$

Thus, in what follows, we assume $\arccos(\frac{r^2+d^2-4R^2}{2rd}) =: \alpha_*(r) < \alpha < \frac{\pi}{2}$. We call α_* the transition angle.

The case $d > 4R$.

- For $0 < r < 2R$ we have

$$\mathscr{C}_{\Omega_{d,R}}(rw) = 2\mathscr{C}_{B_R(0)}(r\mathbf{e}_1). \tag{4.179}$$

- For $2R < r < d - 2R$ we have

$$\mathscr{C}_{\Omega_{d,R}}(rw) = 0. \tag{4.180}$$

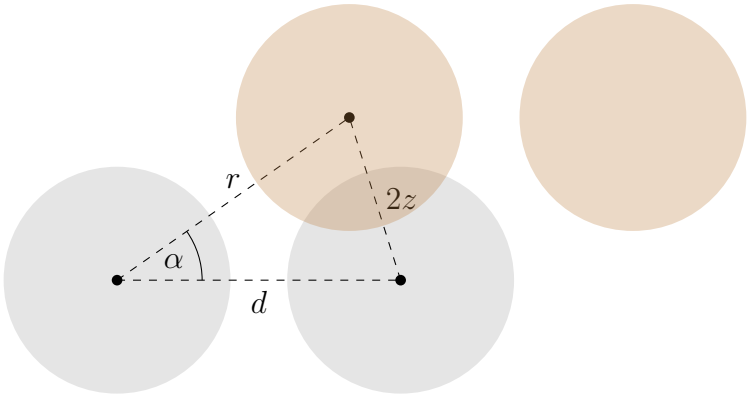

Figure 4.11.: Setup and notation for $\Omega_{d,R}$. The gray circle represent $\Omega_{d,R}$, the brown circles denote $\Omega_{d,R} + rw$.

- For $d - 2R < r < d + 2R$ we have

$$\mathscr{C}_{\Omega_{d,R}}(rw) = 2L(R, \tfrac{\sqrt{r^2+d^2-2drw_1}}{2}). \tag{4.181}$$

- For $r > d + 2R$ we have

$$\mathscr{C}_{\Omega_{d,R}}(rw) = 0. \tag{4.182}$$

The case $2R < d < 4R$**.**

- For $0 < r < d - 2R$ we have

$$\mathscr{C}_{\Omega_{d,R}}(rw) = 2\mathscr{C}_{B_R(0)}(r\mathbf{e}_1). \tag{4.183}$$

- For $d - 2R < r < 2R$ we have

$$\mathscr{C}_{\Omega_{d,R}}(rw) = 2\mathscr{C}_{B_R(0)}(r\mathbf{e}_1) + 2L(R, \tfrac{\sqrt{r^2+d^2-2drw_1}}{2}). \tag{4.184}$$

- For $2R < r < d + 2R$ we have

$$\mathscr{C}_{\Omega_{d,R}}(rw) = 2L(R, \tfrac{\sqrt{r^2+d^2-2drw_1}}{2}). \tag{4.185}$$

- For $r > d + 2R$ we have

$$\mathscr{C}_{\Omega_{d,R}}(rw) = 0. \tag{4.186}$$

The case $d = 2R$**.** We observe that the transition angle in this case is given by $\alpha_*(r) = \arccos(\frac{r}{2d})$.

- For $0 < r < 2R$ we have

$$\mathscr{C}_{\Omega_{d,R}}(rw) = 2\mathscr{C}_{B_R(0)}(r\mathbf{e}_1) + 2L(R, \tfrac{\sqrt{r^2+d^2-2drw_1}}{2}) \tag{4.187}$$

- For $2R < r < 4R$ we have

$$\mathscr{C}_{\Omega_{d,R}}(rw) = 2L(R, \tfrac{\sqrt{r^2+d^2-2drw_1}}{2}). \tag{4.188}$$

- For $r > 4R$ we have

$$\mathscr{C}_{\Omega_{d,R}}(rw) = 0. \tag{4.189}$$

Lack of regularity of Autocorrelation Function for cusp domain We note that $\Omega_{d,R} \in BV_2^\infty$ for all $d > 2R$, and thus the function $\mathfrak{c}_{\Omega_{d,R}}$ is smooth near $r = 0$. However, due to a cusp at $z = 0$, the set $\Omega_{2R,R}$ is not a set with a smooth boundary. Non-smooth boundaries have an effect on the second derivative of the Autocorrelation Function (e.g. if Ω is a polygon, see Section 4.4.4). In this paragraph, we show that the cusp produces a singularity for $c''_{\Omega_{2R,R}}$ as $r \searrow 0$. For notational convenience, we write $d = 2R$.

With the computations above, we find that

$$\mathfrak{c}_{\Omega_{d,R}}(r) = 4\int_0^{\alpha_*(r)} L(R, \tfrac{\sqrt{r^2+d^2-2dr\cos(\alpha)}}{2})\,\mathrm{d}\alpha + 2\mathfrak{c}_{B_R(0)}(r) \qquad \text{for all } 0 < r < 2R. \tag{4.190}$$

However, the first summand is (in contrast to the second summand) not twice differentiable in $r = 0$. To see this, we use the Leibniz Integral Rule to obtain

$$\frac{\mathrm{d}}{\mathrm{d}r}\int_0^{\alpha_*(r)} L(R, \tfrac{\sqrt{r^2+d^2-2dr\cos(\alpha)}}{2})\,\mathrm{d}\alpha \tag{4.191}$$

$$= \alpha_*'(r)L(R,R) - 0 + \int_0^{\alpha_*(r)} \frac{\mathrm{d}}{\mathrm{d}r} L(R, \tfrac{\sqrt{r^2+d^2-2dr\cos(\alpha)}}{2})\,\mathrm{d}\alpha \tag{4.192}$$

$$= \int_0^{\alpha_*(r)} \frac{2R\cos(\alpha) - r}{2}\sqrt{\frac{4rR\cos(\alpha) - r^2}{4R^2 - 4rR\cos(\alpha) + r^2}}\,\mathrm{d}\alpha. \tag{4.193}$$

Deriving again with respect to r we obtain with the Leibniz Integral Rule

$$\frac{\mathrm{d}}{\mathrm{d}r}\int_0^{\alpha_*(r)} \frac{2R\cos(\alpha) - r}{2}\sqrt{\frac{4rR\cos(\alpha) - r^2}{4R^2 - 4rR\cos(\alpha) + r^2}}\,\mathrm{d}\alpha \tag{4.194}$$

$$= \int_0^{\alpha_*(r)} \frac{16(r^2+R^2)R^2\cos^2(\alpha) - 8(r^2+4R^2)rR\cos(\alpha) + r^4 + 8r^2R^2}{2\sqrt{4Rr\cos(\alpha) - r^2}\,(4R^2 - 4rR\cos(\alpha) + r^2)^{3/2}}\,\mathrm{d}\alpha. \tag{4.195}$$

Now, we find that

$$L''(r,R,\alpha) \coloneqq \frac{16(r^2+R^2)R^2\cos^2(\alpha) - 8(r^2+4R^2)rR\cos(\alpha) + r^4 + 8r^2R^2}{2\sqrt{4Rr\cos(\alpha) - r^2}\,(4R^2 - 4rR\cos(\alpha) + r^2)^{3/2}} \tag{4.196}$$

$$= \frac{1}{\sqrt{r}}\,\mathcal{O}(1) \xrightarrow{r\searrow 0} +\infty, \tag{4.197}$$

and consequently using Fatou's Lemma

$$\liminf_{r\searrow 0}\left(\frac{\mathrm{d}}{\mathrm{d}r}\right)^2\int_0^{\alpha_*(r)} L(R,\tfrac{\sqrt{r^2+d^2-2dr\cos(\alpha)}}{2})\,\mathrm{d}\alpha \tag{4.198}$$

$$\leq \int_0^{\frac{\pi}{2}} \liminf_{r\searrow 0}\chi_{(0,\alpha_*(r))}(\alpha)L''(r,R,\alpha)\,\mathrm{d}\alpha = +\infty. \tag{4.199}$$

Hence $c''_{\Omega_{d,R}}(0) = +\infty$.

5. Non-local Isoperimetric Problem

In this chapter we aim to derive an asymptotic expansion as $\varepsilon \to 0$ of a non-local isoperimetric problem of the following form:

$$E_{\gamma,\varepsilon}(\Omega) = \mathrm{Per}(\Omega) - \frac{\gamma}{\varepsilon} \int_{\mathbb{R}^n} \mathcal{K}_\varepsilon(z) \int_{\mathbb{T}^n} |\chi_\Omega(x+z) - \chi_\Omega(x)| \, \mathrm{d}x \, \mathrm{d}z, \tag{5.1}$$

where $\Omega \subset \mathbb{T}^n$, $\gamma > 0$ and $\mathcal{K}_\varepsilon \colon \mathbb{R}^n \longrightarrow \mathbb{R}$ with suitable conditions. As described in Chapter 3, the quantity $E_{\gamma,\varepsilon}$ is an energy model approximating models to describe pattern formation in bio membranes. The regime $\varepsilon \to 0$ corresponds to a macroscopic limit.

The key idea to rewrite $E_{\gamma,\varepsilon}$ in terms of the Autocorrelation function leads to the following representation formula:

$$E_{\gamma,\varepsilon}(\Omega) = \big(1 - \frac{\gamma}{\gamma_{\mathrm{crit}}}\big) \, \mathrm{Per}(\Omega) + 2\gamma \int_0^\infty \Phi_\varepsilon(r)[c'_\Omega(r) - c'_\Omega(0)] \, \mathrm{d}r, \tag{5.2}$$

where c_Ω denotes the Autocorrelation function introduced in Chapter 4 and $\Phi_\varepsilon \colon \mathbb{R}_+ \longrightarrow \mathbb{R}$ arises from $\mathcal{K}_\varepsilon$ and inherits asymptotic behaviour as well as integrability properties from $\mathcal{K}_\varepsilon$. The constant γ_{crit} is explicitly known in terms of the interaction kernel $\mathcal{K}_\varepsilon$. Together with the properties derived for the Autocorrelation Function, this representation gives already crucial insights in the behaviour of the energy:

a) The functional $E_{\gamma,\varepsilon}$ is linear in the space of Autocorrelation functions.

b) The competition of the local and non-local term takes places only in the first order, since the non-local term in (5.2) is non-negative.

c) Using integration by parts, higher order terms in the expansion of $E_{\gamma,\varepsilon}$ correspond to the derivatives of c_Ω evaluated at 0.

This chapter is organised as follows. We will first state the assumptions on the parameters entering (5.1) and then show the reformulation (5.2). In [Section02] we will investigate pointwise properties of the energy as well as compactness. In the third section, we prove Γ–convergence results in different parameter regimes. In the last section, we compute explicit examples building on computations in Chapter 4.

Given $k \in \mathbb{N}$ and a measurable function $f \colon \mathbb{R}^n \longrightarrow \mathbb{R}$, we define the k-th moment of f via

$$\mathfrak{m}_k[f] \coloneqq \int_{\mathbb{R}^n} |z|^k f(z) \, \mathrm{d}z. \tag{5.3}$$

Motivated from the biological model discussed in Chapter 3, we will consider family of functions of the form $\mathcal{K}_\varepsilon(z) = \frac{1}{\varepsilon^n}\mathcal{K}(\frac{z}{\varepsilon})$, where $\mathcal{K}\colon \mathbb{R}^n \longrightarrow \mathbb{R}$ is given, and we pose the following assumptions on the kernel $\mathcal{K}$:

(H1) $\mathcal{K}$ is radial. (Radial Symmetry)

(H2) $\mathfrak{m}_1[\mathcal{K}] < \infty$. (Finite First Moment)

(H3) $\displaystyle\int_{\mathbb{R}^n\setminus B_r(0)} \mathcal{K}(z)\, dz \geq 0$ for all $r > 0$. (Essential Repulsiveness)

With slight abuse of notation, we write $\mathcal{K}(z) = \mathcal{K}(|z|)$ and $\mathfrak{m}_k = \mathfrak{m}_k[\mathcal{K}]$. We also introduce the associated quantity

$$\gamma_{\text{crit}} \coloneqq \frac{n\omega_n}{2\omega_{n-1}}\mathfrak{m}_1^{-1} = \frac{n\omega_n}{2\omega_{n-1}}\left(\int_{\mathbb{R}^n} |z|\,\mathcal{K}(z)\,\mathrm{d}z\right)^{-1}, \tag{5.4}$$

which is finite by (H2). We will quickly comment about the assumptions on the family of kernels.

ad (H1) Radial symmetry assures that the model is isotropic, meaning that there is no preferred direction in the described system. Apart from the physical interpretation, there are two more reasons to include this assumption, namely the kernel in the derivation of the model from Chapter 3 is radially symmetric. The second reason being the radial symmetry of the perimeter functional.

ad (H2) Having a finite first moment allows for an estimate of the non-local term in terms of the variation with the same scaling. More precisely, it allows roughly speaking for an estimate of the form

$$\int_{\mathbb{R}^n} \mathcal{K}(z) \int_{\mathbb{T}^n} |\chi_\Omega(x+z) - \chi_\Omega(x)|\,\mathrm{d}x\,\mathrm{d}z \tag{5.5}$$

$$= \int_{\mathbb{R}^n} |z|\mathcal{K}(z) \int_{\mathbb{T}^n} \frac{|\chi_\Omega(x+z) - \chi_\Omega(x)|}{|z|}\,\mathrm{d}x\,\mathrm{d}z \lesssim \mathrm{Per}(\Omega)\,\mathfrak{m}_1[\mathcal{K}], \tag{5.6}$$

which scales correctly with the local term. In contrast, assuming e.g. $\mathcal{K} \in L^1(\mathbb{R}^n)$ results in a non compatible estimate since the (optimal) isoperimetric inequality yields

$$\int_{\mathbb{R}^n} \mathcal{K}(z) \int_{\mathbb{T}^n} |\chi_\Omega(x+z) - \chi_\Omega(x)|\,\mathrm{d}x\,\mathrm{d}z \lesssim |\Omega|\,\|\mathcal{K}\|_{L^1(\mathbb{R}^n)} \tag{5.7}$$

$$\lesssim \mathrm{Per}(\Omega)^{\frac{n}{n-1}}\|\mathcal{K}\|_{L^1(\mathbb{R}^n)}, \tag{5.8}$$

which scales differently than the local term.

ad (H3) Assumption (H3) is a generalisation of non-negativity. The competing effect of the local and non-local term exists only if it is a difference of two positive quantities,

which is assured by (H3) as it guarantees that Φ in the reformulation is nonnegativ. Moreover, the associated quantity γ_{crit} is non-negative (see Lemma 5.6).

We will now rigorously define the energy functional $E_{\gamma,\varepsilon}$.

Definition 5.1 Let $\mathcal{K}\colon \mathbb{R}^n \longrightarrow \mathbb{R}$ be measurable. Let $\gamma, \varepsilon > 0$ and let $0 < \theta < 1$. We define the class of admissible sets $\mathcal{A} \coloneqq \{\Omega \in BV_n : |\Omega| = \theta\}$ and the energy functional $E_{\gamma,\varepsilon}\colon L^1(\mathbb{T}^n) \longrightarrow \mathbb{R} \cup \{\pm\infty\}$ via

$$E_{\gamma,\varepsilon}[u] \coloneqq \begin{cases} V[u] - \dfrac{\gamma}{\varepsilon} \displaystyle\int_{\mathbb{R}^n} \mathcal{K}_\varepsilon(z) \int_{\mathbb{T}^n} |u(x+z) - u(x)| \,\mathrm{d}x \,\mathrm{d}z & \text{if } u = \chi_\Omega,\ \Omega \in \mathcal{A}, \\ +\infty & \text{else.} \end{cases}$$

We note that $E_{\gamma,\varepsilon}$ is a sharp interface model since $\mathrm{dom}(E_{\gamma,\varepsilon}) \subset \mathcal{A} \subset BV_n$. Moreover, using (5.5) – (5.6), the energy is well-defined assuming the hypothesis (H1) – (H3). Therefore we write $E_{\gamma,\varepsilon}(\Omega) = E_{\gamma,\varepsilon}[\chi_\Omega]$. If $\Omega \in \mathcal{A}$ we can reformulate the energy as

$$E_{\gamma,\varepsilon}(\Omega) = \mathrm{Per}(\Omega) - \frac{\gamma}{\varepsilon} \int_{\mathbb{R}^n} \mathcal{K}_\varepsilon(z) \int_{\mathbb{T}^n} |\chi_\Omega(x+z) - \chi_\Omega(x)| \,\mathrm{d}x \,\mathrm{d}z. \tag{5.9}$$

We remark that the following methods do not rely on the mass constraint, meaning that all the forthcoming results are also true if we set $\mathcal{A} = BV_n$. We end this section by noting that the hypothesis lead to an interaction kernel that forms an approximation of the identity.

Proposition 5.2 Assume $\mathcal{K}$ satisfies (H1) – (H3). Let $\eta_\varepsilon\colon \mathbb{R}^n \longrightarrow \mathbb{R}$ be given by

$$\eta_\varepsilon(z) \coloneqq \frac{1}{\mathfrak{m}_1} \frac{|z|}{\varepsilon} \mathcal{K}_\varepsilon(z) \qquad \text{for all } z \in \mathbb{R}^n. \tag{5.10}$$

Then the family $\{\eta_\varepsilon\}_\varepsilon$ forms an approximation of the identity.

Proof: We note that after the transformation $z \longmapsto \varepsilon z$ we obtain

$$\|\eta_\varepsilon\|_{L^1(\mathbb{R}^n)} = \frac{1}{\mathfrak{m}_1} \int_{\mathbb{R}^n} |z| \, |\mathcal{K}(z)| \,\mathrm{d}z < \infty \tag{5.11}$$

by (H2). Also, by definition and again after the transformation $z \longmapsto \varepsilon z$ we obtain

$$\int_{\mathbb{R}^n} \eta_\varepsilon(z) \,\mathrm{d}z = \frac{1}{\mathfrak{m}_1} \int_{\mathbb{R}^n} |z| \, \mathcal{K}(z) \,\mathrm{d}z = 1. \tag{5.12}$$

Tightness of $\{\eta_\varepsilon\}_\varepsilon$ follows from Fatou's Lemma. More precisely, let $\delta > 0$. Then we obtain with (H2)

$$\limsup_{\varepsilon\to 0} \int_{B_\delta(0)} |\eta_\varepsilon(z)| \,\mathrm{d}z = \frac{1}{\mathfrak{m}_1} \limsup_{\varepsilon\to 0} \int_{B_{\delta/\varepsilon}(0)} |z|\,|\mathcal{K}(z)| \,\mathrm{d}z \tag{5.13}$$

$$\leq \frac{1}{\mathfrak{m}_1} \int_{\mathbb{R}^n} \limsup_{\varepsilon\to 0} |z|\,|\mathcal{K}(z)|\, \chi_{B_{\delta/\varepsilon}(0)}(z) \,\mathrm{d}z = 0. \tag{5.14}$$

Altogether $\{\eta_\varepsilon\}_\varepsilon$ forms an approximation of the identity. ■

5.1. Reformulation in terms of Autocorrelation Function

For the subsequent analysis it is convenient to the radially integrated kernel Φ instead of the kernel $\mathcal{K}$, where

$$\Phi(r) \coloneqq \sigma_n \int_r^\infty \rho^{n-1}\mathcal{K}(\rho)\,\mathrm{d}\rho = \int_{\mathbb{R}^n\setminus B_r(0)} \mathcal{K}(z)\,\mathrm{d}z \qquad \text{for all } r > 0. \tag{5.15}$$

We define $\Phi_\varepsilon(r) \coloneqq \frac{1}{\varepsilon}\Phi(\frac{r}{\varepsilon})$. We collect some basic properties of Φ which follow from our assumptions on $\mathcal{K}$:

Proposition 5.3 Assume $\mathcal{K}$ satisfies (H1) – (H3) and let Φ as in (5.15). Then

a) $\Phi \geq 0$.

b) $\lim\limits_{r\to 0} r\Phi(r) = \lim\limits_{r\to\infty} r\Phi(r) = 0$.

c) $\Phi \in L^1(\mathbb{R}_+)$ and $\displaystyle\int_0^\infty \Phi(r)\,\mathrm{d}r = \int_{\mathbb{R}^n} |z|\,\mathcal{K}(z)\,\mathrm{d}z$.

Proof: By definition of Φ and (H3) we have $\Phi \geq 0$ and

$$\Phi'(r) = -\sigma_n r^{n-1}\mathcal{K}(r) \qquad \text{for all } r > 0. \tag{5.16}$$

By definition of Φ and assumption (H2) we have

$$|R\Phi(R)| \leq \sigma_n R \int_R^\infty \rho^{n-1}|\mathcal{K}(\rho)|\,\mathrm{d}\rho \leq \sigma_n \int_R^\infty \rho^n|\mathcal{K}(\rho)|\,\mathrm{d}\rho \xrightarrow{R\to\infty} 0. \tag{5.17}$$

Moreover, we observe that

$$R\rho^{n-1}|\mathcal{K}(\rho)|\,\chi_{(R,\infty)}(\rho) \leq \rho^n|\mathcal{K}(\rho)| \qquad \text{for all } \rho > 0. \tag{5.18}$$

Thus, the conditions to apply Fatou's Lemma are satisfied (since the right-hand side is integrable by (H2)) and we obtain

$$\limsup_{R\to 0} R\Phi(R) \leq \int_0^\infty \limsup_{R\to 0} R\rho^{n-1}|\mathcal{K}(\rho)|\,\chi_{(R,\infty)}(\rho)\,\mathrm{d}\rho = 0, \tag{5.19}$$

which concludes the proof of b). Integrating by parts we get for $0 < \varrho < R < \infty$

$$\sigma_n \int_\varrho^R r^n \mathcal{K}(r)\,\mathrm{d}r \overset{(5.16)}{=} -\int_\varrho^R r\Phi'(r)\,\mathrm{d}r = -r\,\Phi(r)\Big|_\varrho^R + \int_\varrho^R \Phi(r)\,\mathrm{d}r. \tag{5.20}$$

Using b) in the limits $\varrho \to 0$ and $R \to \infty$, as well as the Dominated Convergence Theorem yields assertion c). ■

We note that with the help of Proposition 5.3 c) we can represent the quantity γ_{crit} from (5.4) in terms of Φ in the following way:

$$\gamma_{\mathrm{crit}} = \frac{n\omega_n}{2\omega_{n-1}} \|\Phi\|^{-1}_{L^1(\mathbb{R}_+)}. \tag{5.21}$$

In particular $\gamma_{\mathrm{crit}} > 0$. Moreover, the assumptions on the kernel $\mathcal{K}$ now imply that the dilated family Φ_ε forms an approximation of the identity:

Corollary 5.4 Assume $\mathcal{K}$ satisfies (H1) – (H3) and let Φ_ε as in (5.15). Let $\varphi_\varepsilon \colon \mathbb{R} \longrightarrow \mathbb{R}$ be given by

$$\varphi_\varepsilon(r) \coloneqq \frac{\Phi_\varepsilon(r)}{\|\Phi\|_{L^1(\mathbb{R}_+)}} \chi_{\mathbb{R}_+}(r) \qquad \text{for all } r \in \mathbb{R}. \tag{5.22}$$

Then the family $\{\varphi_\varepsilon\}_\varepsilon$ forms an approximation of the identity.

Proof: Follows from Proposition 5.2 and Proposition 5.3. ■.

We are now in the position to rewrite the non-local term in $E_{\gamma,\varepsilon}$ in terms of the symmetrised Autocorrelation Function and the integrated kernel Φ.

Lemma 5.5 Assume $\mathcal{K}$ satisfies (H1) – (H3) and let Φ_ε as in (5.15). Then

$$\frac{1}{\varepsilon}\int_{\mathbb{R}^n} \mathcal{K}_\varepsilon(z) \int_{\mathbb{T}^n} |\chi_\Omega(x) - \chi_\Omega(x+z)|\,\mathrm{d}x = -2\int_0^\infty \Phi_\varepsilon(r)\, c'_\Omega(r)\,\mathrm{d}r \quad \text{for all } \Omega \in BV_n. \tag{5.23}$$

Proof: Since u only takes values in $\{0,1\}$ we have with Proposition 4.2

$$\frac{1}{\varepsilon}\int_{\mathbb{R}^n}\mathcal{K}_\varepsilon(z)\int_{\mathbb{T}^n}|\chi_\Omega(x)-\chi_\Omega(x+z)|\,\mathrm{d}x\,\mathrm{d}z \tag{5.24}$$

$$=\frac{1}{\varepsilon}\int_{\mathbb{R}^n}\mathcal{K}_\varepsilon(z)\int_{\mathbb{T}^n}|\chi_\Omega(x)-\chi_\Omega(x+z)|^2\,\mathrm{d}x\,\mathrm{d}z \tag{5.25}$$

$$=\frac{2}{\varepsilon}\int_{\mathbb{R}^n}\mathcal{K}_\varepsilon(z)\left[\int_{\mathbb{T}^n}|\chi_\Omega(x)|^2\,\mathrm{d}x-\int_{\mathbb{T}^n}\chi_\Omega(x)\,\chi_\Omega(x+z)\,\mathrm{d}x\right]\mathrm{d}z \tag{5.26}$$

$$=\frac{2}{\varepsilon}\int_{\mathbb{R}^n}\mathcal{K}_\varepsilon(z)\,[C_\Omega(0)-C_\Omega(z)]\,\mathrm{d}z \tag{5.27}$$

$$=\frac{2\sigma_n}{\varepsilon}\int_0^\infty r^{n-1}\mathcal{K}_\varepsilon(r)\,[c_\Omega(0)-c_\Omega(r)]\,\mathrm{d}r, \tag{5.28}$$

where in the last line we switched to polar coordinates. Let $0<\varrho<R<\infty$. Noting that c_Ω is Lipschitz (see Corollary 4.8), we integrate by parts to obtain

$$\frac{2\sigma_n}{\varepsilon}\int_\varrho^R r^{n-1}\mathcal{K}_\varepsilon(r)\,[c_\Omega(0)-c_\Omega(r)]\,\mathrm{d}r \tag{5.29}$$

$$\overset{(5.16)}{=}-2\int_\varrho^R(\Phi_\varepsilon)'(r)\,[c_\Omega(0)-c_\Omega(r)]\,\mathrm{d}r \tag{5.30}$$

$$=-2\Phi_\varepsilon(r)\,[c_\Omega(0)-c_\Omega(r)]\Big|_\varrho^R-2\int_\varrho^R\Phi_\varepsilon(r)\,c_\Omega'(r)\,\mathrm{d}r. \tag{5.31}$$

Using again Corollary 4.8 we obtain

$$|\Phi_\varepsilon(r)\,[c_\Omega(0)-c_\Omega(r)]|\lesssim r\Phi_\varepsilon(r)\ \mathrm{Per}(\Omega)\qquad\text{for all } r>0. \tag{5.32}$$

Thus the boundary terms in (5.31) vanish in the limit $\varrho\to 0$ and $R\to\infty$ by Proposition 5.3 b). The claim follows from the Dominated Convergence Theorem and the computations above. ■

With this reformulation at hand we derive the following representation formula of the Energy $E_{\gamma,\varepsilon}$:

Theorem 5.6 Let $\gamma>0$ and suppose $\mathcal{K}$ satisfies (H1)–(H3). Let Φ_ε as in (5.15). Then

$$E_{\gamma,\varepsilon}(\Omega)=\left(1-\frac{\gamma}{\gamma_{\mathrm{crit}}}\right)\mathrm{Per}(\Omega)+2\gamma\int_0^\infty\Phi_\varepsilon(r)\,[c_\Omega'(r)-c_\Omega'(0)]\,\mathrm{d}r\qquad\text{for all }\Omega\in BV_n. \tag{5.33}$$

Proof: Acoording to Corollary 4.8 we have $-c_\Omega'(0)=\|c_\Omega'\|_{L^\infty(\mathbb{R}_+)}=\frac{\omega_{n-1}}{n\omega_n}\,\mathrm{Per}(\Omega)$. Since

$\Phi_\varepsilon \in L^1(\mathbb{R}_+)$ (see Proposition 5.3 c)) we obtain

$$\Big(1 - \frac{\gamma}{\gamma_{\text{crit}}}\Big) \operatorname{Per}(\Omega) + 2\gamma \int_0^\infty \Phi_\varepsilon(r)\,[c'_\Omega(r) - c'_\Omega(0)]\,\mathrm{d}r \tag{5.34}$$

$$= \Big(1 - \frac{\gamma}{\gamma_{\text{crit}}}\Big) \operatorname{Per}(\Omega) + 2\gamma \int_0^\infty \Phi_\varepsilon(r)\,c'_\Omega(r)\,\mathrm{d}r \tag{5.35}$$

$$+ 2\gamma \frac{\omega_{n-1}}{n\omega_n} \operatorname{Per}(\Omega) \int_0^\infty \Phi_\varepsilon(r)\,\mathrm{d}r \tag{5.36}$$

$$= \Big(1 - \frac{\gamma}{\gamma_{\text{crit}}}\Big) \operatorname{Per}(\Omega) + 2\gamma \int_0^\infty \Phi_\varepsilon(r)\,c'_\Omega(r)\,\mathrm{d}r + \frac{\gamma}{\gamma_{\text{crit}}} \operatorname{Per}(\Omega) \tag{5.37}$$

$$= \operatorname{Per}(\Omega) + 2\gamma \int_0^\infty \Phi_\varepsilon(r)\,c'_\Omega(r)\,\mathrm{d}r \overset{5.5}{=} E_{\gamma,\varepsilon}(\Omega), \tag{5.38}$$

as claimed. ■

An immediate consequence is a lower bound on the energy $E_{\gamma,\varepsilon}$ in terms of the perimeter functional:

Corollary 5.7 Let $\gamma > 0$ and suppose $\mathcal{K}$ satisfies (H1)–(H3). Then

$$\Big(1 - \frac{\gamma}{\gamma_{\text{crit}}}\Big) \operatorname{Per}(\Omega) \le E_{\gamma,\varepsilon}(\Omega) \qquad \text{for all } \Omega \in BV_n. \tag{5.39}$$

Proof: According to Corollary 4.8 we have $c'_\Omega(r) - c'_\Omega(0) \ge 0$ for all $r > 0$. Since $\Phi_\varepsilon \ge 0$ for all $\varepsilon > 0$, the claim follows from Theorem 5.6. ■

We note that the left-hand side is non-negative as long as $0 < \gamma < \gamma_{\text{crit}}$, which will be helpful later for the proofs of the compactness (see Theorem 5.10) and the liminf inequality in the Γ–convergence results (see Theorem 5.18 and Theorem 5.21).

We next use the reformulation of the energy $E_{\gamma,\varepsilon}$ to show that the lower bound in Corollary 5.7 is asymptotically optimal.

Proposition 5.8 Let $\gamma > 0$ and suppose $\mathcal{K}$ satisfies (H1)–(H3). Then

$$E_{\gamma,\varepsilon}(\Omega) \xrightarrow{\varepsilon \searrow 0} \Big(1 - \frac{\gamma}{\gamma_{\text{crit}}}\Big) \operatorname{Per}(\Omega) \qquad \text{for all } \Omega \in \mathcal{A}. \tag{5.40}$$

Proof: Using (5.28) and the transformation $r \longmapsto \varepsilon r$, the non-local term can be rewritten as

$$\frac{1}{\varepsilon} \int_{\mathbb{R}^n} \mathcal{K}_\varepsilon(z) \int_{\mathbb{T}^n} |\chi_\Omega(x+z) - \chi_\Omega(x)|\,\mathrm{d}x\,\mathrm{d}z = 2\sigma_n \int_0^\infty r^{n-1} \mathcal{K}(r) \frac{c_\Omega(0) - c_\Omega(\varepsilon r)}{\varepsilon}\,\mathrm{d}r. \tag{5.41}$$

We note with the help of Corollary 4.8

$$\left| r^{n-1}\mathcal{K}(r)\frac{c_\Omega(0)-c_\Omega(\varepsilon r)}{\varepsilon}\right| \lesssim r^n\mathcal{K}(r)\ \mathrm{Per}(\Omega), \qquad \lim_{\varepsilon\to 0}\frac{c_u(0)-c_u(\varepsilon r)}{\varepsilon} = -r\,c_u'(0). \quad (5.42)$$

Using the Dominated Convergence Theorem and Corollary 4.8 we obtain

$$\frac{1}{\varepsilon}\int_{\mathbb{R}^n}\mathcal{K}_\varepsilon(z)\int_{\mathbb{T}^n}|u(x+z)-u(x)|\,\mathrm{d}x\,\mathrm{d}z \quad (5.43)$$

$$\xrightarrow{\varepsilon\searrow 0} -2c_\Omega'(0)\int_0^\infty r^n\mathcal{K}(r)\,\mathrm{d}r = -\frac{1}{\gamma_{\mathrm{crit}}}\mathrm{Per}(\Omega). \quad (5.44)$$

Using Theorem 5.6 proves the claim. ■

We remark that Proposition 5.8 was proven in [BKMC23, Proposition 4.4] under the additional assumption that Ω is a polytope. Thus Proposition 5.8 improves the statement in [BKMC23].

Corollary 5.9 Suppose $\mathcal{K}$ satisfies (H1)–(H3) and let Φ_ε as in (5.15). Then

$$\int_0^\infty \Phi_\varepsilon(r)\,[c_\Omega'(r)-c_\Omega'(0)]\,\mathrm{d}r \xrightarrow{\varepsilon\searrow 0} 0 \qquad \text{for all } \Omega\in BV_n. \quad (5.45)$$

Proof: Follows immediately from Theorem 5.6 and Proposition 5.8. ■

5.2. Compactness and Non-Compactness of the Energy Functional

In this section, we collect compactness and non-compactness properties of the energy functional $E_{\gamma,\varepsilon}$. To allow for a more general class of parameters, we will now consider $\gamma=\gamma_\varepsilon$. In summary, we will show that:

- $E_{\gamma_\varepsilon,\varepsilon}$ is compact if $\limsup_{\varepsilon\to 0}\gamma_\varepsilon<\gamma_{\mathrm{crit}}$.
- $E_{\gamma_\varepsilon,\varepsilon}$ is not compact, if $\gamma_{\mathrm{crit}}<\liminf_{\varepsilon\to 0}\gamma_\varepsilon\le\limsup_{\varepsilon\to 0}\gamma_\varepsilon<\infty$.
- If $\gamma_{\mathrm{crit}}<\liminf_{\varepsilon\to 0}\gamma_\varepsilon\le\limsup_{\varepsilon\to 0}\gamma_\varepsilon<\infty$, then there does not exist a rescaling $\mathbf{R}$, such that $\mathbf{R}^{-1}(\varepsilon)E_{\gamma_\varepsilon,\varepsilon}$ is compact.

These results identify sub- and supercritical parameter regimes for the functional $E_{\gamma,\varepsilon}$. The failure of compactness is reflected in the representation formula from Theorem 5.6

(see also Corollary 5.7)

$$E_{\gamma,\varepsilon}(\Omega) = \Big(1 - \frac{\gamma}{\gamma_{\text{crit}}}\Big) \operatorname{Per}(\Omega) + 2\gamma \int_0^\infty \Phi_\varepsilon(r)\,[c'_\Omega(r) - c'_\Omega(0)]\,\mathrm{d}r \qquad \text{for all } \Omega \in BV_n. \tag{5.46}$$

If $\gamma < \gamma_{\text{crit}}$, then the energy is non-negative and more importantly is bounded from below by the perimeter functional and therefore inherits compactness properties from the compact imbedding of BV into L^1 (see Theorem 2.10). If $\gamma > \gamma_{\text{crit}}$, then the energy is potentially negative and oscillations are preferred as in those situations the energy now decreases.

The most interesting case to us is the critical case $\gamma_\varepsilon \sim \gamma_{\text{crit}}$ as there potentially exist rescalings to restore compactness. Of the highest importance is the connection of rescalings $\mathbf{R}$ and the factor governing the local term $1 - \frac{\gamma_\varepsilon}{\gamma_{\text{crit}}}$. However, in some cases, the choice of the interaction kernel $\mathcal{K}$ does not allow for the existence of a rescaling to restore compactness (at least not under the assumptions (H1) – (H3), see Lemma 5.17).

We will first look at the subcritical case.

Theorem 5.10 Let $\gamma_\varepsilon > 0$ and assume $\limsup_{\varepsilon\to 0} \gamma_\varepsilon < \gamma_{\text{crit}}$. Suppose $\mathcal{K}$ satisfies (H1)–(H3). Let $\Omega_\varepsilon \in BV_n$ such that $\limsup_{\varepsilon\to 0} E_{\gamma_\varepsilon,\varepsilon}(\Omega_\varepsilon) < \infty$. Then there exists $\Omega \in \mathcal{A}$ and a subsequence (not relabeled), such that $|\Omega \triangle \Omega_\varepsilon| \to 0$.

Proof: Without loss of generality we can assume $\Omega_\varepsilon \in \mathcal{A}$, otherwise the energy would be asymptotically unbounded. Let $0 < 2\delta < \gamma_{\text{crit}} - \limsup_{\varepsilon\to 0} \gamma_\varepsilon$. By passing to a convergent subsequence (not relabeled), we can assume that $\gamma_\varepsilon + \delta < \gamma_{\text{crit}}$ for $\varepsilon > 0$ sufficiently small. Thus by Corollary 5.7 we obtain

$$0 < \frac{\delta}{\gamma_{\text{crit}}} \operatorname{Per}(\Omega_\varepsilon) \le \big(1 - \frac{\gamma_\varepsilon}{\gamma_{\text{crit}}}\big) \operatorname{Per}(\Omega_\varepsilon) \overset{5.7}{\le} E_{\gamma_\varepsilon,\varepsilon}(\Omega_\varepsilon). \tag{5.47}$$

Again, passing to a subsequence (not relabeled) we find $\operatorname{Per}(\Omega_\varepsilon) \lesssim 1$. Using the compact embedding of BV into L^1 (see Theorem 2.10) finishes the proof. ■

The case of constant sequences $\gamma_\varepsilon = \gamma < \gamma_{\text{crit}}$ was proven in [BKMC23, Theorem 2.1].

The non-compactness results will mostly rely on the construction of a sequence $\Omega_\varepsilon \in \mathcal{A}$ such that there does not exist an L^1 convergent subsequence. The following lemma will provide a suitable candidate by constructing oscillating laminates (see Figure 5.1).

Lemma 5.11 Let $0 < \theta < 1$. Let $S \coloneqq (0,\theta) \times \mathbb{T}^{n-1} \subset \mathbb{T}^n$. Let $S_k \coloneqq kS$ for all $k \in \mathbb{N}$. Then:

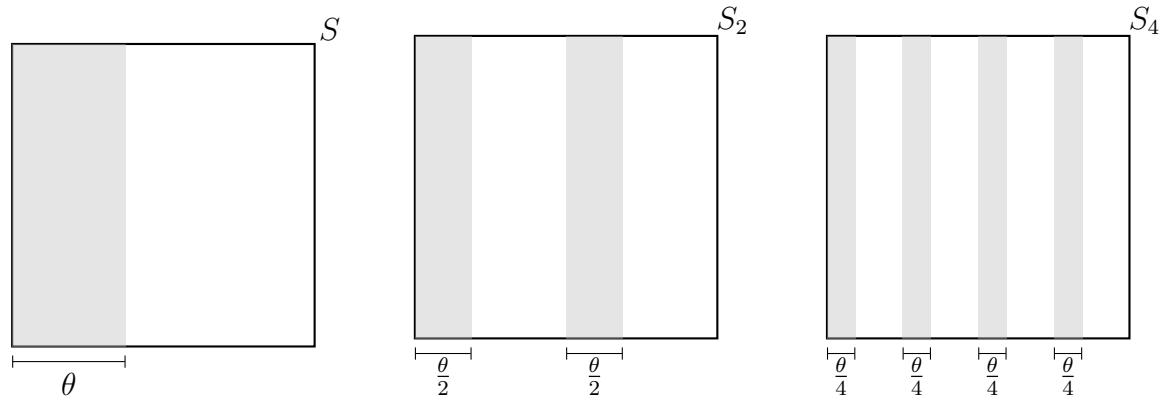

Figure 5.1.: Construction of sequence of oscillating laminates.

a) $|S_k| = \theta$ for all $k \in \mathbb{N}$.

b) $\mathrm{Per}(S_k) = 2^k$ for all $k \in \mathbb{N}$.

c) There does not exist an L^1 convergent subsequence.

Proof: The first two assertions are trivial. To show the third assertion, we assume there exists a subsequence (not relabeled) and $v \in L^1(\mathbb{T}^n, \{0,1\})$, such that $\chi_{S_k} =: v_k \to v$ in L^1 as $k \to \infty$. Then $\|v\|_{L^1(\mathbb{T}^n)} = \theta$. We note that $v_k \overset{*}{\rightharpoonup} \theta$ in L^∞ as $k \to \infty$ (see [BD98, Example 2.7]) and thus

$$\|v_k - v\|_{L^1(\mathbb{T}^n)} = \int_{\mathbb{T}^n} v_k(x)\,\mathrm{d}x + \int_{\mathbb{T}^n} v(x)\,\mathrm{d}x - 2\int_{\mathbb{T}^n} v_k(x)\,v(x)\,\mathrm{d}x \tag{5.48}$$

$$\xrightarrow{k\to\infty} 2\theta - 2\theta^2 \neq 0, \tag{5.49}$$

a contradiction. ■

With the help of Lemma 5.11 we will now show non-compactness in the supercritical regime.

Theorem 5.12 Let $\gamma_\varepsilon > 0$ and assume $\gamma_{\mathrm{crit}} < \liminf_{\varepsilon\to 0} \gamma_\varepsilon \leq \limsup_{\varepsilon\to 0} \gamma_\varepsilon < \infty$. Suppose $\mathcal{K}$ satisfies (H1)–(H3). Then there exists $\Omega_\varepsilon \in \mathcal{A}$ such that $\limsup_{\varepsilon\to 0} E_{\gamma_\varepsilon,\varepsilon}(\Omega_\varepsilon) < \infty$, but there does not exist an L^1–convergent subsequence of Ω_ε.

Proof: The assumptions on the sequence γ_ε imply that there exist $\gamma_*, \gamma^*, \varepsilon_0 > 0$, such that

$$\gamma_{\mathrm{crit}} < \gamma_* < \gamma_\varepsilon < \gamma^* < \infty \qquad \text{for all } 0 < \varepsilon < \varepsilon_0, \tag{5.50}$$

which in turn implies for all $\Omega \in BV_n$ (with Theorem 5.6)

$$E_{\gamma_\varepsilon,\varepsilon}(\Omega) \leq \big(1 - \frac{\gamma_*}{\gamma_{\text{crit}}}\big) \operatorname{Per}(\Omega) + 2\gamma^* \int_0^\infty \Phi_\varepsilon(r)[c'_\Omega(r) - c'_\Omega(0)]\,\mathrm{d}r \quad \text{for all } 0 < \varepsilon < \varepsilon_0. \tag{5.51}$$

Using the sequence from Lemma 5.11 and Corollary 5.9, we obtain

$$\int_0^\infty \Phi_\varepsilon(r)[c'_{S_k}(r) - c'_{S_k}(0)]\,\mathrm{d}r \xrightarrow{\varepsilon \searrow 0} 0. \tag{5.52}$$

Hence, for all $k \in \mathbb{N}$ there exists $\bar{\varepsilon}(k)$ such that

$$\int_0^\infty \Phi_\varepsilon(r)[c'_{S_k}(r) - c'_{S_k}(0)]\,\mathrm{d}r < \frac{1}{k} \qquad \text{for all } 0 < \varepsilon < \bar{\varepsilon}(k). \tag{5.53}$$

For $\frac{1}{2}\min\{\frac{1}{k+1}, \bar{\varepsilon}(k+1), \varepsilon_0\} \leq \varepsilon \leq \frac{1}{2}\min\{\frac{1}{k}, \bar{\varepsilon}(k), \varepsilon_0\}$, we choose $\Omega_\varepsilon = S_k$. Then there does not exist an L^1–convergent subsequence (see Lemma 5.11) and

$$E_{\gamma,\varepsilon}(\Omega_\varepsilon) \overset{(5.51)}{\leq} \big(1 - \frac{\gamma_*}{\gamma_{\text{crit}}}\big) \operatorname{Per}(\Omega_\varepsilon) + 2\gamma^* \int_0^\infty \Phi_\varepsilon(r)[c'_{\Omega_\varepsilon}(r) - c'_{\Omega_\varepsilon}(0)]\,\mathrm{d}r \tag{5.54}$$

$$\overset{\gamma_{\text{crit}} < \gamma_*}{\leq} 2\gamma^* \int_0^\infty \Phi_\varepsilon(r)[c'_{\Omega_\varepsilon}(r) - c'_{\Omega_\varepsilon}(0)]\,\mathrm{d}r \overset{(5.53)}{\leq} \frac{2\gamma^*}{k} \lesssim 1, \tag{5.55}$$

from which the claim follows. ■

Under the assumption of (H1) – (H3), the condition $\limsup_{\varepsilon\to 0} \gamma_\varepsilon < \infty$ cannot be omited since otherwise the parameter γ_ε might change the scaling of the non-local term, e.g. $\gamma_\varepsilon = \frac{\gamma}{\varepsilon}$ (see also (5.5) – (5.7)).

Theorem 5.10 identifies the subcritical parameter regime $0 \leq \gamma < \gamma_{\text{crit}}$ and the supercritical parameter regime $\gamma > \gamma_{\text{crit}}$. We learn that the local term dominates in the subcritical regime, while in the supercritical regime the destabilising effect of the non–local interaction takes over. The failure of compactness is reflected in uniform lower bounds of the energy and the behaviour of minimising sequences:

Corollary 5.13 Let $\gamma_\varepsilon > 0$ and suppose that $\mathcal{K}$ satisfies (H1) – (H3).

a) Let $\limsup_{\varepsilon\to 0} \gamma_\varepsilon \leq \gamma_{\text{crit}}$. Then there exists $\varepsilon^* > 0$, such that $E_{\gamma_\varepsilon,\varepsilon} \geq 0$ for every $0 < \varepsilon < \varepsilon^*$.

b) Let $\gamma_{\text{crit}} < \liminf_{\varepsilon\to 0} \gamma_\varepsilon \leq \limsup_{\varepsilon\to 0} \gamma_\varepsilon < \infty$. Then there exists a sequence $\Omega_\varepsilon \in \mathcal{A}$ such that

$$E_{\gamma_\varepsilon,\varepsilon}(\Omega_\varepsilon) \xrightarrow{\varepsilon \searrow 0} -\infty. \tag{5.56}$$

Moreover $\liminf_{\varepsilon\to 0} \operatorname{Per}(\Omega_\varepsilon) = \infty$ for any sequence such that (5.56) holds.

Proof: Assertion a) follows directly from Proposition 5.7. In order to show assertion b) we use the notation as in the proof of Theorem 5.12. Then $\mathrm{Per}(\Omega_\varepsilon) \xrightarrow{\varepsilon\searrow 0} +\infty$ and

$$E_{\gamma,\varepsilon}(\Omega_\varepsilon) \overset{(5.51)}{\leq} \big(1 - \frac{\gamma_*}{\gamma_{\mathrm{crit}}}\big)\,\mathrm{Per}(\Omega_\varepsilon) + 2\gamma^* \int_0^\infty \Phi_\varepsilon(r)[c'_{\Omega_\varepsilon}(r) - c'_{\Omega_\varepsilon}(0)]\,\mathrm{d}r \tag{5.57}$$

$$\overset{(5.53)}{\leq} \big(1 - \frac{\gamma_*}{\gamma_{\mathrm{crit}}}\big)\,\mathrm{Per}(\Omega_\varepsilon) + \frac{2\gamma^*}{k}, \tag{5.58}$$

from which the claim follows since $\gamma_* > \gamma_{\mathrm{crit}}$. In order to prove the necessity of a sequence with unbounded perimeter, we argue by contradiction: assume that (after selection of a subsequence) $\mathrm{Per}(\Omega_\varepsilon) \lesssim 1$, then $-1 \lesssim E_{\gamma,\varepsilon}[u_\varepsilon]$ by Proposition 5.7, which contradicts (5.56). ■

Before we turn to the critical parameter regime, we define what we mean by a rescaling function:

Definition 5.14 Let $\mathbf{R} \in C^0(\mathbb{R}_+)$. $\mathbf{R}$ is called a **Rescaling**, if $\mathbf{R} \geq 0$ and $\mathbf{R}(\varepsilon) \xrightarrow{\varepsilon\searrow 0} \infty$.

We have seen in Theorem 5.12 that the energy functional does not have compactness properties in the supercritical regime. The following lemma shows that there does not exist a rescaling to restore compactness.

Theorem 5.15 Let $\mathbf{R}$ be a rescaling and let $\gamma_\varepsilon > 0$ such that $\gamma_{\mathrm{crit}} < \liminf_{\varepsilon\to 0} \gamma_\varepsilon \leq \limsup_{\varepsilon\to 0} \gamma_\varepsilon < \infty$. Suppose $\mathcal{K}$ satisfies (H1)–(H3). Then there exists $\Omega_\varepsilon \in \mathcal{A}$ such that $\mathbf{R}(\varepsilon) E_{\gamma_\varepsilon,\varepsilon}(\Omega_\varepsilon) \xrightarrow{\varepsilon\searrow 0} -\infty$.

Proof: We use the notation as in the proof of Theorem 5.12. Then $\mathrm{Per}(\Omega_\varepsilon) \xrightarrow{\varepsilon\searrow 0} +\infty$ and

$$E_{\gamma,\varepsilon}(\Omega_\varepsilon) \overset{(5.51)}{\leq} \big(1 - \frac{\gamma_*}{\gamma_{\mathrm{crit}}}\big)\,\mathrm{Per}(\Omega_\varepsilon) + 2\gamma^* \int_0^\infty \Phi_\varepsilon(r)[c'_{\Omega_\varepsilon}(r) - c'_{\Omega_\varepsilon}(0)]\,\mathrm{d}r \tag{5.59}$$

$$\overset{(5.53)}{\leq} \big(1 - \frac{\gamma_*}{\gamma_{\mathrm{crit}}}\big)\,\mathrm{Per}(\Omega_\varepsilon) + \frac{2\gamma^*}{k}. \tag{5.60}$$

We will construct a subsequence of Ω_ε to ensure divergence to $-\infty$. In particular, for every $\varepsilon > 0$ we find $\delta_\varepsilon > 0$ such that

$$\mathbf{R}(\varepsilon)\big(1 - \frac{\gamma_*}{\gamma_{\mathrm{crit}}}\big)\,\mathrm{Per}(\Omega_\delta) > \frac{1}{\varepsilon} \qquad \text{for all } 0 < \delta < \delta_\varepsilon. \tag{5.61}$$

Now, let $\bar\varepsilon := \frac{1}{2}\min\{\varepsilon, \delta_\varepsilon\}$, then choosing the subsequence $\bar\Omega_\varepsilon := \Omega_{\bar\varepsilon}$ provides a sequence with the desired properties. ■

We will now shift our focus to the critical regime $\gamma_\varepsilon \sim \gamma_{\text{crit}}$.

Theorem 5.16 Let $\mathbf{R}$ be a rescaling and let $\gamma_\varepsilon > 0$ such that $\liminf_{\varepsilon\to 0}(1 - \frac{\gamma_\varepsilon}{\gamma_{\text{crit}}})\mathbf{R}(\varepsilon) > 0$. Suppose $\mathcal{K}$ satisfies (H1)–(H3). Let $\Omega_\varepsilon \in BV_n$ such that $\limsup_{\varepsilon\to 0} \mathbf{R}(\varepsilon)E_{\gamma_\varepsilon,\varepsilon}(\Omega_\varepsilon) < \infty$. Then there exists $\Omega \in \mathcal{A}$ and a subsequence (not relabeled), such that $|\Omega \triangle \Omega_\varepsilon| \to 0$.

Proof: By assumption there exists $\sigma > 0$ such that for $\varepsilon > 0$ sufficiently small we have $\sigma < (1 - \frac{\gamma_\varepsilon}{\gamma_{\text{crit}}})\mathbf{R}(\varepsilon)$. Using Corollary 5.7 we obtain

$$\sigma \operatorname{Per}(\Omega_\varepsilon) \leq \mathbf{R}(\varepsilon)\big(1 - \frac{\gamma_\varepsilon}{\gamma_{\text{crit}}}\big) \operatorname{Per}(\Omega_\varepsilon) \leq \mathbf{R}(\varepsilon)E_{\gamma_\varepsilon,\varepsilon}(\Omega_\varepsilon). \tag{5.62}$$

Passing to a subsequence (not relabeled) we find $\operatorname{Per}(\Omega_\varepsilon) \lesssim 1$. Using the compact embedding of BV into L^1 (see Theorem 2.10) finishes the proof. ■

We will end this section that there does not always exist a rescaling in the critical regime to restore compactness:

Lemma 5.17 Let $\mathbf{R}$ be a rescaling. Suppose $\mathcal{K}$ satisfies (H1)–(H3) and additionally assume that $\operatorname{supp}(\mathcal{K})$ is compact. Then there exists $\Omega_\varepsilon \in \mathcal{A}$ such that $\limsup_{\varepsilon\to 0} \mathbf{R}(\varepsilon)E_{\gamma_{\text{crit}},\varepsilon}(\Omega_\varepsilon) < \infty$, but there does not exist an L^1-convergent subsequence of Ω_ε.

Proof: We use the notation as in the proof of Theorem 5.12. Then $\operatorname{Per}(\Omega_\varepsilon) \xrightarrow{\varepsilon\searrow 0} +\infty$ and Theorem 5.6 yields

$$E_{\gamma_{\text{crit}},\varepsilon}(\Omega_\varepsilon) = 2\gamma_{\text{crit}} \int_0^\infty \Phi_\varepsilon(r)[c'_{\Omega_\varepsilon}(r) - c'_{\Omega_\varepsilon}(0)]\,\mathrm{d}r. \tag{5.63}$$

Since Ω_ε is a sequence of laminates, there exists $R_\varepsilon > 0$ such that $c'_{\Omega_\varepsilon}(r) = c'_{\Omega_\varepsilon}(0)$ for all $0 < r < R_\varepsilon$. With this at hand, we construct a subsequence of Ω_ε to ensure $E_{\gamma_{\text{crit}},\varepsilon}(\Omega_\varepsilon) = 0$ for all $\varepsilon > 0$. Thus, the energy is bounded and as a subsequence of Ω_ε, there does not exist a converging subsequence (see also Lemma 5.11).

Since $\mathcal{K}$ has compact support, so does Φ. Thus we can choose $0 < \delta \ll 1$ such that $\operatorname{supp}(\Phi_\delta) \subset [0, R_\varepsilon)$. Hence for every $\varepsilon > 0$ we find $\delta_\varepsilon > 0$ such that

$$\int_0^\infty \Phi_\delta(r)[c'_{\Omega_\varepsilon}(r) - c'_{\Omega_\varepsilon}(0)]\,\mathrm{d}r = 0 \qquad \text{for all } 0 < \delta < \delta_\varepsilon. \tag{5.64}$$

Now, let $\bar{\varepsilon} \coloneqq \frac{1}{2}\min\{\varepsilon, \delta_\varepsilon\}$, then choosing the subsequence $\bar{\Omega}_\varepsilon \coloneqq \Omega_{\bar{\varepsilon}}$ provides a sequence with the desired properties. ■

All the non-compactness results relied on carefully chosen oscillations and Lemma 5.11 to either bound the energy, or make it diverge to $-\infty$. However, laminates are no sets of finite perimeter in $\mathbb{R}^n$. In order to still achieve non-compactness in the full space setting, we instead use annuli $A_{\rho,R} \coloneqq B_R(0) \setminus B_\rho(0)$. In particular, choosing $\rho^n = R^n - \frac{\theta}{\omega_n}$, we have $|A_{\rho,R}| = \theta$, $\mathrm{Per}(A_{\rho,R}) = \sigma_n(R^{n-1} + \rho^{n-1})$, but $A_{\rho,R}$ does not have a convergent subsequence as $R \to \infty$. The techniques to prove non-compactness in the full space setting carry over from the periodic setting.

5.3. Asymptotic Expansion as $\varepsilon \to 0$

This section deals with the asymptotic expansion of the energy functional $E_{\gamma,\varepsilon}$ as $\varepsilon \to 0$. We will use the framework of Γ–convergence to show asymptotic behaviour.

As was seen in the last section, we can only hope to find a reasonable limit functional in the subcritical and critical parameter regime. While the subcritical regime does not require rescaling, the choice of the rescaling in the critical regime has a crucial effect on the asymptotic behaviour of the energy functional.

As a reminder, given a Banach space X, we say that a sequence $F_\varepsilon \colon X \longrightarrow \mathbb{R} \cup \{\pm\infty\}$ **Γ–converges** to $F \colon X \longrightarrow \mathbb{R} \cup \{\pm\infty\}$ as $\varepsilon \to 0$, if the following conditions hold:

- **Liminf–inequality:** For every $x \in X$ and every sequence $x_\varepsilon \in X$ with $x_\varepsilon \to x$ it holds
$$\liminf_{\varepsilon \to 0} F_\varepsilon(x_\varepsilon) \geq F(x). \tag{5.65}$$
- **Limsup–inequality** For every $x \in X$ there exists a sequence $x_\varepsilon \in X$, such that $x_\varepsilon \to x$ and
$$\limsup_{\varepsilon \to 0} F_\varepsilon(x_\varepsilon) \leq F(x). \tag{5.66}$$

In that case, we denote $F_\varepsilon \xrightarrow{\Gamma} F$. We will start with the subcritical regime:

Theorem 5.18 Let $\gamma_\varepsilon > 0$ and assume $\gamma^* \coloneqq \limsup_{\varepsilon \to 0} \gamma_\varepsilon < \gamma_{\mathrm{crit}}$. Suppose $\mathcal{K}$ satisfies (H1)–(H3). Then $E_{\gamma_\varepsilon,\varepsilon} \xrightarrow{\Gamma} (1 - \frac{\gamma^*}{\gamma_{\mathrm{crit}}})\,\mathrm{Per}$ in the L^1-topology.

Proof: *Liminf inequality:* By Theorem 5.10 we can assume without loss of generality that $\Omega_\varepsilon, \Omega \in \mathcal{A}$ and $|\Omega_\varepsilon \triangle \Omega| \to 0$. The assumptions on γ_ε imply

$$0 < 1 - \frac{\gamma^*}{\gamma_{\mathrm{crit}}} = \liminf_{\varepsilon \to 0} 1 - \frac{\gamma_\varepsilon}{\gamma_{\mathrm{crit}}}, \tag{5.67}$$

and thus by the lower semicontinuity of the perimeter and Theorem 5.7

$$0 \leq \big(1 - \frac{\gamma^*}{\gamma_{\text{crit}}}\big) \operatorname{Per}(\Omega) = \big(1 - \frac{\gamma^*}{\gamma_{\text{crit}}}\big) \operatorname{Per}(\Omega) = \Big(\liminf_{\varepsilon\to 0} 1 - \frac{\gamma_\varepsilon}{\gamma_{\text{crit}}}\Big) \operatorname{Per}(\Omega) \tag{5.68}$$

$$\leq \Big(\liminf_{\varepsilon\to 0} 1 - \frac{\gamma_\varepsilon}{\gamma_{\text{crit}}}\Big)\Big(\liminf_{\varepsilon\to 0} \operatorname{Per}(\Omega_\varepsilon)\Big) \tag{5.69}$$

$$\leq \liminf_{\varepsilon\to 0} \big(1 - \frac{\gamma_\varepsilon}{\gamma_{\text{crit}}}\big) \operatorname{Per}(\Omega_\varepsilon) \tag{5.70}$$

$$\leq \liminf_{\varepsilon\to 0} E_{\gamma_\varepsilon,\varepsilon}(\Omega_\varepsilon). \tag{5.71}$$

Limsup inequality: The case $\Omega \notin \mathcal{A}$ is trivial, so let $\Omega \in \mathcal{A}$. We choose the constant recovery sequence $\Omega_\varepsilon = \Omega$. Let $\delta > 0$, then there exists $\varepsilon_\delta > 0$ such that for all $0 < \varepsilon < \varepsilon_\delta$

$$E_{\gamma_\varepsilon,\varepsilon}(\Omega) = \big(1 - \frac{\gamma_\varepsilon}{\gamma_{\text{crit}}}\big) \operatorname{Per}(\Omega) + 2\gamma_\varepsilon \int_0^\infty \Phi_\varepsilon(r)[c'_\Omega(r) - c'_\Omega(0)]\,\mathrm{d}r \tag{5.72}$$

$$\leq \big(1 - \frac{\gamma^*}{\gamma_{\text{crit}}} + \delta\big) \operatorname{Per}(\Omega) + 2\gamma_{\text{crit}} \int_0^\infty \Phi_\varepsilon(r)[c'_\Omega(r) - c'_\Omega(0)]\,\mathrm{d}r, \tag{5.73}$$

where we used Theorem 5.6 in the first line. The non-local term on the right-hand side vanishes as $\varepsilon \to 0$ by Corollary 5.9 and thus we obtain

$$\limsup_{\varepsilon\to 0} E_{\gamma_\varepsilon,\varepsilon}(\Omega) \leq \big(1 - \frac{\gamma^*}{\gamma_{\text{crit}}}\big) \operatorname{Per}(\Omega) + \delta \operatorname{Per}(\Omega). \tag{5.74}$$

Since δ was arbitrary, the limsup inequality follows. ■

The result of Theorem 5.18 in case of a constant sequence $\gamma_\varepsilon = \gamma \leq \gamma_{\text{crit}}$ was shown in [BKMC23].

5.3.1. Higher Order Expansion

In this section, we will restrict ourselves to the case $n = 2$. Similar to the introduction of the function Φ in (5.15) due to an integration by parts, we need an integrated kernel for convergence in higher orders of the energy $E_{\gamma,\varepsilon}$. Thus we introduce

$$\Psi_\varepsilon(r) \coloneqq \frac{1}{\varepsilon}\Psi(\tfrac{r}{\varepsilon}), \qquad \Psi(r) \coloneqq \int_r^\infty \Phi(\rho)\,\mathrm{d}\rho \qquad \text{for all } r > 0. \tag{5.75}$$

Similar to Proposition 5.3 and Corollary 5.4 we collect properties of the function Ψ and the family $\{\Psi_\varepsilon\}_\varepsilon$.

Proposition 5.19 Assume $\mathcal{K}$ satisfies (H1) – (H3) and assume additionally $\mathfrak{m}_2 < \infty$. Let Φ as in (5.15) and Ψ as in (5.75). Then

a) $\Psi \geq 0$.

b) $\lim\limits_{r\to 0} r\Psi(r) = \lim\limits_{r\to\infty} r\Psi(r) = 0$.

c) $\Psi \in L^1(\mathbb{R}_+)$ and $\displaystyle\int_0^\infty \Psi(r)\,\mathrm{d}r = \frac{1}{2}\int_{\mathbb{R}^n} |z|^2\,\mathcal{K}(z)\,\mathrm{d}z$.

Proof: Assertion a) follows from $\Phi \geq 0$ (see Proposition 5.3 a)). Before we will show the remaining assertions, we note that the assumption $\mathfrak{m}_2 < \infty$ improves upon the properties of Φ shown in Proposition 5.3, namely

$$\lim_{r\to\infty} r^2\Phi(r) = 0, \qquad \int_0^\infty r\Phi(r)\,\mathrm{d}r = \frac{1}{2}\int_{\mathbb{R}^n} |z|^2\,\mathcal{K}(z)\,\mathrm{d}z. \tag{5.76}$$

To see the first claim, we observe that

$$r^2\Phi(r) = \sigma_n \int_r^\infty r^2\rho^{n-1}\mathcal{K}(\rho)\,\mathrm{d}\rho \leq \sigma_n \int_r^\infty \rho^{n+1}\mathcal{K}(\rho)\,\mathrm{d}\rho \xrightarrow{r\to\infty} 0, \tag{5.77}$$

where in the last line we used $\mathfrak{m}_2 < \infty$. Now we obtain for $0 < r < R < \infty$ via integration by parts

$$\int_r^R \rho\Phi(\rho)\,\mathrm{d}\rho = \frac{1}{2}\rho^2\Phi(\rho)\Big|_r^R + \frac{\sigma_n}{2}\int_r^R \rho^{n+1}\mathcal{K}(\rho)\,\mathrm{d}\rho. \tag{5.78}$$

Using the Dominated Convergence Theorem in the limits $r \to 0$ and $R \to \infty$ (since $\mathfrak{m}_2 < \infty$) as well as (5.77) yields

$$\int_0^\infty \rho\Phi(\rho)\,\mathrm{d}\rho = \frac{\sigma_n}{2}\int_0^\infty \rho^{n+1}\mathcal{K}(\rho)\,\mathrm{d}\rho = \frac{1}{2}\int_{\mathbb{R}^n} |z|^2\,\mathcal{K}(z)\,\mathrm{d}z. \tag{5.79}$$

Now we can show the remaining assertions. First, we notice that

$$R\Psi(R) = \int_R^\infty R\Phi(\rho)\,\mathrm{d}\rho \leq \int_R^\infty \rho\Phi(\rho)\,\mathrm{d}\rho \xrightarrow{R\to\infty} 0. \tag{5.80}$$

Moreover, as $\Psi(0) = \|\Phi\|_{L^1(\mathbb{R}_+)} < \infty$, we have $r\Psi(r) \xrightarrow{r\to 0} 0$. Lastly, let $0 < r < R < \infty$. Then using integration by parts

$$\int_r^R \Psi(\rho)\,\mathrm{d}\rho = \rho\Psi(\rho)\Big|_r^R + \int_r^R \rho\Phi(\rho)\,\mathrm{d}\rho. \tag{5.81}$$

Using the Dominated Convergence Theorem in the limits $r \to 0$ and $R \to \infty$ yields

$$\int_0^\infty \Psi(\rho)\,\mathrm{d}\rho = \int_0^\infty \rho\Phi(\rho)\,\mathrm{d}\rho = \frac{1}{2}\int_{\mathbb{R}^n} |z|^2\,\mathcal{K}(z)\,\mathrm{d}z, \tag{5.82}$$

as claimed. ■

Corollary 5.20 Assume $\mathcal{K}$ satisfies (H1) – (H3) and additionally $\mathfrak{m}_2 < \infty$. Let Ψ_ε as in (5.75). Let $\psi_\varepsilon \colon \mathbb{R} \longrightarrow \mathbb{R}$ be given by

$$\psi_\varepsilon(r) \coloneqq \frac{\Psi_\varepsilon(r)}{\|\Psi\|_{L^1(\mathbb{R}_+)}} \chi_{\mathbb{R}_+}(r) \qquad \text{for all } r \in \mathbb{R}. \tag{5.83}$$

Then the family $\{\psi_\varepsilon\}_\varepsilon$ forms an approximation of the identity.

Proof: Follows from Proposition 5.19. ■

Using the just proven properties of Ψ, we are able to prove the following Γ–convergence result for the rescaled energy functional $\frac{1}{\varepsilon} E_{\gamma_\varepsilon,\varepsilon}$ in the critical regime.

Theorem 5.21 Let $\gamma_\varepsilon > 0$ and assume $\frac{1}{\varepsilon}(1 - \frac{\gamma_\varepsilon}{\gamma_{\text{crit}}}) \xrightarrow{\varepsilon \searrow 0} \sigma > 0$. Suppose $\mathcal{K}$ satisfies (H1)–(H3) and additionally $\mathfrak{m}_2 < \infty$. Then $\frac{1}{\varepsilon} E_{\gamma_\varepsilon,\varepsilon} \xrightarrow{\Gamma} \sigma \operatorname{Per}$ in the L^1–topology.

Proof: *Liminf inequality:* Using Theorem 5.16 we can assume without loss of generality that $\Omega_\varepsilon, \Omega \in \mathcal{A}$ and $|\Omega_\varepsilon \triangle \Omega| \to 0$. Let $0 < \delta < \frac{\sigma}{2}$. Then there exists $\varepsilon^* > 0$ such that for all $0 < \varepsilon < \varepsilon^*$ we have

$$0 < \sigma - \delta < \frac{1}{\varepsilon}\big(1 - \frac{\gamma_\varepsilon}{\gamma_{\text{crit}}}\big). \tag{5.84}$$

Thus by the lower semicontinuity of the perimeter and Theorem 5.7 we obtain

$$\begin{aligned}
0 < (\sigma - \delta) \operatorname{Per}(\Omega) &\leq \Big(\liminf_{\varepsilon \to 0} \frac{1}{\varepsilon}\big(1 - \frac{\gamma_\varepsilon}{\gamma_{\text{crit}}}\big) \Big) \operatorname{Per}(\Omega) && (5.85)\\
&\leq \Big(\liminf_{\varepsilon \to 0} \frac{1}{\varepsilon}\big(1 - \frac{\gamma_\varepsilon}{\gamma_{\text{crit}}}\big) \Big) \Big(\liminf_{\varepsilon \to 0} \operatorname{Per}(\Omega_\varepsilon) \Big) && (5.86)\\
&\leq \liminf_{\varepsilon \to 0} \frac{1}{\varepsilon}\big(1 - \frac{\gamma_\varepsilon}{\gamma_{\text{crit}}}\big) \operatorname{Per}(\Omega_\varepsilon) && (5.87)\\
&\leq \liminf_{\varepsilon \to 0} \frac{1}{\varepsilon} E_{\gamma_\varepsilon,\varepsilon}(\Omega_\varepsilon). && (5.88)
\end{aligned}$$

Rearranging the terms leads to

$$\sigma \operatorname{Per}(\Omega) \leq \delta \operatorname{Per}(\Omega) + \liminf_{\varepsilon \to 0} \frac{1}{\varepsilon} E_{\gamma_\varepsilon,\varepsilon}(\Omega_\varepsilon). \tag{5.89}$$

Since $\delta > 0$ was arbitrary, the liminf inequality follows.

Limsup inequality: The case $\Omega \notin \mathcal{A}$ is trivial. We first focus on the case $\Omega \in \mathcal{A} \cap BV_2^\infty$ and choose the constant recovery sequence $\Omega_\varepsilon = \Omega$. Since $\Omega \in BV_2^\infty$, there exists $R > 0$

such that $c_\Omega \in C^\infty((0,2R])$ (see Theorem 4.10). We use Theorem 5.6 to obtain

$$\frac{1}{\varepsilon}E_{\gamma_\varepsilon,\varepsilon}(\Omega) = \frac{1}{\varepsilon}\big(1-\frac{\gamma_\varepsilon}{\gamma_{\text{crit}}}\big)\operatorname{Per}(\Omega) + \frac{2\gamma_\varepsilon}{\varepsilon}\int_0^\infty \Phi_\varepsilon(r)[c_\Omega'(r)-c_\Omega'(0)]\,\mathrm{d}r \tag{5.90}$$

and claim that the non-local term converges to 0.

We split the non-local term as follows

$$\frac{1}{\varepsilon}\int_0^\infty \Phi_\varepsilon(r)[c_\Omega'(r)-c_\Omega'(0)]\,\mathrm{d}r = \frac{1}{\varepsilon}\int_0^R \Phi_\varepsilon(r)[c_\Omega'(r)-c_\Omega'(0)]\,\mathrm{d}r \tag{5.91}$$

$$+\frac{1}{\varepsilon}\int_R^\infty \Phi_\varepsilon(r)[c_\Omega'(r)-c_\Omega'(0)]\,\mathrm{d}r \tag{5.92}$$

$$=: I_\varepsilon + J_\varepsilon, \tag{5.93}$$

and estimate both integrals seperately. Using the regularity of the Autocorrelation Function, we can integrate by parts to obtain

$$I_\varepsilon = -\Big[\Psi_\varepsilon(r)[c_\Omega'(r)-c_\Omega'(0)]\Big]_0^R + \int_0^R \Psi_\varepsilon(r)c_\Omega''(r)\,\mathrm{d}r \tag{5.94}$$

$$= \Psi_\varepsilon(R)[c_\Omega'(R)-c_\Omega'(0)] + \int_0^R \Psi_\varepsilon(r)c_\Omega''(r)\,\mathrm{d}r \xrightarrow{\varepsilon\to 0} 0 + \|\Psi\|_{L^1(\mathbb{R}_+)}c_\Omega''(0) = 0, \tag{5.95}$$

where Ψ_ε is defined in (5.75) and in the last line we used Corollary 5.20 and Corollary 4.12. For the quantity J_ε we use the fact that $\mathfrak{m}_2 < \infty$ by assumption and (5.79) to obtain

$$|J_\varepsilon| \le 2\operatorname{Per}(\Omega)\frac{1}{\varepsilon}\int_{\frac{R}{\varepsilon}}^\infty \Phi(r)\,\mathrm{d}r \le \frac{2\operatorname{Per}(\Omega)}{R}\int_{\frac{R}{\varepsilon}}^\infty r\Phi(r)\,\mathrm{d}r \xrightarrow{\varepsilon\to 0} 0. \tag{5.96}$$

Altogether we obtain

$$\limsup_{\varepsilon\to 0}\frac{1}{\varepsilon}E_{\gamma_\varepsilon,\varepsilon}(\Omega) \le \limsup_{\varepsilon\to 0}\frac{1}{\varepsilon}\big(1-\frac{\gamma_\varepsilon}{\gamma_{\text{crit}}}\big)\operatorname{Per}(\Omega) = \sigma\operatorname{Per}(\Omega), \tag{5.97}$$

which was the claim. For general sets $\Omega \in \mathcal{A}$ we use a diagonal sequence. More precisely: there exists a sequence of smooth sets $\Omega_k \in \mathcal{A}\cap BV_2^\infty$ such that (see Lemma 2.18)

$$|\Omega_k \triangle \Omega| \xrightarrow{k\to\infty} 0, \qquad |\operatorname{Per}(\Omega_k)] - \operatorname{Per}(\Omega)| \xrightarrow{k\to\infty} 0. \tag{5.98}$$

By the computations above we have $\frac{1}{\varepsilon}E_{\gamma_\varepsilon,\varepsilon}(\Omega_k) \xrightarrow{\varepsilon\searrow 0} \sigma\operatorname{Per}(\Omega_k)$ for any $k\in\mathbb{N}$. Hence, for all $k\in\mathbb{N}$ there exists $\varepsilon^*(k)$ such that

$$|E_{\gamma_\varepsilon,\varepsilon}(\Omega_k) - \sigma\operatorname{Per}(\Omega_k)| < \frac{1}{k} \qquad \text{for all } 0<\varepsilon<\varepsilon^*. \tag{5.99}$$

For $\frac{1}{2}\min\{\frac{1}{k+1}, \varepsilon^*(k+1)\} < \varepsilon < \frac{1}{2}\min\{\frac{1}{k}, \varepsilon^*(k)\}$ we choose $\Omega_\varepsilon = \Omega_k$. Then

$$|\Omega_\varepsilon \triangle \Omega| \xrightarrow{\varepsilon\to 0} 0, \qquad |\operatorname{Per}(\Omega_\varepsilon) - \operatorname{Per}(\Omega)| \xrightarrow{\varepsilon\to 0} 0, \qquad E_{\gamma_\varepsilon,\varepsilon}(\Omega_k) \overset{(5.99)}{\leq} \sigma \operatorname{Per}(\Omega_k) + \frac{1}{k}, \tag{5.100}$$

from which the limsup inequality follows. ■

We note that the liminf inequality in the Γ–convergence result does not require higher moments of the kernel due to the pointwise estimate shown in (5.62). The higher moment condition is needed in the proof of the limsup inequality only. Moreover, a significant change occurs in the limsup inequality as the constant sequence in general cannot be used as a recovery sequence, one example being polygons. Indeed, repeating the same computations for a polytope $P \subset \mathbb{T}^2$ as in (5.91)–(5.96), we find that

$$E_{\gamma_\varepsilon,\varepsilon}(P) \xrightarrow{\varepsilon\searrow 0} \sigma \operatorname{Per}(P) + 2\gamma_{\text{crit}}\|\Psi\|_{L^1(\mathbb{R}_+)} c_P''(0) > \sigma \operatorname{Per}(\Omega), \tag{5.101}$$

where we used Corollary 4.18.

5.4. Energy Computations

In this section, we discuss several examples. Important for the modelling is the fundamental solution $\mathcal{K}$ of the Helmholtz equation $\mathcal{K} - \Delta\mathcal{K} = \delta_0$. We will mainly restrict to the case $n = 2$, where the Helmholtz kernel is given by $\mathcal{K}(z) = \frac{1}{2\pi}K_0(|z|)$, where $K_0 \colon \mathbb{R}_+ \longrightarrow \mathbb{R}_+$ is the Modified Bessel Function of the second kind (see Appendix Lemma A.14).

In what follows we will use the notation Rem to denote a remainder term which is vanishing as $\varepsilon \to 0$ based on the decay of the interaction kernel $\mathcal{K}$. More precisely, using the notation of the proof of Theorem 5.21, we denote

$$\text{Rem} = J_\varepsilon = \int_R^\infty \Phi_\varepsilon(r)[c_\Omega'(r) - c_\Omega'(0)]\,\mathrm{d}r \lesssim 2\operatorname{Per}(\Omega)\int_{\frac{R}{\varepsilon}}^\infty \Phi(r)\,\mathrm{d}r, \tag{5.102}$$

of which the asymptotic behaviour as $\varepsilon \to 0$ is only dependent on the decay of Φ and therefore only dependent of $\mathcal{K}$.

5.4.1. Energy of Balls

Building upon computations in Section 4.4.1, and using Proposition 5.8 and Theorem 5.21, we obtain for $0 < \rho < 1$ and $0 < \varepsilon \ll 1$

$$E_{\gamma,\varepsilon}(B_\rho) = 2\pi\rho\big(1 - \frac{\gamma}{\gamma_{\text{crit}}}\big) + \varepsilon^2\frac{\gamma}{\rho}\frac{\gamma_{\text{sec}}}{\gamma_{\text{crit}}} + \text{Rem}, \tag{5.103}$$

where Rem is the remainder term as described in (5.102). Here, the constant γ_{sec} in the second order is given by

$$\gamma_{\text{sec}} \coloneqq \frac{\pi}{6}\frac{\mathfrak{m}_3}{\mathfrak{m}_1}. \tag{5.104}$$

5.4.2. Energy of Laminates

For general laminates $S \subset \mathbb{T}^n$ with N components we know that $c_S'(r) - c_S'(0) = 0$ near $r = 0$ (see (4.136) – (4.139)). Thus the energy can be computed to be

$$E_{\gamma,\varepsilon}(S) = \big(1 - \frac{\gamma}{\gamma_{\text{crit}}}\big)2^N + \text{Rem}\,. \tag{5.105}$$

In particular, there do not occur higher order contributions in the ε–expansion.

Evenly spaced laminates: As we have seen in Section 5.2, multiple stripes are preferred to a single stripe in the supercritical regime $\gamma > \gamma_{\text{crit}}$. Moreover, if in addition $\mathcal{K} \in L^1(\mathbb{R}^n)$, then we observe that

$$E_{\gamma,\varepsilon}(\Omega) \geq -\frac{\gamma}{\varepsilon}\int_{\mathbb{R}^n} \mathcal{K}_\varepsilon(z) \int_{\mathbb{T}^n} |\chi_\Omega(x+z) - \chi_\Omega(x)|\,\mathrm{d}x\,\mathrm{d}z \geq -\frac{2\gamma}{\varepsilon}\|\mathcal{K}\|_{L^1(\mathbb{R}^n)}, \tag{5.106}$$

and thus is bounded from below.

In Lemma 4.16 we computed the Autocorrelation Function for a single laminate for $n = 2$. Thus, given the volume fraction $0 < \theta < 1$, the parameters $\varepsilon, \gamma > 0$ and the interaction kernel $\mathcal{K}$, we can explicitly compute the energy of a single laminate with the help of Theorem 5.6 even in the supercritical regime. In addition, we are able to compute the energy of k evenly spaced laminates through dilation. More precisely, let $S \coloneqq (0,\theta) \times \mathbb{T} \subset \mathbb{T}^2$ be a single laminate, we can dilate $S_k \coloneqq kS$ to have k laminates which have volume fraction θ. Inserting in the energy functional, we obtain

$$E_{\gamma,\varepsilon}(S_k) = kE_{\gamma,k\varepsilon}(S). \tag{5.107}$$

In that case, the function $F_{\gamma,\varepsilon,\theta}\colon k \longmapsto kE_{\gamma,k\varepsilon}(S)$ might attain its minimum. In order to find the minimum, we find critical points through the equation $F'_{\gamma,\varepsilon,\theta} = 0$. We obtain

$$\frac{1}{2}\frac{\mathrm{d}}{\mathrm{d}k}F_{\gamma,\varepsilon,\theta}(k) = \frac{\mathrm{d}}{\mathrm{d}k}k\Big[1 + \gamma\int_0^\infty \Phi_{k\varepsilon}(r)\,c_S'(r)\,\mathrm{d}r\Big] \tag{5.108}$$

$$= 1 + \gamma\int_0^\infty \Phi_{k\varepsilon}(r)\,c_S'(r)\,\mathrm{d}r + k\gamma\int_0^\infty c_S'(r)\,\frac{\mathrm{d}}{\mathrm{d}k}\Phi_{k\varepsilon}(r)\,\mathrm{d}r \tag{5.109}$$

$$= 1 + \gamma\int_0^\infty c_S'(r)\frac{\mathrm{d}}{\mathrm{d}k}\big[k\Phi_{k\varepsilon}(r)\big]\,\mathrm{d}r. \tag{5.110}$$

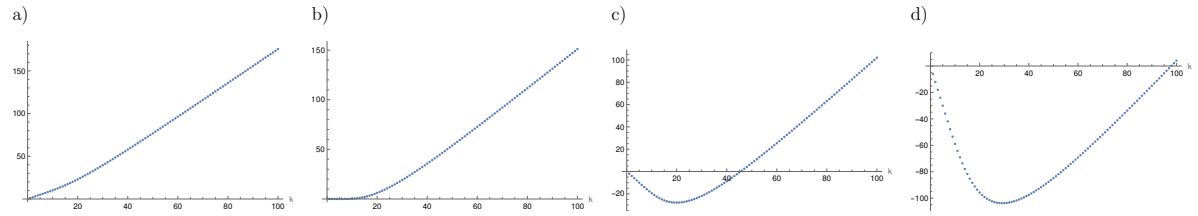

Figure 5.2.: Values of $E_{\gamma,\varepsilon}(S_k)$ for the Helmholtz kernel $\mathcal{K} - \Delta\mathcal{K} = \delta_0$ (with $\gamma_{\text{crit}} = 1$) for different values of γ and fixed $\varepsilon = \frac{1}{2}$. The different values are a) $\gamma = \frac{1}{2}$, b) $\gamma = 1$, c) $\gamma = 2$, d) $\gamma = 4$.

We compute

$$\frac{\mathrm{d}}{\mathrm{d}k}\big[k\Phi_{k\varepsilon}(r)\big] = \frac{\mathrm{d}}{\mathrm{d}k}\big[\frac{1}{\varepsilon}\Phi(\tfrac{r}{k\varepsilon})\big] = \frac{1}{\varepsilon}\Phi'(\tfrac{r}{k\varepsilon})\,\big(-\frac{r}{k^2\varepsilon}\big) \tag{5.111}$$

$$= -\frac{1}{k\varepsilon}\,\frac{r}{k\varepsilon}\Phi'(\tfrac{r}{k\varepsilon}) = -(\mathrm{id}\Phi')_{k\varepsilon}(r) = \sigma_2(\mathrm{id}^2\mathcal{K})_{k\varepsilon}(r). \tag{5.112}$$

Inserting in the above computations shows

$$\frac{1}{2}\frac{\mathrm{d}}{\mathrm{d}k}F_{\gamma,\varepsilon,\theta}(k) = 1 + \gamma\sigma_2\int_0^\infty c_S'(r)(\mathrm{id}^2\mathcal{K})_{k\varepsilon}(r)\,\mathrm{d}r \overset{!}{=} 0. \tag{5.113}$$

Rearranging the terms we obtain the criticality condition:

$$\boxed{\int_0^\infty r^2\mathcal{K}(r)\,c_S'(k\varepsilon r)\,\mathrm{d}r = -\frac{1}{2\pi\gamma}}$$

We observe that, under the additional assumption that $\mathcal{K}$ is a continuous function, for every $\gamma > \gamma_{\text{crit}}$ there exists $t = k\varepsilon$ such that the criticality condition holds. Indeed, we compute

$$\int_0^\infty r^2\mathcal{K}(r)\,c_S'(tr)\,\mathrm{d}r \xrightarrow{t\searrow 0} -\frac{2}{\pi}\int_0^\infty r^2\mathcal{K}(r)\,\mathrm{d}r = -\frac{1}{2\pi\gamma_{\text{crit}}}, \tag{5.114}$$

$$\int_0^\infty r^2\mathcal{K}(r)\,c_S'(tr)\,\mathrm{d}r \xrightarrow{t\to\infty} 0, \tag{5.115}$$

where we used [KS23, Proposition 2.4 *(vi)*] in last line. After the transformation $r \longmapsto \frac{r}{t}$ we find that the integral is continuous with respect to t, so the claim follows with the Intermediate Value Theorem.

In summary, given $\varepsilon > 0$ and $\gamma > \gamma_{\text{crit}}$, we find $k_* > 1$ through the criticality condition such that S_{k^*} is a better competitor than S_k for every $k \in \mathbb{N}$. In particular, the interpretation for $E_{\gamma,\varepsilon}$ as a biological model described in Chapter 3 is that fine scale patterns form in the supercritical regime.

5.4.3. Energy of Polytopes

As we have seen in the proofs of Proposition 5.8 and Theorem 5.21, the methods relied on the smoothness of the Autocorrelation Function near $r = 0$. Even though polytopes

are not in the class BV_2^∞, Lemma 4.17 shows that the corresponding Autocorrelation Function is smooth. Thus the calculations and estimates carry over and we obtain for a polytope $P \subset \mathbb{T}^2$:

$$E_{\gamma,\varepsilon}(P) = \big(1 - \frac{\gamma}{\gamma_{\text{crit}}}\big) \operatorname{Per}(P) + \varepsilon\gamma \|\Psi\|_{L^1(\mathbb{R}_+)} c_P''(0) + \text{Rem} \tag{5.116}$$

where $\Psi \in L^1(\mathbb{R}_+)$ is given in (5.75) and Rem is a remainder term depending on the decay of $\mathcal{K}$. Apart for laminates, the quantity $c_P''(0)$ is positive (see Corollary 4.18).

Polygons as recovery sequences: It is worth noting that due to the fact that $c_P^{(k)}(0) = 0$ for all $k \geq 3$ (see Lemma 4.17) there is no higher order contribution in the ε–expansion. In spite of this, polytopes do not make good candidates for recovery sequences for higher order convergence.

To see this, assume $\gamma_\varepsilon > 0$ such that $\frac{1}{\varepsilon^2}(1 - \frac{\gamma_\varepsilon}{\gamma_{\text{crit}}}) \xrightarrow{\varepsilon \searrow 0} \sigma > 0$, which would correspond to a next order rescaling (compare to Theorem 5.21). Let $\Omega = B_\rho(0)$ with $\rho < \frac{1}{8}$ and consider Ξ_N to be a regular polytope with N edges such that (see Figure 5.3)

$$|\Xi_N| = |\Omega|, \qquad \operatorname{Per}(\Xi_N) \xrightarrow{N\to\infty} \operatorname{Per}(\Omega). \tag{5.117}$$

For this demonstration, we additionally assume $\mathcal{K} = \chi_{B_1(0)}$, which satisfies (H1)–(H3) and $\mathfrak{m}_3 < \infty$. Then $\operatorname{supp}(\Phi) \subset [0,1]$ and we compute for all $0 < r < 1$

$$\Phi(r) = \pi(1 - r^2), \qquad \|\Phi\|_{L^1} = \frac{2\pi}{3}, \tag{5.118}$$

$$\Psi(r) = \frac{\pi}{3}(r^3 - 3r + 2), \qquad \|\Psi\|_{L^1} = \frac{\pi}{4}, \tag{5.119}$$

$$\tag{5.120}$$

where Ψ is as in (5.75). Moreover we compute

$$\gamma_{\text{crit}} = \frac{3}{4}, \qquad \gamma_{\text{sec}} = \frac{\pi}{10}, \tag{5.121}$$

where γ_{sec} is as in (5.104).

The quantity R_N from (4.141) will be important for our computations as it determines in which range the Autocorrelation Function c_{Ξ_N} is a polynomial. Since Ξ_N is convex, we find that R_N is given by the length of an edge. We find that

$$|\Xi_N| = N R_N h_N, \tag{5.122}$$

where h_N is the height of one of the identical isoceles triangles. Using trigonometry we

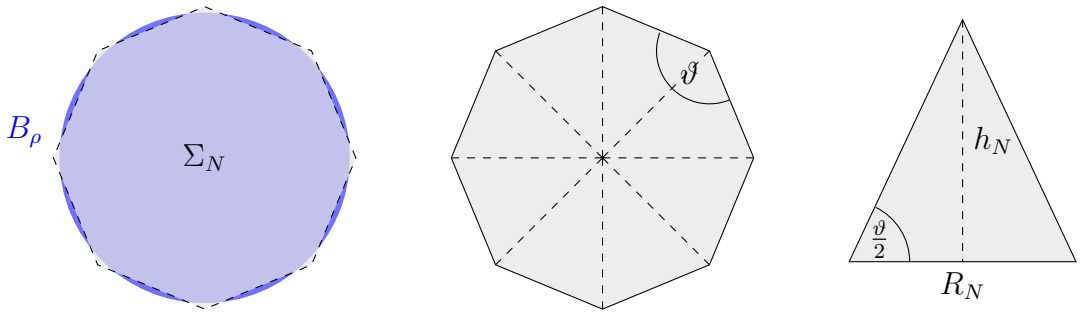

Figure 5.3.: Setup and notation for Ξ_N.

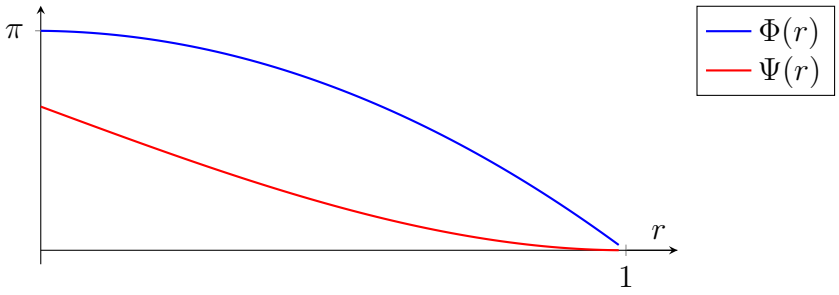

Figure 5.4.: Plots of the functions Φ and Ψ corresponding to $\mathcal{K} = \chi_{B_1}$.

obtain $\tan(\frac{\vartheta}{2}) = \frac{h_N}{R_N/2}$ and thus

$$|\Xi_N| = NR_N h_N = \frac{N}{2} R_N^2 \tan(\tfrac{\vartheta}{2}) \qquad \Longrightarrow \qquad R_N^2 = \frac{2|\Xi_N|}{N} \cot(\tfrac{\vartheta}{2}). \tag{5.123}$$

Using the Laurent Series of the cotangent and plugging in $\vartheta = \pi \frac{N-2}{N}$ we obtain that

$$R_{\Xi_N} = \frac{\sqrt{2\pi|\Xi_N|}}{N} + \mathcal{O}(\tfrac{1}{N^2}). \tag{5.124}$$

Moreover, the quantity $c''_{\Xi_N}(0)$ is given by (see (4.170))

$$c''_{\Xi_N}(0) = \frac{2\pi}{3N} + \mathcal{O}(\tfrac{1}{N^3}). \tag{5.125}$$

We are now in the position to compute the energy of the polytopes Ξ_N. Using Lemma 4.17 we obtain for $0 < \varepsilon < \frac{\sqrt{2\pi|\Omega|}}{N} < R_N$

$$\frac{1}{\varepsilon^2} \int_0^\infty \Phi_\varepsilon(r)[c'_{\Xi_N}(r) - c'_{\Xi_N}(0)]\,\mathrm{d}r = \frac{1}{\varepsilon^2} \int_0^\varepsilon \Phi_\varepsilon(r)[c'_{\Xi_N}(r) - c'_{\Xi_N}(0)]\,\mathrm{d}r \tag{5.126}$$

$$= \frac{c''_{\Xi_N}(0)}{\varepsilon^2} \int_0^\varepsilon r\Phi_\varepsilon(r)\,\mathrm{d}r \tag{5.127}$$

$$= \frac{\|\Psi\|_{L^1(\mathbb{R}_+)}}{\varepsilon} c''_{\Xi_N}(0) = \frac{\pi^2}{6N\varepsilon} + \frac{1}{N\varepsilon}\mathcal{O}(\tfrac{1}{N^2}). \tag{5.128}$$

Due to the constraint on ε, the optimal choice for the parameters is $N\varepsilon = \sqrt{2\pi|\Omega|} = \sqrt{2}\pi\rho$,

from which we obtain

$$\frac{1}{\varepsilon^2}\int_0^\infty \Phi_\varepsilon(r)[c'_{\Xi_N}(r) - c'_{\Xi_N}(0)]\,\mathrm{d}r = \frac{\pi}{6\sqrt{2}\rho} + \mathcal{O}(\tfrac{1}{N^2}). \tag{5.129}$$

In the limit $\varepsilon \searrow 0$ (which in turn makes $N \to \infty$) we obtain

$$E_{\gamma_\varepsilon,\varepsilon}(\Xi_N) \xrightarrow{\varepsilon\searrow 0} \sigma\,\mathrm{Per}(\Omega) + 2\gamma_{\mathrm{crit}}\frac{\pi}{6\sqrt{2}\rho} = \sigma\,\mathrm{Per}(\Omega) + \frac{3\pi}{12\sqrt{2}\rho} > \sigma\,\mathrm{Per}(\Omega) + \frac{1}{80\rho}, \tag{5.130}$$

where the right-hand side corresponds to the energy of a ball given in (5.103).

5.4.4. Energy of Annuli

In Section 4.4.2, we have computed the full space Autocorrelation Function of an annulus $A_{\rho,R} \coloneqq B_R(0) \setminus B_\rho(0)$. As the Autocorrelation Function of $A_{\rho,R}$ is tightly connected to the Autocorrelation Function of B_R and B_ρ, we aim to derive a formula of the energy of an annulus in terms of the energy of the corresponding balls. We are using the following representation formula of the energy:

$$E_{\gamma,\varepsilon}(\Omega) = \mathrm{Per}(\Omega) - \gamma\int_{\mathbb{R}^n}\mathcal{K}(z)\int_{\mathbb{R}^n}|\chi_\Omega(x+z) - \chi_\Omega(x)|\,\mathrm{d}x\,\mathrm{d}z \tag{5.131}$$

$$= \mathrm{Per}(\Omega) + 2\gamma\int_0^\infty \Phi_\varepsilon(r)\,\mathfrak{c}'_\Omega(r)\,\mathrm{d}r. \tag{5.132}$$

Using the explicit formula for the Autocorrelation Function of the annulus, we compute

$$\int_0^\infty \Phi_\varepsilon(r)\,\mathfrak{c}'_{A_{\rho,R}}(r)\,\mathrm{d}r = \int_0^{2\rho}\Phi_\varepsilon(r)\,\mathfrak{c}'_{B_\rho}(r)\,\mathrm{d}r + \int_0^{2R}\Phi(r)\,\mathfrak{c}'_{B_R}(r)\,\mathrm{d}r \tag{5.133}$$

$$+ 2\int_{R-\rho}^{R+\rho}\Phi_\varepsilon(r)\,\frac{\mathrm{d}}{\mathrm{d}r}\big[L(\rho, \tfrac{R^2-\rho^2+r^2}{2r} - r) - L(R, \tfrac{R^2-\rho^2+r^2}{2r})\big]\,\mathrm{d}r, \tag{5.134}$$

where $L(R,d)$ is defined in (4.116). We compute

$$\frac{\mathrm{d}}{\mathrm{d}r}L(\rho, \tfrac{R^2-\rho^2+r^2}{2r} - r) = \frac{r^2+R^2-\rho^2}{2r^3} \tag{5.135}$$

$$\times\sqrt{(r-R-\rho)(\rho-r-R)(r-R+\rho)(r+R+\rho)}, \tag{5.136}$$

$$\frac{\mathrm{d}}{\mathrm{d}r}L(R, \tfrac{R^2-\rho^2+r^2}{2r}) = \frac{r^2-R^2+\rho^2}{2r^3} \tag{5.137}$$

$$\times\sqrt{(r-R-\rho)(\rho-r-R)(r-R+\rho)(r+R+\rho)}. \tag{5.138}$$

Thus

$$\frac{\mathrm{d}}{\mathrm{d}r}\big[L(\rho,\tfrac{R^2-\rho^2+r^2}{2r}-r)-L(R,\tfrac{R^2-\rho^2+r^2}{2r})\big] \tag{5.139}$$

$$=\frac{R^2-\rho^2}{r^3}\sqrt{(r-R-\rho)(\rho-r-R)(r-R+\rho)(r+R+\rho)}. \tag{5.140}$$

Altogether we obtain for the non-local term

$$\int_0^\infty \Phi_\varepsilon(r)\,\mathfrak{c}'_{A_{\rho,R}}(r)\,\mathrm{d}r=\int_0^{2\rho}\Phi_\varepsilon(r)\,\mathfrak{c}'_{B_\rho}(r)\,\mathrm{d}r+\int_0^{2R}\Phi_\varepsilon(r)\,\mathfrak{c}'_{B_R}(r)\,\mathrm{d}r$$
$$+2(R^2-\rho^2)\int_{R-\rho}^{R+\rho}\Phi_\varepsilon(r)\frac{\sqrt{(r-R-\rho)(\rho-r-R)(r-R+\rho)(r+R+\rho)}}{r^3}\,\mathrm{d}r.$$

Hence the energy of an annulus can be computed by

$$E_{\gamma,\varepsilon}(A_{\rho,R})=E_{\gamma,\varepsilon}(B_\rho)+E_{\gamma,\varepsilon}(B_R)$$
$$+4\gamma(R^2-\rho^2)\int_{R-\rho}^{R+\rho}\Phi_\varepsilon(r)\frac{\sqrt{(r-R-\rho)(\rho-r-R)(r-R+\rho)(r+R+\rho)}}{r^3}\,\mathrm{d}r.$$

6. Conclusion

In this thesis, we analysed the Autocorrelation Function (see Chapter 4) and the non-local isoperimetric energy (see Chapter 5)

$$E_{\gamma,\varepsilon}(\Omega) = \mathrm{Per}(\Omega) - \frac{\gamma}{\varepsilon}\int_{\mathbb{R}^n} \mathcal{K}_\varepsilon(z) \int_{\mathbb{T}^n} |\chi_\Omega(x+z) - \chi_\Omega(x)|\,\mathrm{d}x\,\mathrm{d}z.$$

We have seen that the geometry of a set $\Omega \subset \mathbb{T}^n$ is deeply connected to regularity properties of the corresponding Autocorrelation Function c_Ω. In particular, smoothness of the boundary implies smoothness of c_Ω near the origin (see Theorem 4.10), and we have established formulae for derivatives of the Autocorrelation Function at the origin (see Corollary 4.8, Corollary 4.12 and Corollary 4.15, see also Lemma 4.11, Corollary 4.18).

Using the Autocorrelation Function, we reformulated the energy functional $E_{\gamma,\varepsilon}$ as (see Theorem 5.6)

$$E_{\gamma,\varepsilon}(\Omega) = \big(1 - \frac{\gamma}{\gamma_{\mathrm{crit}}}\big)\,\mathrm{Per}(\Omega) + 2\gamma \int_0^\infty \Phi_\varepsilon(r)[c_\Omega'(r) - c_\Omega'(0)]\,\mathrm{d}r,$$

which provided crucial insight to establish an asymptotic expansion as $\varepsilon \to 0$. We found a parameter γ_{crit} which seperated sub- and supercritical regimes in which the energy showed different compactness properties. In particular, in the subcritical regime $\gamma < \gamma_{\mathrm{crit}}$, the energy functional is compact, in the supercritical regime $\gamma > \gamma_{\mathrm{crit}}$, the energy is not compact (see Section 5.2). In addition, we derived the Γ–limits in the subcritical regime (see Theorem 5.18), and for the rescaled energy in the critical regime (see Theorem 5.21).

We compared the diffuse energy model $\mathcal{F}_{q,\varepsilon}$ to the sharp interface analogue $E_{\gamma,\varepsilon}$ and explained in which way they can be seen as mechano-chemical models describing pattern formation processes in biological membranes (see Section 3.2). We found that the models share qualitative behaviour in that there exist sub- and supercritical parameter regimes with respect to the relative strength of the non-local interaction, i.e. the parameters q and γ. However, they are quantitavely different as the regimes do not match for both energy models (see Section 3.3).

A. Appendix

Lemma A.1 There exists a Dirac sequence $\psi_\varepsilon \in C^\infty(\mathbb{T}^n)$, i.e. the sequence has the following properties:

a) $\operatorname{supp}(\psi_\varepsilon) = \overline{B_\varepsilon(0)}$ for all $0 < \varepsilon < \frac{1}{2}$.

b) $\sup_\varepsilon \|\psi_\varepsilon\|_{L^1(\mathbb{T}^n)} \lesssim 1$.

c) $\displaystyle\int_{\mathbb{T}^n} \psi_\varepsilon(x)\,\mathrm{d}x = 1$ for all $0 < \varepsilon < \frac{1}{2}$.

d) For every $r > 0$ and $\delta > 0$ there exists $\varepsilon_0(r, \delta) > 0$, such that

$$\int_{\mathbb{T}^n \setminus B_r(0)} |\psi_\varepsilon(x)|\,\mathrm{d}x < \delta \qquad \text{for all } \varepsilon < \varepsilon_0. \tag{A.1}$$

Proof: Let $\psi \in C_c^\infty(\mathbb{R}^n)$ be the standard convolution kernel

$$\psi(x) \coloneqq \begin{cases} \exp(\frac{1}{1-|x|^2}) & \text{for all } x \in B_1(0), \\ 0 & \text{else.} \end{cases} \tag{A.2}$$

Define the dilated kernel $\psi_\varepsilon(x) \coloneqq \frac{1}{\varepsilon^n}\psi(\frac{x}{\varepsilon})$ for all $x \in \mathbb{R}^n$. Then $\operatorname{supp}(\psi_\varepsilon) = \overline{B_\varepsilon(0)}$ and thus for $\varepsilon < \frac{1}{2}$ we find $\operatorname{supp}(\psi_\varepsilon)$ is compactly embedded into $\mathcal{Q}^n$. Thus there exists a periodic extension of ψ_ε to $\mathbb{R}^n$ and therefore we find $\psi_\varepsilon \in C^\infty(\mathbb{T}^n)$ for all $0 < \varepsilon < \frac{1}{2}$. The claimed assertions follow as in the Euclidean case. ■

As usual for Dirac sequences, having $f \in L^p(\mathbb{T}^n)$ for $1 \le p < \infty$, it holds $f * \eta_k \to f$ in $L^p(\mathbb{T}^n)$ as $k \to \infty$ (see [Gra08, Section 1.2.4]).

Lemma A.2 Let $f, g \in L^1(\mathbb{T}^n)$. Then $\operatorname{supp}(f * g) \subset \operatorname{supp}(f) + \operatorname{supp}(g)$.

Proof. The proof is motivated by [Rud91, Theorem 6.35 and Theorem 6.37].

Let $x \in \mathbb{T}^n$ and define

$$K_x \coloneqq \operatorname{supp}(f) \cap (x - \operatorname{supp}(g)) = \{y \in \mathbb{T}^n : y \in \operatorname{supp}(f) \text{ and } x - y \in \operatorname{supp}(g)\}. \quad \text{(A.3)}$$

We find that

$$(f * g)(x) = \int_{\mathbb{T}^n} f(y)\, g(x-y)\, \mathrm{d}y = \int_{K_x} f(y)\, g(x-y)\, \mathrm{d}y \qquad \text{for all } x \in \mathbb{T}^n. \quad \text{(A.4)}$$

Assume $x \notin \operatorname{supp}(f) + \operatorname{supp}(g)$, that is there do not exist $z_f \in \operatorname{supp}(f)$ and $z_g \in \operatorname{supp}(g)$ such that $x - z_f = z_g$. Thus $K_x = \emptyset$ and $(f * g)(x) = 0$. Hence $\operatorname{supp}(f * g) \subset \operatorname{supp}(f) + \operatorname{supp}(g)$ as claimed. ■

Theorem A.3 The inclusion mapping $i : W^{1,1}(\mathbb{T}^n) \longrightarrow L^1(\mathbb{T}^n)$ is a compact operator.

Proof: Follows from [Heb99, Theorem 2.9] since $\mathbb{T}^n$ is a closed Riemannian manifold. ■

Lemma A.4 Let $f \in C^\infty(\mathbb{T}^n)$. Then there exists $C > 0$ such that for all $k \in \mathbb{N}$ there exists an affine linear function $f_k \in C^0(\mathbb{T}^n)$ such that

$$\|f - f_k\|_{W^{1,1}(\mathbb{T}^n)} \leq \frac{C}{k} \|f\|_{W^{1,1}(\mathbb{T}^n)}. \quad \text{(A.5)}$$

Proof: As $f \in C^\infty(\mathbb{T}^n)$ there exists a representative $F \in C^\infty(\mathbb{R}^n)$ which is $\mathcal{Q}^n$ periodic, i.e.

$$F(x+z) = F(x) \qquad \text{for all } x \in \mathbb{R}^n,\ z \in \mathbb{Z}^n. \quad \text{(A.6)}$$

We now use a finite element approximation of F: let $\sigma_0 \subset \mathbb{R}^n$ be the unit simplex (with affine independent vertices $\{0, \mathbf{e}_1, \ldots, \mathbf{e}_n\}$). Then through periodic refinement we obtain a family of subdivision $\mathcal{T}^k$ such that for $\sigma_k \in \mathcal{T}^k$ we have $\operatorname{diam}(\sigma_k) \leq \frac{\operatorname{diam}(\sigma_0)}{k}$. We can now apply [BS94, Theorem 4.4.20] to obtain an affine linear function $F_k \in C^0(\mathcal{Q}^n)$ such that

$$\|F - F_k\|_{W^{1,1}(\mathcal{Q}^n)} \lesssim \frac{1}{k} \|F\|_{W^{1,1}(\mathcal{Q}^n)}, \quad \text{(A.7)}$$

where the constant depends on n and $\operatorname{diam}(\sigma_0)$. By the choice of the subdivisions, the function F_k can be extended periodically to $\mathbb{R}^n$, and thus can be identified with an affine linear function $f_k \in C^0(\mathbb{T}^n)$. Using (A.7) we find

$$\|f - f_k\|_{W^{1,1}(\mathbb{T}^n)} = \|F - F_k\|_{W^{1,1}(\mathcal{Q}^n)} \lesssim \frac{1}{k} \|F\|_{W^{1,1}(\mathcal{Q}^n)} = \frac{1}{k} \|f\|_{W^{1,1}(\mathbb{T}^n)}, \quad \text{(A.8)}$$

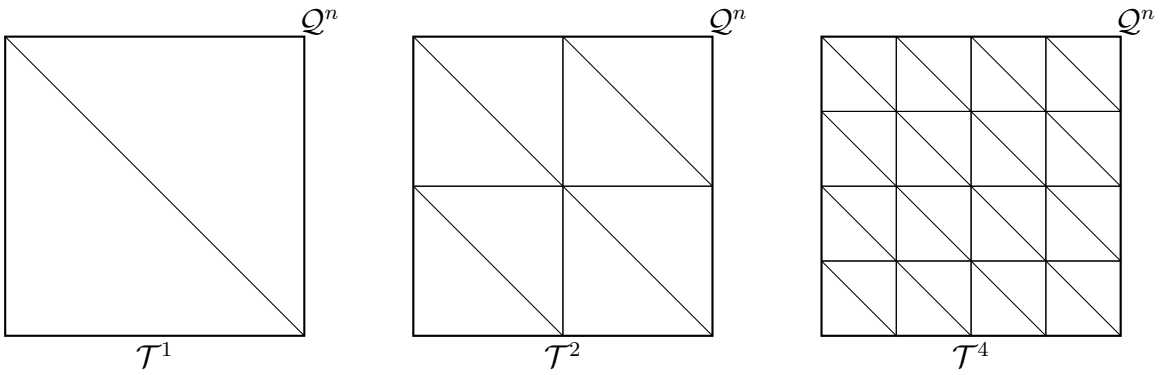

Figure A.1.: Subdivisions $\mathcal{T}^k$ for $\mathcal{Q}^n$.

which proves the claim. ■

Lemma A.5 Let $A_1, A_2, A_3 \subset \mathbb{T}^n$ be measurable. Then

$$|A_1 \cap A_2| - |A_1 \cap A_3| \leq |A_2 \setminus A_3| \leq |A_2| - |A_2 \cap A_3|. \tag{A.9}$$

Proof: The proof is motivated by [Gal11, Proposition 5].

Since $A_1 \cap A_2 \cap A_3 \subset A_1 \cap A_3$ and $A_1 \cap A_2 \cap A_3 \subset A_1 \cap A_2$ we obtain

$$|A_1 \cap A_2| - |A_1 \cap A_3| \leq |A_1 \cap A_2| - |A_1 \cap A_2 \cap A_3| = |(A_1 \cap A_2) \setminus (A_1 \cap A_2 \cap A_3)|. \tag{A.10}$$

The claim follows from the inclusion $(A_1 \cap A_2) \setminus (A_1 \cap A_2 \cap A_3) \subset A_2 \setminus A_3$. ■

Lemma A.6 Let $\vartheta_l, \vartheta_r \in (0, 2\pi)$. Let $\varpi(\,\cdot\,, \vartheta_l, \vartheta_r)\colon (0, 2\pi) \longrightarrow \mathbb{R}$ be as in (4.156). Then

$$\frac{1}{2\pi} \int_0^{2\pi} |\sin(\alpha)|\, \varpi(\alpha, \vartheta_l, \vartheta_r)\, \mathrm{d}\alpha \tag{A.11}$$

$$= \frac{1}{2\pi}(1 + (\pi - \vartheta_r)\cot(\vartheta_r)) + \frac{1}{2\pi}(1 + (\pi - \vartheta_r)\cot(\vartheta_l)). \tag{A.12}$$

Proof: The deficit function is dependent on the relation between ϑ_r and ϑ_l (see Figure A.2). Due to the geometry, the deficit itself separates into (see Figure 4.10 a))

$$\varpi(\alpha, \vartheta_l, \vartheta_r) = \varpi_l(\alpha, \vartheta_l) + \varpi_r(\alpha, \vartheta_r). \tag{A.13}$$

Due to reflectional symmetry and the fact $c''_\Omega = c''_{\Omega^c}$, the cases to consider reduces to the following six cases. Moreover, we only need to consider $\pi < \alpha < 2\pi$. We adapt the

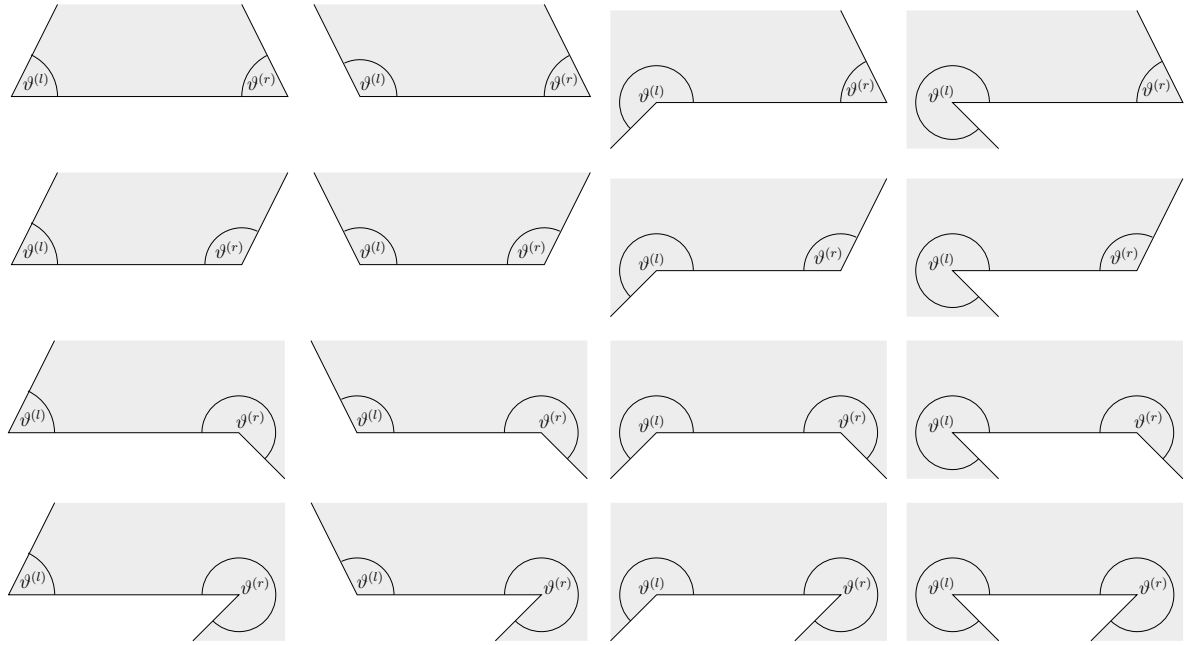

Figure A.2.: Different cases depending on acute or obtuse angles.

notation as in the proof of Lemma 4.18 and write $w = (w_1, w_2) = (\cos(\alpha), \sin(\alpha)) \in \mathbb{S}^1$.

- $0 < \vartheta_l \leq \frac{\pi}{2}$ and $0 < \vartheta_r \leq \frac{\pi}{2}$: We compute for the left deficit

$$\varpi_l(\alpha, \vartheta_l) = \begin{cases} 0 & \text{for all } \pi < \alpha < \pi + \vartheta_l, \\ w_1 + \frac{|w_2|}{\tan(\vartheta_l)} & \text{for all } \pi + \vartheta_l < \alpha < 2\pi. \end{cases} \tag{A.14}$$

  We compute for the right deficit

$$\varpi_r(\alpha, \vartheta_r) = \begin{cases} -w_1 + \frac{|w_2|}{\tan(\vartheta_r)} & \text{for all } \pi < \alpha < 2\pi - \vartheta_r, \\ 0 & \text{for all } 2\pi - \vartheta_r < \alpha < 2\pi. \end{cases} \tag{A.15}$$

- $0 < \vartheta_i^{(l)} \leq \frac{\pi}{2}$ and $\frac{\pi}{2} < \vartheta_i^{(r)} \leq \pi$: We compute for the left deficit

$$\varpi_l(\alpha, \vartheta_l) = \begin{cases} 0 & \text{for all } \pi < \alpha < \pi + \vartheta_l, \\ w_1 + \frac{|w_2|}{\tan(\vartheta_l)} & \text{for all } \pi + \vartheta_l < \alpha < 2\pi. \end{cases} \tag{A.16}$$

  Using $-\tan(\pi - x) = \tan(x)$ we compute for the right deficit

$$\varpi_r(\alpha, \vartheta_r) = \begin{cases} -w_1 + \frac{|w_2|}{\tan(\vartheta_r)} & \text{for all } \pi < \alpha < 2\pi - \vartheta_r, \\ 0 & \text{for all } 2\pi - \vartheta_r < \alpha < 2\pi. \end{cases} \tag{A.17}$$

- $0 < \vartheta_i^{(l)} \leq \frac{\pi}{2}$ and $\pi < \vartheta_i^{(r)} \leq \frac{3\pi}{2}$: We compute for the left deficit

$$\varpi_l(\alpha, \vartheta_l) = \begin{cases} 0 & \text{for all } \pi < \alpha < \pi + \vartheta_l, \\ w_1 + \frac{|w_2|}{\tan(\vartheta_l)} & \text{for all } \pi + \vartheta_l < \alpha < 2\pi. \end{cases} \tag{A.18}$$

Using $-\tan(\pi - x) = \tan(x)$ we compute for the right deficit

$$\varpi_r(\alpha, \vartheta_r) = \begin{cases} 0 & \text{for all } \pi < \alpha < \pi + \vartheta_r, \\ w_1 - \frac{|w_2|}{\tan(\vartheta_r)} & \text{for all } \pi + \vartheta_r < \alpha < 2\pi. \end{cases} \tag{A.19}$$

- $0 < \vartheta_i^{(l)} \leq \frac{\pi}{2}$ and $\frac{3\pi}{2} < \vartheta_i^{(r)} \leq 2\pi$: We compute for the left deficit

$$\varpi_l(\alpha, \vartheta_l) = \begin{cases} 0 & \text{for all } \pi < \alpha < \pi + \vartheta_l, \\ w_1 + \frac{|w_2|}{\tan(\vartheta_l)} & \text{for all } \pi + \vartheta_l < \alpha < 2\pi. \end{cases} \tag{A.20}$$

Using $-\tan(2\pi - x) = \tan(x)$ we compute for the right deficit

$$\varpi_r(\alpha, \vartheta_r) = \begin{cases} 0 & \text{for all } \pi < \alpha < 3\pi - \vartheta_r, \\ w_1 - \frac{|w_2|}{\tan(\vartheta_r)} & \text{for all } 3\pi - \vartheta_r < \alpha < 2\pi. \end{cases} \tag{A.21}$$

- $\frac{\pi}{2} < \vartheta_i^{(l)} \leq \pi$ and $\frac{\pi}{2} < \vartheta_i^{(r)} \leq \pi$: We compute for the left deficit

$$\varpi_l(\alpha, \vartheta_l) = \begin{cases} 0 & \text{for all } \pi < \alpha < \pi + \vartheta_l, \\ w_1 + \frac{|w_2|}{\tan(\vartheta_l)} & \text{for all } \pi + \vartheta_l < \alpha < 2\pi. \end{cases} \tag{A.22}$$

Using $-\tan(\pi - x) = \tan(x)$ we compute for the right deficit

$$\varpi_r(\alpha, \vartheta_r) = \begin{cases} -w_1 + \frac{|w_2|}{\tan(\vartheta_r)} & \text{for all } \pi < \alpha < 2\pi - \vartheta_r, \\ 0 & \text{for all } 2\pi - \vartheta_r < \alpha < 2\pi. \end{cases} \tag{A.23}$$

- $\frac{\pi}{2} < \vartheta_i^{(l)} \leq \pi$ and $\pi < \vartheta_i^{(r)} \leq \frac{3\pi}{2}$: We compute for the left deficit

$$\varpi_l(\alpha, \vartheta_l) = \begin{cases} 0 & \text{for all } \pi < \alpha < \pi + \vartheta_l, \\ w_1 + \frac{|w_2|}{\tan(\vartheta_l)} & \text{for all } \pi + \vartheta_l < \alpha < 2\pi. \end{cases} \tag{A.24}$$

Using $-\tan(\pi - x) = \tan(x)$ we compute for the right deficit

$$\varpi_r(\alpha, \vartheta_r) = \begin{cases} 0 & \text{for all } \pi < \alpha < \pi + \vartheta_r, \\ w_1 - \frac{|w_2|}{\tan(\vartheta_r)} & \text{for all } \pi + \vartheta_r < \alpha < 2\pi. \end{cases} \tag{A.25}$$

In any case, integrating over all $0 < \alpha < 2\pi$ results in

$$\frac{1}{2\pi}\int_0^{2\pi} |w_2|\varpi(\alpha, \vartheta_r, \vartheta_l)\,\mathrm{d}\alpha = -\frac{1}{\pi}\int_\pi^{2\pi} \sin(\alpha)\,(\varpi_r(\alpha, \vartheta_r) + \varpi_l(\alpha, \varpi_l))\,\mathrm{d}\alpha \tag{A.26}$$

$$= \frac{1}{2\pi}(1 + (\pi - \vartheta_r)\cot(\vartheta_r)) \tag{A.27}$$

$$+ \frac{1}{2\pi}(1 + (\pi - \vartheta_r)\cot(\vartheta_l)), \tag{A.28}$$

from which we obtain the claim. ■

A.1. Geometric Relations

Lemma A.7 Let $E \in BV_n$. Then

$$\lim_{r\to 0} \frac{|E \cap B_r(x)|}{|B_r(x)|} = \frac{1}{2} \qquad \text{for } \mathscr{H}^{n-1} \text{ almost every } x \in \partial E. \tag{A.29}$$

Proof: Follows from [Mag12, Remark 15.3 and Corollary 15.8]. ■

Theorem A.8 Let $f\colon \mathbb{T}^n \longrightarrow \mathbb{R}$ be smooth. Then

$$|\{x \in \mathbb{T}^n : \mathrm{D}_x f = 0\}| = 0. \tag{A.30}$$

Proof: See e.g. [BJ82, Chapter 6] and [GP74, Chapter 1.7]. ■

As a reminder, given two smooth manifolds M, N and a smooth map $f\colon M \longrightarrow N$, we define the Jacobian via

$$\mathrm{Jac}_f(x) \coloneqq \det(\mathrm{D}_x f\, \mathrm{D}_x f^*)^{\frac{1}{2}} \qquad \text{for all } x \in M. \tag{A.31}$$

Theorem A.9 Let $k \in \mathbb{N}_0$ and $n \in \mathbb{N}$. Let M be a compact Riemannian manifold of dimension $n + k$ and N be a compact Riemannian manifold of dimension k. Let $F \in C^\infty(M, N)$. Then for all $\varphi \in L^1(M)$

$$\int_M \varphi\ \mathrm{Jac}_F\ \mathrm{d}\mathscr{H}^{n+k} = \int_N \Big(\int_{F^{-1}(\{y\})} \varphi(x)\,\mathrm{d}\mathscr{H}^k(x) \Big)\,\mathrm{d}\mathscr{H}^n(y). \tag{A.32}$$

Proof: See [BZ88, Theorem 13.4.2 and Corollary 13.4.6]. ■

A.2. Integral Identities

Lemma A.10 Let $v \in \mathbb{S}^{n-1}$. Then

$$\int_{\mathbb{S}^{n-1}} |v \cdot w| \, \mathrm{d}\mathscr{H}^{n-1}(w) = 2\omega_{d-1}, \tag{A.33}$$

where $\omega_d \coloneqq |\{x \in \mathbb{R}^d : |x| < 1\}|$.

Proof: Using the invariance under rotations of the Hausdorff measure, we have

$$\int_{\mathbb{S}^{n-1}} |v \cdot w| \, \mathrm{d}\mathscr{H}^{n-1}(w) = \int_{\mathbb{S}^{n-1}} |\mathbf{e}_n \cdot w| \, \mathrm{d}\mathscr{H}^{n-1}(w). \tag{A.34}$$

Let $B^{n-1} \coloneqq \{x \in \mathbb{R}^{n-1} : |x| < 1\}$. Then we can parametrise the sphere via $\varphi_\pm \colon B^{n-1} \longrightarrow \mathbb{S}^{n-1}$, $x \longmapsto (x, \pm\sqrt{1-|x|^2})$. Using the formula for parametrised areas, we obtain

$$\int_{\mathbb{S}^{n-1}} |w_n| \, \mathrm{d}\mathscr{H}^{n-1}(w) = 2 \int_{B^{n-1}} \sqrt{1-|x|^2} \sqrt{1 + \frac{|x|^2}{1-|x|^2}} \, \mathrm{d}x = 2\omega_{n-1}, \tag{A.35}$$

as claimed. ■

Lemma A.11 Let $r > 0$, $k \in \mathbb{N}$ and $0 < \theta < 1$. Then

$$\int_{\operatorname{acos}(\frac{k+\theta}{r})}^{\operatorname{acos}(\frac{k}{r})} \sin^{n-2}(\alpha) \, \mathrm{d}\alpha = \frac{1}{r^{n-2}} \int_k^{k+\theta} (r^2 - z^2)^{\frac{n-3}{2}} \, \mathrm{d}z. \tag{A.36}$$

Proof: We substitute $z = \cos(\alpha)$ to obtain

$$\begin{aligned}
\int_{\operatorname{acos}(\frac{k+\theta}{r})}^{\operatorname{acos}(\frac{k}{r})} \sin^{n-2}(\alpha) \, \mathrm{d}\alpha &= \int_{\operatorname{acos}(\frac{k+\theta}{r})}^{\operatorname{acos}(\frac{k}{r})} (1 - \cos^2(\alpha))^{\frac{n-2}{2}} \, \mathrm{d}\alpha && \text{(A.37)} \\
&= \int_{\frac{k+\theta}{r}}^{\frac{k}{r}} (1-z^2)^{\frac{n-2}{2}} \frac{-1}{\sqrt{1-z^2}} \, \mathrm{d}z && \text{(A.38)} \\
&= \int_{\frac{k}{r}}^{\frac{k+\theta}{r}} (1-z^2)^{\frac{n-3}{2}} \, \mathrm{d}z && \text{(A.39)} \\
&= \frac{1}{r^{n-2}} \int_k^{k+\theta} (r^2 - z^2)^{\frac{n-3}{2}} \, \mathrm{d}z, && \text{(A.40)}
\end{aligned}$$

as claimed. ■

Lemma A.12 Let $r > 0$, $k \in \mathbb{N}$ and $0 < \theta < 1$. Then

$$\int_{\operatorname{acos}(\frac{k+\theta}{r})}^{\operatorname{acos}(\frac{k}{r})} \sin^{n-2}(\alpha)\cos(\alpha)\,\mathrm{d}\alpha = \frac{1}{r^{n-1}}\int_{k}^{k+\theta} t(r^2-t^2)^{\frac{n-3}{2}}\,\mathrm{d}t \tag{A.41}$$

$$= \frac{r^{-(n-1)}}{n-1}\Big[(r^2-k^2)^{\frac{n-1}{2}} - (r^2-(k+\theta)^2)^{\frac{n-1}{2}}\Big] \tag{A.42}$$

Proof: We substitute $z = \cos(\alpha)$ to obtain

$$\int_{\operatorname{acos}(\frac{k+\theta}{r})}^{\operatorname{acos}(\frac{k}{r})} \sin^{n-2}(\alpha)\cos(\alpha)\,\mathrm{d}\alpha = \int_{\operatorname{acos}(\frac{k+\theta}{r})}^{\operatorname{acos}(\frac{k}{r})} (1-\cos^2(\alpha))^{\frac{n-2}{2}}\cos(\alpha)\,\mathrm{d}\alpha \tag{A.43}$$

$$= \int_{\frac{k+\theta}{r}}^{\frac{k}{r}} (1-z^2)^{\frac{n-2}{2}} z\frac{-1}{\sqrt{1-z^2}}\,\mathrm{d}z \tag{A.44}$$

$$= \int_{\frac{k}{r}}^{\frac{k+\theta}{r}} (1-z^2)^{\frac{n-3}{2}} z\,\mathrm{d}z \tag{A.45}$$

$$= \frac{1}{r^{n-1}}\int_{k}^{k+\theta} z(r^2-z^2)^{\frac{n-3}{2}}\,\mathrm{d}z. \tag{A.46}$$

Now substituting $u = 1 - z^2$ yields

$$\frac{1}{r^{n-1}}\int_{k}^{k+\theta} z(r^2-z^2)^{\frac{n-3}{2}}\,\mathrm{d}z = -\frac{1}{2r^{n-1}}\int_{r^2-(k+\theta)^2}^{r^2-k^2} u^{\frac{n-3}{2}}\,\mathrm{d}u \tag{A.47}$$

$$= \frac{r^{-(n-1)}}{n-1}\Big[(r^2-k^2)^{\frac{n-1}{2}} - (r^2-(k+\theta)^2)^{\frac{n-1}{2}}\Big], \tag{A.48}$$

as claimed. ■

A.3. Interaction Kernels

In the following section we present some examples of admissible kernels. As described in Chapter 3, the kernel satisfying $\mathcal{K} - \Delta\mathcal{K} = \delta_0$ is relevant for mechano-chemical models.

Lemma A.13 Let $\mathcal{K} \in L^1(\mathbb{R}^n)$ be the unique solution to $\mathcal{K} - \Delta\mathcal{K} = \delta_0$. Then

$$\int_{\mathbb{R}^n} |z|\,\mathcal{K}(z)\,\mathrm{d}z = \sqrt{\pi}\,\Gamma(\tfrac{n+1}{2})\,\Gamma(\tfrac{n}{2})^{-1} \tag{A.49}$$

and the associated critical value $\gamma_{\text{crit}} = 1$.

Proof: We first note that the equation can be solved explicitly with Fourier methods. More precisely

$$\mathcal{F}\mathcal{K}(\xi) \coloneqq \int_{\mathbb{R}^n} \mathcal{K}(z)\, e^{-2\pi \mathbf{i} z\cdot\xi}\, dz = \frac{1}{1+(2\pi)^2|\xi|^2} \qquad \text{for all } \xi \in \mathbb{R}^n. \tag{A.50}$$

Since the Fourier transform is an injective map $\mathcal{F} : L^1(\mathbb{R}^n) \longrightarrow C_b^0(\mathbb{R}^n)$, the solution $\mathcal{K}$ is unique. Since $\hat{\mathcal{K}}$ is radial, so is $\mathcal{K}$ and thus (H1). Employing polar coordinates, $\mathcal{K}$ solves

$$\mathcal{K}(r) - \frac{n-1}{r}\mathcal{K}'(r) - \mathcal{K}''(r) = 0 \qquad \text{for all } r > 0. \tag{A.51}$$

Substituting $\mathcal{K}(r) \coloneqq r^{1-\frac{n}{2}} g(r)$, we obtain

$$r^2 g''(r) + r g'(r) - (r^2 + (\tfrac{n}{2}-1)^2) g(r) = 0 \qquad \text{for all } r > 0. \tag{A.52}$$

This is the modified Bessel equation. The unique decaying solution is given by $g = K_{\frac{n}{2}-1}$, where K_ν denotes the decaying modified Bessel function of the second kind of genus $\nu \geq 0$, i.e.

$$K_\nu(r) = \int_0^\infty \cosh(\nu t)\, e^{-r\,\cosh(t)} dt \qquad \text{for all } r > 0. \tag{A.53}$$

Altogether, we obtain

$$\mathcal{K}(z) = a|z|^{1-\frac{n}{2}} K_{\frac{n}{2}-1}(|z|) \qquad \text{for all } z \in \mathbb{R}^n, \tag{A.54}$$

where $a = (2\pi)^{-\frac{n}{2}}$ such that $\|\mathcal{K}\|_{L^1(\mathbb{R}^n)} = 1$. Since $K_\nu \geq 0$ for all $\nu \geq 0$, it follows (H3). The identity (A.49) and (H2) follow from [GR15, p.676]. ■

Fractional versions of the Helmholtz equations also produce admissible kernels.

Lemma A.14 Let $s \in (1,2)$ and let $\mathcal{K}^{(s)} \in L^1(\mathbb{R}^n)$ be the unique solution to

$$\mathcal{K}^{(s)} + (-\Delta)^{\frac{s}{2}} \mathcal{K}^{(s)} = \delta_0 \qquad \text{in } \mathbb{R}^n. \tag{A.55}$$

Then $\mathcal{K}^{(s)}$ satisfies (H1) – (H3).

Proof: We first note that the equation can be solved explicitly with Fourier methods.

More precisely

$$\mathcal{F}\mathcal{K}^{(s)}(\xi) \coloneqq \int_{\mathbb{R}^n} \mathcal{K}^{(s)}(z)\, e^{-2\pi \mathbf{i} z\cdot\xi}\, dz = \frac{1}{1+(2\pi)^s|\xi|^s} \qquad \text{for all } \xi \in \mathbb{R}^n. \tag{A.56}$$

Since the Fourier transform is an injective map $\mathcal{F} : L^1(\mathbb{R}^n) \longrightarrow C_b^0(\mathbb{R}^n)$, the solution of (A.55) is unique. Since $\hat{\mathcal{K}}^{(s)}$ is radial, so is $\mathcal{K}^{(s)}$ and thus (H1). Using [MW21, Lemma 1.2] we obtain that $\mathcal{K}^{(s)} \geq 0$ and $|\mathcal{K}^{(s)}(r)| \lesssim r^{-n-s}$ for $r \geq 1$ which directly yield both (H2) and (H3). ■

The following family of kernels (so called Bessel kernels) are taken from [Peg21].

Lemma A.15 Let $\alpha, \kappa > 0$ and $\mathfrak{B}_{\alpha,\kappa} \in L^1(\mathbb{R}^n)$ be the unique solution to

$$(\mathrm{id} - \kappa\Delta)^{\frac{\alpha}{2}} \mathfrak{B}_{\alpha,\kappa} = \delta_0 \qquad \text{in } \mathbb{R}^n. \tag{A.57}$$

Then $\mathfrak{B}_{\alpha,\kappa}$ satisfies (H1) – (H3) and the associated critical value is given by

$$\gamma_{\mathrm{crit}} = \frac{1}{2}\sqrt{\frac{\pi}{\kappa}} \frac{\Gamma(\frac{\alpha}{2})}{\Gamma(\frac{1+\alpha}{2})} \frac{\Gamma(1+\frac{n}{2})^2}{\Gamma(\frac{1+n}{2})^2}. \tag{A.58}$$

Proof: See [Peg21, Proposition 3.10]. ■

A.4. Graph Representation for Autocorrelation Function

Let $R > 0$ and $f \in C^\infty([-2R, 2R])$, such that $(f')^{-1}(\{0\}) = \{\bar{x}\}$. Without loss of generality, we can assume $f''(\bar{x}) \neq 0$, since otherwise we may look at the function $f_\varepsilon(x) \coloneqq f(x) + \frac{\varepsilon}{2}(x-\bar{x})^2$ and then take the limit $\varepsilon \to 0$. We assume there exists $x \in C^\infty((0, R])$ such that $f(x(r)+r) = f(x(r))$ for all $r \in (0, R]$.

Lemma A.16 Let f, x and $\bar{x}$ be as described above. Then $f'(x(r)) \xrightarrow{r\to 0} 0$ and $x(r) \xrightarrow{r\to 0} \bar{x}$.

Proof: We use a Taylor expansion of f to deduce

$$0 = f(x(r)+r) - f(x(r)) = r f'(x(r)) + \mathcal{O}(r^2), \tag{A.59}$$

from which we obtain $f'(x(r)) \xrightarrow{r\to 0} 0$ since f and x are smooth. Since by assumption $(f')^{-1}(\{0\}) = \{\bar{x}\}$, the claim follows. ■

The following limit will be useful in the computations to come.

Lemma A.17 Let f, x and $\bar{x}$ be as described above. Then

$$\frac{f'(x(r))}{r} \xrightarrow{r\searrow 0} -\frac{1}{2}f''(\bar{x}). \tag{A.60}$$

Proof: We define

$$Y \coloneqq \lim_{r\searrow 0} \frac{f'(x(r))}{r}. \tag{A.61}$$

We intend to use l'Hospital's Lemma to compute Y. We note that by the Implicit Function Theorem

$$x'(r) = -\frac{f'(x(r)+r)}{f'(x(r)+r) - f'(x(r))} \qquad \text{for all } 0 < r < R. \tag{A.62}$$

We compute using a Taylor Expansion

$$\frac{(f'(x(r)))'}{r'} = \frac{f''(x(r))x'(r)}{1} = -f''(x(r))\frac{f'(x(r)+r)}{f'(x(r)+r) - f'(x(r))} \tag{A.63}$$

$$= -f''(x(r))\,\frac{f'(x(r)) + rf''(x(r)) + \mathcal{O}(r^2)}{rf''(x(r)) + \mathcal{O}(r^2)} \tag{A.64}$$

$$= -f''(x(r))\Big[\frac{f'(x(r))}{r}\frac{1}{f''(x(r)) + \mathcal{O}(r)} + 1\Big]. \tag{A.65}$$

Using Lemma A.16 we find $Y = -Y - f''(\bar{x})$, which means $Y = -\frac{1}{2}f''(\bar{x})$. ■

For notational convenience, we will define the function $F\colon (0, R] \longrightarrow \mathbb{R}$ via

$$F(r) \coloneqq 2\int_{x(r)}^{x(r)+r} f(y)\,\mathrm{d}y \qquad \text{for all } r \in (0, R). \tag{A.66}$$

We note that integrals of this form appear in the analysis of c_Ω and its derivatives as in (4.75) and subsequent proofs.

Lemma A.18 Let F as in (A.66). Then

$$F''(r) \xrightarrow{r\searrow 0} 0. \tag{A.67}$$

Proof: We write $f' = f'(x(r))$ etc. We note that $x(r) \to \bar{x}$ as $r \to 0$ by Lemma A.16. We

use a Taylor expansion of f to deduce

$$F''(r) = \frac{2r^2[(f')^3 f''' - (f')^2(f'')^2] + r^3[(f')^2 f'' f''' + (f')^3 f'''' - 2f'(f'')^3]}{r^3(f'')^3 + \mathcal{O}(r^4)} + \mathcal{O}(r) \quad \text{(A.68)}$$

$$= 2\frac{(f')^2}{r}\frac{f'f''' - (f'')^2}{(f'')^3 + \mathcal{O}(r^4)} + f'\frac{f'f''f''' + (f')^2 f'''' - 2(f'')^3}{f'' + \mathcal{O}(r^4)} + \mathcal{O}(r) \quad \text{(A.69)}$$

Applying Lemma A.16 and Lemma A.17 proves the claim. ■

Lemma A.19 Let F as in (A.66). Then

$$F'''(r) \xrightarrow{r\searrow 0} -\frac{1}{2}f''(\bar{x}). \quad \text{(A.70)}$$

Proof: We write $f' = f'(x(r))$ etc. We note that $x(r) \to \bar{x}$ as $r \to 0$ by Lemma A.16. We use a Taylor expansion of f to deduce

$$F'''(r) = \frac{6r^3(f')^2(f'')^4 + 6r^4 f'(f'')^5 + r^5(f'')^6 + f'\mathcal{O}(r^5)}{r^5(f'')^5 + \mathcal{O}(r^6)} + \mathcal{O}(r) \quad \text{(A.71)}$$

$$= 6\frac{(f')^2}{r^2}\frac{(f'')^4}{(f'')^5 + \mathcal{O}(r)} + 6\frac{f'}{r}\frac{(f'')^5}{(f'')^5 + \mathcal{O}(r)} + \frac{f''}{1 + \mathcal{O}(r)} + f'\frac{\mathcal{O}(1)}{1 + \mathcal{O}(r)}\mathcal{O}(r). \quad \text{(A.72)}$$

Applying Lemma A.16 and Lemma A.17 we obtain

$$F'''(r) \xrightarrow{r\searrow 0} 6\big(-\tfrac{1}{2}f''(\bar{x})\big)^2\frac{1}{f''(\bar{x})} + 6\big(-\tfrac{1}{2}f''(\bar{x})\big) + f''(\bar{x}) = -\frac{1}{2}f''(\bar{x}) \quad \text{(A.73)}$$

as claimed. ■

List of Symbols

$\mathbb{N}$	Set of positive integers starting from 1
$\mathbb{Z}^n$	Set of n-dimensional vectors with integer entries
$\mathbb{R}^n$	Euclidean space
$\mathbf{e}_i$	Standard unit vector in $\mathbb{R}^n$
$\mathbb{R}_+$	Positive real numbers
$\mathbb{T}^n$	Unit Flat Torus
$\mathcal{Q}^n$	Primitive cell of $\mathbb{T}^n$
$\mathsf{T}_x X$	Tangent space of X at x
$\mathsf{T}X$	Tangent bundle of X
$\mathsf{N}_x X$	Normal space of X at x
$\mathsf{N}X$	Normal bundle of X
$B_r(x)$	Ball or radius r with centre x
$\mathbb{S}^{n-1}$	Unit sphere in $\mathbb{R}^n$
$x \cdot y$	Standard scalar product in $\mathbb{R}^n$, Riemannian metric in $\mathbb{T}^n$
$\lvert x - y \rvert$	Distance between x and y
$\mathscr{B}(X)$	Borel σ–Algebra of X
$\lvert \Omega \rvert$	Measure of a set
$\mathscr{H}^{n-1}$	$n-1$ dimensional Hausdorff measure
$A + z$	$\{a + z : a \in A\}$
$A \triangle B$	Symmetric difference of two sets
ω_n	Measure of unit ball in $\mathbb{R}^n$
σ_n	Hausdorff measure of unit sphere in $\mathbb{R}^n$
χ_Ω	Indicator function of a set Ω
$L^p(X)$	Lebesgue space
$W^{1,p}(X)$	Sobolev space
$\lVert f \rVert_{L^p(X)}$	L^p norm of f
$\lVert f \rVert_{W^{1,p}(X)}$	Sobolev norm of f
$C^0(X)$	Space of continuous functions
$C^\infty(X)$	Space of smooth functions
$C^\infty(X, \mathbb{R}^n)$	Space of smooth vector fields
$C_c^\infty(\mathbb{R}^n)$	Space of smooth functions with compact support
$BV(X)$	Space of functions with bounded variation
BV_n	Sets of finite perimeter in $\mathbb{T}^n$
BV_n^∞	Smooth sets of finite perimeter in $\mathbb{R}^n$ (see Definition 2.17)
$\mathcal{A}$	Class of admissible functions for non-local isoperimetric problem
$\nabla_w f$	Directional derivative along w
∇f	Gradient of f

$\nabla \cdot F$	Divergence of a vector field F
$\mathrm{D}_x f$	Differential of a map between two manifolds
Jac_f	Jacobian of f
$V_w[f]$	Directional variation of f along w
$V[f]$	Variation of f
$\mathrm{Per}(\Omega)$	Variation of χ_Ω
$f * g$	Convolution of f and g
$\mathcal{O}$	Landau symbol
A^*	Adjoint of A
$v^\perp$	Counter clockwise rotated vector, $(v_1, v_2)^\perp = (v_2, -v_1)$
ν	Gauß map
$x^\perp$	Counter clockwise rotation of x
$\exp_x$	Exponential map at x
$\mathscr{C}_\Omega$	Covariogram of a set Ω in $\mathbb{R}^n$
$\mathfrak{c}_\Omega$	Autocorrelation Function of a set Ω in $\mathbb{R}^n$
C_Ω	Covariogram of a set Ω in $\mathbb{T}^n$
c_Ω	Autocorrelation Function of a set Ω in $\mathbb{T}^n$
$E_{\gamma,\varepsilon}$	Non-local isoperimetric energy
$\mathcal{K}$	Integration kernel in non-local isoperimetric energy
Φ, Ψ	Integrated kernels (see (5.15) and (5.75) respectively)
γ_{crit}	Critical parameter of non-local isoperimetric energy (see (5.4))
$\mathfrak{m}_k[\mathcal{K}]$	k-th moment of $\mathcal{K}$
$A \lesssim B$	It exists $C > 0$ such that $A \leq CB$
$F_\varepsilon \xrightarrow{\Gamma} F$	F_ε converges in the sense of Γ–convergence to F

Bibliography

[AB15] G. Averkov and G. Bianchi. Covariograms generated by valuations. *Int. Math. Res. Not. IMRN*, 2015(19):9277–9329, 2015.

[ACO09] G. Alberti, R. Choksi, and F. Otto. Uniform energy distribution for an isoperimetric problem with long-range interactions. *J. Amer. Math. Soc.*, 22(2):569–605, 2009.

[ADPM11] L. Ambrosio, G. Da Prato, and A. Mennucci. *Introduction to measure theory and integration*, volume 10 of *Appunti. Scuola Normale Superiore di Pisa (Nuova Serie) [Lecture Notes. Scuola Normale Superiore di Pisa (New Series)]*. Edizioni della Normale, Pisa, 2011.

[AFM13] E. Acerbi, N. Fusco, and M. Morini. Minimality via second variation for a nonlocal isoperimetric problem. *Comm. Math. Phys.*, 322(2):515–557, 2013.

[AJL+02] B. Alberts, A. Johnson, J. Lewis, M. Raff, K. Roberts, and P. Walter. Molecular biology of the cell. 2002.

[BBM01] J. Bourgain, H. Brezis, and P. Mironescu. Another look at Sobolev spaces. In *Optimal control and partial differential equations*, pages 439–455. IOS, Amsterdam, 2001.

[BD98] A. Braides and A. Defranceschi. *Homogenization of multiple integrals*, volume 12 of *Oxford Lecture Series in Mathematics and its Applications*. The Clarendon Press, Oxford University Press, New York, 1998.

[Bia02] G. Bianchi. Determining convex polygons from their covariograms. *Adv. in Appl. Probab.*, 34(2):261–266, 2002.

[BJ82] T. Bröcker and K. Jänich. *Introduction to differential topology*. Cambridge University Press, Cambridge-New York, 1982. Translated from the German by C. B. Thomas and M. J. Thomas.

[BKMC23] D. Brazke, H. Knüpfer, and A. Marciniak-Czochra. Γ-limit for a sharp interface model related to pattern formation on biomembranes. *Calc. Var. Partial Differential Equations*, 62(3):Paper No. 94, 18, 2023.

[BS94] S. Brenner and L. Scott. *The mathematical theory of finite element methods*, volume 15 of *Texts in Applied Mathematics*. Springer-Verlag, New York, 1994.

[BZ88] Y. Burago and V. Zalgaller. *Geometric inequalities*, volume 285 of *Grundlehren der mathematischen Wissenschaften [Fundamental Principles of Mathematical Sciences]*. Springer-Verlag, Berlin, 1988. Translated from the Russian by A. B. Sosinskii, Springer Series in Soviet Mathematics.

[Can70] P. Canham. The minimum energy of bending as a possible explanation of the biconcave shape of the human red blood cell. *Journal of Theoretical Biology*, 26(1):61–81, 1970.

[CDMFL11] M. Chermisi, G. Dal Maso, I. Fonseca, and G. Leoni. Singular perturbation models in phase transitions for second-order materials. *Indiana Univ. Math. J.*, 60(2):367–409, 2011.

[CMM20] A. Cucchi, A. Mellet, and N. Meunier. A Cahn-Hilliard model for cell motility. *SIAM J. Math. Anal.*, 52(4):3843–3880, 2020.

[CN20] A. Cesaroni and M. Novaga. Second-order asymptotics of the fractional perimeter as $s \to 1$. *Math. Eng.*, 2(3):512–526, 2020.

[CP10] R. Choksi and M. Peletier. Small volume fraction limit of the diblock copolymer problem: I. Sharp-interface functional. *SIAM J. Math. Anal.*, 42(3):1334–1370, 2010.

[Cri18] R. Cristoferi. On periodic critical points and local minimizers of the Ohta-Kawasaki functional, 2018.

[CS06] R. Choksi and P. Sternberg. Periodic phase separation: the periodic Cahn-Hilliard and isoperimetric problems. *Interfaces Free Bound.*, 8(3):371–392, 2006.

[CS13] M. Cicalese and E. Spadaro. Droplet minimizers of an isoperimetric problem with long-range interactions. *Comm. Pure Appl. Math.*, 66(8):1298–1333, 2013.

[CSZ11] M. Cicalese, E. Spadaro, and C. Zeppieri. Asymptotic analysis of a second-order singular perturbation model for phase transitions. *Calc. Var. Partial Differential Equations*, 41(1-2):127–150, 2011.

[DÓ2] J. Dávila. On an open question about functions of bounded variation. *Calc. Var. Partial Differential Equations*, 15(4):519–527, 2002.

[EH21] C. Elliott and L. Hatcher. Domain formation via phase separation for spherical biomembranes with small deformations. *European J. Appl. Math.*, 32(6):1127–1152, 2021.

[EHS22] C. Elliott, L. Hatcher, and B. Stinner. On the sharp interface limit of a phase field model for near spherical two phase biomembranes. *Interfaces Free Bound.*, 24(2):263–286, 2022.

[EL11] X. Emery and C. Lantuéjoul. Geometric covariograms, indicator variograms and boundaries of planar closed sets. *Math. Geosci.*, 43(8):905–927, 2011.

[FHLZ16] I. Fonseca, G. Hayrapetyan, G. Leoni, and B. Zwicknagl. Domain formation in membranes near the onset of instability. *J. Nonlinear Sci.*, 26(5):1191–1225, 2016.

[Gal11] Bruno Galerne. Computation of the perimeter of measurable sets via their covariogram. Applications to random sets. *Image Anal. Stereol.*, 30(1):39–51, 2011.

[GeB93] K. Groß e Brauckmann. New surfaces of constant mean curvature. *Math. Z.*, 214(4):527–565, 1993.

[GMP22] M. Goldman, B. Merlet, and M. Pegon. Uniform $C^{1,\alpha}$-regularity for almost-minimizers of some nonlocal perturbations of the perimeter, 2022. preprint.

[GMS13] D. Goldman, C. Muratov, and S. Serfaty. The Γ-limit of the two-dimensional Ohta-Kawasaki energy. I. Droplet density. *Arch. Ration. Mech. Anal.*, 210(2):581–613, 2013.

[GMS14] D. Goldman, C. Muratov, and S. Serfaty. The Γ-limit of the two-dimensional Ohta-Kawasaki energy. Droplet arrangement via the renormalized energy. *Arch. Ration. Mech. Anal.*, 212(2):445–501, 2014.

[GP74] V. Guillemin and A. Pollack. *Differential topology*. Prentice-Hall, Inc., Englewood Cliffs, NJ, 1974.

[GR15] I. Gradshteyn and I. Ryzhik. *Table of integrals, series, and products*. Elsevier/Academic Press, Amsterdam, eighth edition, 2015.

[Gra08] L. Grafakos. *Classical Fourier analysis*, volume 249 of *Graduate Texts in Mathematics*. Springer, New York, second edition, 2008.

[GZ98] R. Gardner and G. Zhang. Affine inequalities and radial mean bodies. *Amer. J. Math.*, 120(3):505–528, 1998.

[Heb99] E. Hebey. *Nonlinear analysis on manifolds: Sobolev spaces and inequalities*, volume 5 of *Courant Lecture Notes in Mathematics*. New York University, Courant Institute of Mathematical Sciences, New York; American Mathematical Society, Providence, RI, 1999.

[Hel73] W. Helfrich. Elastic properties of lipid bilayers: theory and possible experiments. *Zeitschrift für Naturforschung C*, 28(11-12):693–703, 1973.

[HG96] J. Hu and R. Granek. Buckling of amphiphilic monolayers induced by head-tail asymmetry. *Journal de Physique II*, 6(7):999–1022, 1996.

[HZ01] W. Huttner and J. Zimmerberg. Implications of lipid microdomains for membrane curvature, budding and fission: Commentary. *Current opinion in cell biology*, 13(4):478–484, 2001.

[JP17] V. Julin and G. Pisante. Minimality via second variation for microphase separation of diblock copolymer melts. *J. Reine Angew. Math.*, 729:81–117, 2017.

[KG10] Y. Kaizuka and J. Groves. Bending-mediated superstructural organizations in phase-separated lipid membranes. *New J. Phys*, 12, 2010.

[KS23] H. Knüpfer and W. Shi. Second order expansion for the nonlocal perimeter functional. *Comm. Math. Phys.*, 398(3):1371–1402, 2023.

[KSA06] S. Komura, N. Shimokawa, and D. Andelman. Tension-induced morphological transition in mixed lipid bilayers. *Langmuir*, 22, 2006.

[LA87] S. Leibler and D. Andelman. Ordered and curved meso-structures in membranes and amphiphilic films. *Journal de Physique*, 48(11):2013–2018, 1987.

[Leo13] G. Leoni. Gamma convergence and applications to phase transitions. *CNA Lecture Notes, CMU, in preparation*, 2013.

[LL15] J. Lorent and I. Levental. Structural determinants of protein partitioning into ordered membrane domains and lipid rafts. *Chemistry and Physics of Lipids*, 192(SI):23–32, 2015.

[Mag12] F. Maggi. *Sets of finite perimeter and geometric variational problems*, volume 135 of *Cambridge Studies in Advanced Mathematics*. Cambridge University Press, Cambridge, 2012. An introduction to geometric measure theory.

[Mat86] G. Matheron. Le covariogramme géométrique des compacts convexes de $\mathbb{R}^{@}$. *Technical Report N/2/86/G, Centre de Géostatistique, Ecole des mines de Paris*, 1986.

[MC70] C. Mallows and J. Clark. Linear-intercept distributions do not characterize plane sets. *J. Appl. Probability*, 7:240–244, 1970.

[Mod87] L. Modica. The gradient theory of phase transitions and the minimal interface criterion. *Arch. Rational Mech. Anal.*, 98:123–142, 1987.

[MP22] B. Merlet and M. Pegon. Large mass rigidity for a liquid drop model in 2D with kernels of finite moments. *Journal de l'École polytechnique — Mathématiques*, 9:63–100, 2022.

[MRS93] M. Meyer, S. Reisner, and M. Schmuckenschläger. The volume of the intersection of a convex body with its translates. *Mathematika*, 40(2):278–289, 1993.

[MS14] M. Morini and P. Sternberg. Cascade of minimizers for a nonlocal isoperimetric problem in thin domains. *SIAM J. Math. Anal.*, 46(3):2033–2051, 2014.

[MS19] C. Muratov and T. Simon. A nonlocal isoperimetric problem with dipolar repulsion. *Comm. Math. Phys.*, 372(3):1059–1115, 2019.

[MS20] A. Mondino and C. Scharrer. Existence and regularity of spheres minimising the Canham-Helfrich energy. *Arch. Ration. Mech. Anal.*, 236(3):1455–1485, 2020.

[MW21] A. Mellet and Y. Wu. An isoperimetric problem with a competing nonlocal singular term. *Calc. Var. Partial Differential Equations*, 60(3):Paper No. 106, 40, 2021.

[MW23] A. Mellet and Y. Wu. Γ-convergence of some nonlocal perimeters in bounded domains with general boundary conditions. *SIAM J. Math. Anal.*, 55(4):3226–3261, 2023.

[Nag93] W. Nagel. Orientation-dependent chord length distributions characterize convex polygons. *J. Appl. Probab.*, 30(3):730–736, 1993.

[Peg21] M. Pegon. Large mass minimizers for isoperimetric problems with integrable nonlocal potentials. *Nonlinear Anal.*, 211:Paper No. 112395, 48, 2021.

[PYG06] R. Parthasarathy, C. Yu, and J. Groves. Curvature-modulated phase separation in lipid bilayer membranes. *Langmuir*, 22(11):5095–5099, 2006.

[RF10] H. Royden and P. Fitzpatrick. *Real analysis*. Pearson, fourth edition, 2010.

[RKG05] S. Rozovsky, Y. Kaizuka, and J. Groves. Formation and spatio-temporal evolution of periodic structures in lipid bilayers. *Jour. Am. Chem. Soc.*, 127(1):36–37, 2005.

[Ros05] A. Ros. The isoperimetric problem. In *Global theory of minimal surfaces*, volume 2 of *Clay Math. Proc.*, pages 175–209. Amer. Math. Soc., Providence, RI, 2005.

[RS05] L. Rajendran and K. Simons. Lipid rafts and membrane dynamics. *Journal of Cell Science*, 118(6):1099–1102, 2005.

[Rud91] W. Rudin. *Functional analysis*. International Series in Pure and Applied Mathematics. McGraw-Hill, Inc., New York, second edition, 1991.

[RW00] X. Ren and J. Wei. On the multiplicity of solutions of two nonlocal variational problems. *SIAM J. Math. Anal.*, 31:909–924, 2000.

[SI97] K. Simons and E. Ikonen. Functional rafts in cell membranes. *Nature.*, 1997.

[SMNT17] N. Shimokawa, R. Mukai, M. Nagata, and M. Takagi. Formation of modulated phases and domain rigidification in fatty acid-containing lipid membranes. *Physical Chemistry Chemical Physics*, 19(20):13252–13263, 2017.

[SP13] S. Sonnino and A. Prinetti. Membrane domains and the "lipid raft" concept. *Current Medicinal Chemistry*, 20(1):4–21, 2013.

[Tan96] T. Taniguchi. Shape deformation and phase separation dynamics of two-component vesicles. *Physical review letters*, 76(23):4444, 1996.

[Wil17] F. Willot. Mean covariogram of cylinders and applications to Boolean random sets. *Izv. Nats. Akad. Nauk Armenii Mat.*, 52(6):62–76, 2017.